N71-36442

FINAL TECHNICAL REPORT

# CHARGED PARTICLE RADIATION DAMAGE IN SEMICONDUCTORS, XVI:

# STUDY AND DETERMINATION OF AN OPTIMUM DESIGN FOR SPACE UTILIZED LITHIUM DOPED SOLAR CELLS, PART II

CASE FILE
COPY

15 JULY 1971

13154-6022-R0-00

Contract No. 952554

JET PROPULSION LABORATORY
CALIFORNIA INSTITUTE OF TECHNOLOGY
PASADENA, CALIFORNIA

TRW
SYSTEMS GROUP

ONE SPACE PARK • REDONDO BEACH, CALIFORNIA 90278

# FINAL REPORT
# STUDY AND DETERMINATION OF AN OPTIMUM DESIGN FOR SPACE UTILIZED LITHIUM-DOPED SOLAR CELLS, PART II

15 July 1971

13154-6022-R0-00


Prepared by:

R. G. Downing

J.R. Carter, Jr.

Approved by:

A.M.Liebschutz



Contract 952554



Jet Propulsion Laboratory
California Institute of Technology
Pasadena, California

TRW Systems Group
One Space Park
Redondo Beach, California 90278



This work was performed for the Jet Propulsion Laboratory, California Institute of Technology, as sponsored by the National Aeronautics and Space Administration under Conctract NAS 7-100.

## PREFACE

This report concludes a two year study, under Contract 952554, for the Jet Propulsion Laboratory, Pasadena, California. Mr. Paul Berman of JPL was the technical monitor for the program. The report also represents the last of a series of sixteen reports, covering studies of "Charged Particle Radiation Damage in Semiconductors." The first report of this series was "Experimental Proton Irradiation of Solar Cells", dated 15 September 1961, under NAS 5-613. In behalf of all the workers who have contributed to these studies, the current investigators gratefully acknowledge the support and encouragement of the Jet Propulsion Laboratory, and various organizations and individuals of the National Aeronautics and Space Administration who have directed our work during the past decade.

TABLE OF CONTENTS


| | Page |
|---|---|
| ABSTRACT | viii |
| SUMMARY | ix |
| I. INTRODUCTION | 1 |
| II. LITHIUM-DOPED SOLAR CELL EVALUATION | 2 |
| A. Centralab Solar Cells | 4 |
| B. Heliotek Solar Cells | 11 |
| C. Electron Energy Dependence | 14 |
| D. Incremental Irradiation | 16 |
| E. Solar Simulator Measurements | 18 |
| III. KINETICS OF LITHIUM IN IRRADIATED SOLAR CELLS | 21 |
| A. Removal Rates, Low Oxygen Cells | 21 |
| B. Removal Rates, High Oxygen Cells | 25 |
| C. Capacitance Measurements | 31 |
| D. Lithium Counterdoped n/p Solar Cells | 33 |
| IV. CONCLUSIONS | 36 |
| V. NEW TECHNOLOGY | 38 |
| VI. PAPERS AND PUBLICATIONS GENERATED | 38 |
| REFERENCES | 39 |

# LIST OF ILLUSTRATIONS


Page

TABLES

I LITHIUM SOLAR CELL MANUFACTURING PARAMETERS . . . . . 40

II FLOAT ZONE SILICON CELL RECOVERY CHARACTERISTICS . . . . . 41

III CRUCIBLE LITHIUM SOLAR CELL RECOVERY CHARACTERISTICS, $60^{o}$ RECOVERY . . . . . 42

IV LITHIUM DIFFUSION MATRIX C13 SERIES: MAXIMUM, MEAN AND MINIMUM DONOR CONCENTRATION AT JUNCTION: VOLTAGE-CAPACITANCE RELATIONSHIP . . . . . 43

V SOLAR SIMULATOR MEASUREMENTS . . . . . 44

FIGURES

1 RECOVERY OF GROUP C11A SOLAR CELLS, $3x10^{15}$ $e/cm^2$ . . . . . 45

2 RECOVERY OF GROUP C11B SOLAR CELLS, $3x10^{15}$ $e/cm^2$ . . . . . 46

3 RECOVERY OF GROUP C11D SOLAR CELLS, $3x10^{15}$ $e/cm^2$ . . . . . 47

4 RECOVERY OF GROUP C11C SOLAR CELLS, $3x10^{14}$ $e/cm^2$ . . . . . 48

5 RECOVERY OF GROUP C11C SOLAR CELLS, $3x10^{15}$ $e/cm^2$ . . . . . 49

6 DONOR CONCENTRATION VS. DIFFUSION TIME . . . . . 50

7 SHORT CIRCUIT CURRENT VS. DONOR CONCENTRATION, C13A, C13B . . . . . 51

8 SHORT CIRCUIT CURRENT VS. DONOR CONCENTRATION, C13C, C13D . . . . . 52

9 SHORT CIRCUIT CURRENT VS. DONOR CONCENTRATION, C13E, C13F . . . . . 53

10 SHORT CIRCUIT CURRENT VS. DONOR CONCENTRATION, C13G, C13H . . . . . 54

11 SHORT CIRCUIT CURRENT VS. DONOR CONCENTRATION, C13I, C13J . . . . . 55

12 DIFFUSION LENGTH VS. ELECTRON FLUENCE . . . . . 56

LIST OF ILLUSTRATIONS (Continued)


| | | Page |
|---|---|---|
| FIGURES | | |
| 13 | SHORT CIRCUIT CURRENT VS. DIFFUSION LENGTH . . . . . | 57 |
| 14 | SHORT CIRCUIT CURRENT VS. ELECTRON FLUENCE . . . . . | 58 |
| 15 | SHORT CIRCUIT CURRENT RECOVERY, Q.C. CELLS, AT 60°C . . . . | 59 |
| 16 | SHORT CIRCUIT CURRENT RECOVERY, Q.C. CELLS, AT 60°C . . . . . | 60 |
| 17 | SHORT CIRCUIT CURRENT RECOVERY, Q.C. CELLS, AT 60°C . . . . . | 61 |
| 18 | SHORT CIRCUIT CURRENT RECOVERY, Q.C. CELLS, AT 60°C . . . . . | 62 |
| 19 | SHORT CIRCUIT CURRENT RECOVERY, Q.C. CELLS, AT 60°C . . . . . | 63 |
| 20 | SHORT CIRCUIT CURRENT RECOVERY, Q. C. CELLS, AT 60°C . . . . . | 64 |
| 21 | SHORT CIRCUIT CURRENT RECOVERY, Q.C. CELLS, AT 60°C . . . . . | 65 |
| 22 | SHORT CIRCUIT CURRENT RECOVERY, Q.C. CELLS, AT 60°C . . . . . | 66 |
| 23 | SHORT CIRCUIT CURRENT RECOVERY, Q.C. CELLS, AT 60°C . . . . . | 67 |
| 24 | SHORT CIRCUIT CURRENT RECOVERY, Q.C. CELLS, AT 60°C . . . . . | 68 |
| 25 | SHORT CIRCUIT CURRENT DURING RECOVERY, Q.C. CELLS . . . . . | 69 |
| 26 | SHORT CIRCUIT CURRENT DURING RECOVERY, Q.C. CELLS . . . . . | 70 |
| 27 | SHORT CIRCUIT CURRENT DURING RECOVERY, Q.C. CELLS . . . . . | 71 |
| 28 | SHORT CIRCUIT CURRENT DURING RECOVERY, Q.C. CELLS . . . . . | 72 |
| 29 | SHORT CIRCUIT CURRENT DURING RECOVERY, Q.C. CELLS . . . . . | 73 |
| 30 | SHORT CIRCUIT CURRENT DURING RECOVERY, Q.C. CELLS . . . . . | 74 |
| 31 | SHORT CIRCUIT CURRENT DURING RECOVERY, Q.C. CELLS . . . . . | 75 |
| 32 | SHORT CIRCUIT CURRENT DURING RECOVERY, Q.C. CELLS . . . . . | 76 |
| 33 | SHORT CIRCUIT CURRENT DURING RECOVERY, Q.C. CELLS . . . . . | 77 |
| 34 | SHORT CIRCUIT CURRENT DURING RECOVERY, Q.C. CELLS . . . . . | 78 |
| 35 | RECOVERY OF GROUP H1A SOLAR CELLS, $3x10^{14}$ e/cm$^2$ . . . . . | 79 |

LIST OF ILLUSTRATIONS (Continued)


| | | Page |
|---|---|---|
| FIGURES | | |
| 36 | RECOVERY OF GROUP H1A SOLAR CELLS, $3x10^{15}$ e/cm$^2$ | 80 |
| 37 | RECOVERY OF GROUP H4A SOLAR CELLS, $3x10^{14}$ e/cm$^2$ | 81 |
| 38 | RECOVERY OF GROUP H4A SOLAR CELLS, $3x10^{15}$ e/cm$^2$ | 82 |
| 39 | RECOVERY OF GROUP H2A SOLAR CELLS, $3x10^{14}$ e/cm$^2$ | 83 |
| 40 | RECOVERY OF GROUP H2A SOLAR CELLS, $3x10^{15}$ e/cm$^2$ | 84 |
| 41 | RECOVERY OF GROUP H5A1 SOLAR CELLS, $3x10^{14}$ e/cm$^2$ | 85 |
| 42 | RECOVERY OF GROUP H5A1 SOLAR CELLS, $3x10^{15}$ e/cm$^2$ | 86 |
| 43 | RECOVERY OF GROUP H5A2 SOLAR CELLS, $3x10^{14}$ e/cm$^2$ | 87 |
| 44 | RECOVERY OF GROUP H5A2 SOLAR CELLS, $3x10^{15}$ e/cm$^2$ | 88 |
| 45 | RECOVERY OF GROUP H5A3 SOLAR CELLS, $3x10^{14}$ e/cm$^2$ | 89 |
| 46 | RECOVERY OF GROUP H5A3 SOLAR CELLS, $3x10^{15}$ e/cm$^2$ | 90 |
| 47 | SHORT CIRCUIT CURRENT RECOVERY, 28 MeV | 91 |
| 48 | SHORT CIRCUIT CURRENT VS. ELECTRON FLUENCE | 92 |
| 49 | CRITICAL FLUENCE VS. ELECTRON ENERGY | 93 |
| 50 | SHORT CIRCUIT CURRENT CHANGES DURING INCREMENTAL IRRADIATION | 94 |
| 51 | CARRIER REMOVAL IN CELL H1A-6903 | 95 |
| 52 | CARRIER REMOVAL IN CELL H4A-7595 | 96 |
| 53 | CARRIER REMOVAL IN CELL H2A-6993 | 97 |
| 54 | CARRIER REMOVAL IN CELL H5A1-7164 | 98 |
| 55 | CARRIER REMOVAL IN CELL H5A-7169 | 99 |
| 56 | REMOVAL RATE, HELIOTEK, LOPEX | 100 |
| 57 | CARRIER REMOVAL IN CELLS OF C11C GROUP | 101 |
| 58 | REMOVAL RATES OF CELLS OF C11C GROUP | 102 |

LIST OF ILLUSTRATIONS (Continued)


| | | Page |
|---|---|---|
| 59 | CARRIER REMOVAL IN CELL OF C11A AND C11D GROUPS . . . . . | 103 |
| 60 | REMOVAL RATES OF CELLS OF C11A AND C11D GROUPS . . . . . | 104 |
| 61 | REMOVAL RATE VS. LITHIUM DONOR CONCENTRATION . . . . . | 105 |
| 62 | DONOR CONCENTRATION VS. BARRIER WIDTH, C13A-6 . . . . . | 106 |
| 63 | DONOR CONCENTRATION VS. BARRIER WIDTH, C13E-5 . . . . . | 107 |
| 64 | LITHIUM DONOR LOSS DURING RECOVERY, $3x10^{14}$ $e/cm^2$ . . . | 108 |
| 65 | DONOR CONCENTRATION DURING RECOVERY, C13A-1 . . . . . | 109 |
| 66 | CHANGE IN LITHIUM DONOR CONCENTRATION AND DIFFUSION LENGTH DURING RECOVERY, C13A-1 . . . . . | 110 |
| 67 | DONOR CONCENTRATION DURING RECOVERY, C13D-1 . . . . . | 111 |
| 68 | CHANGE IN LITHIUM DONOR CONCENTRATION AND DIFFUSION LENGTH DURING RECOVERY, C13D-1 . . . . . | 112 |
| 69 | LITHIUM DONOR CONCENTRATION VS. GRADIENT, LOW OXYGEN CELLS . . . . . | 113 |
| 70 | LITHIUM DONOR CONCENTRATION VS. GRADIENT, HIGH OXYGEN CELLS . . . . . | 114 |
| 71 | EXPONENT "n" VS. GRADIENT, HIGH OXYGEN CELLS . . . . . | 115 |
| 72 | LITHIUM COUNTERDOPED DIODE, WACKER FZ . . . . . | 116 |
| 73 | LITHIUM COUNTERDOPED DIODE, T.I. LOPEX . . . . . | 117 |
| 74 | LITHIUM COUNTERDOPED n/p SOLAR CELL . . . . . | 118 |

## ABSTRACT

Several groups of lithium-doped solar cells were evaluated for hardness to 1 MeV electron irradiation. The groups represent programmed variations in manufacturing technique. The cells exhibiting highest recovered powers were fabricated with relatively low lithium donor concentration at the junction within a range of 2 - $4x10^{14}$ Li/$cm^3$. The lower lithium donor concentrations have produced cells of equal or superior efficiency to conventional n/p cells. Lithium diffusions of 8 hours at 325$^{o}$C have produced excellent cells. Other factors such as boron diffusion source and lithium source area variation do not appear to significantly affect radiation hardness. Solar simulator measurements were made on many cells representing cell groups showing the highest recovered outputs. These results confirm that lithium-doped solar cells, fabricated to an optimum design, are superior in hardness to conventional n/p solar cells.

Changes in the lithium donor concentration during the recovery of irradiated cells were monitored by capacitance-voltage measurements. The donor loss which occurs during recovery is directly related to the initial lithium donor concentration. The lithium donor loss which occurs during recovery is highly non-linear with electron fluence. A physical model of the recovery process is proposed in which the defects formed during irradiation act as nuclei for the precipitation of lithium donors. The coalescence of lithium neutralizes recombination centers and causes cell output levels to increase.

## SUMMARY

A two year program was conducted to determine the optimum design for lithium-doped solar cells, which would be suitable for space applications. This work was accomplished by evaluation of solar cells produced for JPL by other contractors. The evaluation consisted of characterizing the as-received cells as to the quantity and distribution of lithium donors in the cells. The cells were irradiated with 1 MeV electron fluences of $3x10^{14}$ and $3x10^{15}$ $e/cm^2$. The cell response was determined by the I-V output characteristics under 100 $mw/cm^2$ 2800°K Tungsten illumination. The cells made from float zone or Lopex silicon were stored at room temperature after irradiation, and those made from quartz crucible silicon were stored at 60°C. Cell response was determined periodically after irradiation.

The manufacturing parameters varied , including silicon resistivity and oxygen content, boron diffusion source, lithium diffusion source area coverage, and lithium diffusion schedule. The results of the irradiation evaluation indicated that the lithium diffusion schedule and the oxygen concentration (i.e., float zone or quartz crucible silicon) are the major factors of practical importance in the behavior of irradiated lithium-doped solar cells. The role of oxygen concentration has been covered in Part I. of this final report. The most important factor optimization of the lithium cells is concentration of lithium donors near the junction. This quantity affects the cell performance in several ways. The results indicate that a lithium donor concentration between 2 to $4x10^{14}$ $cm^{-3}$ at the junction is desired for optimum radiation hardness. Lithium donor concentrations above this range result in slightly lower output levels after recovery from irradiation and lower initial power output. Although cells

with higher lithium donor concentrations recover more rapidly after irradiation, this quality is of questionable value in a real time space environment.

The results indicated that cells with optimum lithium donor concentrations can be produced with efficiencies equal to or superior to those of commercial n/p cells. After irradiations of $3x10^{14}$ e/cm$^2$, the optimum lithium-doped cells recover to $I_{sc}$ values in the range of 53-56 ma (tungsten). At the higher fluence of $3x10^{15}$ e/cm, the optimum cell recovers to $I_{sc}$ values of 40 to 44 ma (tungsten). Lithium diffusion schedules of 8 hours at 325$^{o}$C successfully produce the desired concentration of lithium donors at the junction. The lower lithium diffusion temperatures also offer the advantage of reduced spread in lithium donor concentration within a production group.

A group of lithium-doped solar cells was irradiated with 28 MeV electrons. The results indicate that lithium-doped cells have a tenfold advantage over conventional n/p cells in this environment. These data are necessary for calculations of the cell degradation in the space environment.

Studies of lithium-doped cell degradation during incremental irradiations were made in an attempt to produce an accelerated radiation evaluation more nearly approaching a real time test. The results of the incremental irradiations were very similar to those for fast irradiation followed by long recoveries. Further work is necessary to verify these results or confirm the usefulness of incremental irradiation testing.

To provide a better basis for the comparison of irradiation results for lithium-doped cells with those of conventional n/p cells, the cells which recovered to the highest output levels were tested under simulated solar illumination of 140 mw/cm$^2$ with an X25L simulator. The results

indicate that optimum design lithium-doped cells recover to a maximum power output 24 mw after $3x10^{14}$ e/cm$^2$ and 20 mw after $3x10^{15}$ e/cm$^2$.

Studies of the changes in the lithium donor concentration which occur during irradiation and recovery were studied by means of capacitance-voltage measurements. The results previously reported in Part I. of this report indicated that oxygen-vacancy pairs are the predominant defects formed during irradiation of lithium-doped cells. The recent studies of the changes during the recovery process indicate that precipitation of the lithium donors on radiation defects occurs during recovery. This conclusion was reached because of the highly non-linear changes in the lithium-donor concentration, during recovery, relative to the particle fluence or defect concentration. The changes in lithium-donor concentration which occur during recovery appear to be directly related to the original lithium-donor concentration.

Measurements of the minority carrier diffusion lengths of lithium-doped cells during the recovery period were compared with the changes in the lithium-donor concentration. The results indicate that both changes occur within a very similar time scheme, and probably are related.

Attempts were made to investigate the behavior of p-type lithium counterdoped silicon devices in a radiation environment. The first work involving Schottky barrier diodes indicated significant recovery of diffusion length after irradiation. When counterdoping was introduced in n/p solar cells, only a small recovery occurred after irradiation. Further work is necessary to determine if the effect can be of practical significance.

# I. INTRODUCTION

This final report culminates activities during the second and final 12-month period under JPL Contract No. 952554 in the study of lithium-doped solar cells. Interest in the field began with Vavilov's report of a radiation resistant diode made with lithium-doped, crucible grown silicon.[1] Wysocki later reported lithium-doped solar cells which degraded under electron irradiation, but rapidly recovered at room temperature.[2] Floating zone silicon, with its characteristic lower oxygen concentration, was used to achieve this result. Subsequent work in this laboratory indicated that a similar but slower recovery also occurs in lithium-doped, quartz-crucible,silicon solar cells.

A series of studies was conducted by RCA and TRW to evaluate the various factors influencing the behavior of irradiated lithium-doped solar cells.[3-8] The various developments and improvements which have affected the behavior of lithium cells were reviewed in Part I of this final report.[5] In addition, the work of several investigators has confirmed a physical model of the behavior of lithium-doped solar cells during irradiation. The most important task remaining is that of improving the cell output levels, which can be achieved during the recovery stage.

During our previous work it was noted that electron irradiated, lithium-doped solar cells would recover to power output levels somewhat greater than those of a similarly irradiated 10 ohm-cm n/p solar cell. All lithium-doped cells did not recover to these levels, but many groups did. The evidence indicated that identifiable manufacturing parameters determine which lithium-doped cells exhibit superior behavior. In the past year's work, additional manufacturing parameters have been examined to seek means of further increasing the recovered power levels. The maximum

recovered output values observed after irradiation of $3x10^{15}$ 1 MeV e/cm$^2$ also exceeded those for conventional n/p cells, but no significant increase was observed in these levels as compared to cells evaluated during the first year of this contract. Manufacturing changes produced lithium-doped cells which were superior at the lower electron fluence of $3x10^{14}$ e/cm$^2$. Lithium-doped solar cells previously were often inferior at the lower fluences because of lower outputs before irradiation. Improvements in the pre-irradiation power levels have been made to the point that the highest efficiency cells now made are the lithium-doped cells. This improvement is in part due to the effect of lithium-doping on cell $V_{oc}$ values. This effect is illustrated in the cells of group C13. The as-received $V_{oc}$ values of this group average above 0.6v. Similarly doped cells without lithium would have $V_{oc}$ values of only 0.55v.

The changes in lithium concentration during irradiation and recovery have been further studied during this report period. The evidence indicates that simple ion pairing of lithium donors and recombination centers is not the recovery mechanism. The results indicate a nonlinearity, with fluence, of lithium reacting during recovery and, in many cases, a larger number than one lithium donor reacting with each radiation defect. These results require a modification of the recovery model to the extent that a "precipitation" of lithium occurs on the radiation defects. Correlations between the changes in lithium donor concentration during recovery and the recovery of minority carrier diffusion length after irradiation have an approximate agreement.

## II. LITHIUM-DOPED SOLAR CELL EVALUATION

During the past year, lithium-doped solar cells manufactured by

Centralab and Heliotek have been irradiated with 1 MeV electrons and their recovery characteristics have been studied. Several different processing techniques were represented in these cells, including different diffusion schedules, gases, and varying percentage of lithium coverage of the rear surface. Data for cell groups C11A through C11D, C13A through C13J, H1A, H2A, H4A, H5A1, H5A2, and H5A3, are listed in Table I. Cells of all groups received radiation exposure to 1 MeV electrons. Tungsten I-V characteristics and capacitance vs. voltage measurements were then obtained as a function of time at either room temperature or 60°C. The general radiation damage and recovery characteristics of each cell group are summarized in Tables II and III. The recovered levels given in the tables are as of July 1971 (end of contract period) and take into account any redegradation that may have occurred. In general, it can be observed that the higher lithium concentrations at the junction result in lower initial characteristics, and more rapid annealing rates while, with lower lithium concentrations, higher initial output and slower recovery rates exist. It should be noted that most cell groups tested were superior to the contemporary n/p cells in recovered level. The initial short circuit current of many of the cells studied was inferior to the contemporary n/p cells.

Most previous evaluations of lithium-doped solar cell radiation hardness have been done by a fast irradiation to the desired fluence, followed by a recovery period. This type of evaluation may have only limited validity as an accelerated space radiation environment. A second approach has been low flux irradiation with a beta particle source. This is a cumbersome procedure which is practically limited to fluences in the range of $3 \times 10^{14}$ e/cm$^2$. We have investigated an alternate method in which electron fluence is applied incrementally with intervening recovery periods. These results are compared to those from a single fast radiation followed by recovery.

A limited study was made of the behavior of lithium-doped cells under irradiation with 28 MeV electrons. These data were needed for calculations of radiation degradation due to the spectrum of particle energies found in space. For practical reasons, our evaluations of solar cells have been reported in terms of response to 2800$^{0}$K Tungsten illumination of approximately 100 mw/cm$^{2}$. Such data are adequate for comparative studies of radiation degradation, but are of little value for evaluation by spacecraft designers. For this reason we have selected 20 irradiated and recovered cells, which represent important cell groups, types, fluences, and energies, for measurement under a solar simulator. These measurements are of particular value in the comparison of lithium-doped solar cells with conventional cells.

A. Centralab Cells

The Centralab cells submitted for evaluation were all fabricated from quartz crucible grown silicon, with the exception of group C11C. The variable of boron dopant gas was investigated by diffusing the p-type front surface with boron trichloride in the case of group C11A and boron tribromide in the case of group C11B. The short circuit current values of cells received in group C11B were rather low (53 ma) compared to those of group C11A. This difference is not believed to be related to the use of boron tribromide. It is known that when Texas Instruments manufactured solar cells, their p-type diffusions were made with boron tribromide. A second important difference between the cells of these two groups is concentration of lithium found at the junction. Although the cells of both C11A and C11B groups were lithium diffused in the same manner (480 min. at 325$^{0}$C), the data in Table I indicate that group C11A cells contain twice the lithium concentration of cells of group C11B.This difference is not considered to

be related to use of boron tribromide. The effect of this lower lithium concentration can be seen in the 60°C recovery data in Table III and in Figures 1 and 2. The cells of group C11A are nearly fully recovered 200 hours after irradiation; however, those of C11B appear to be only half recovered at a comparable recovery time. This slower recovery is probably due to the lower lithium concentration. The recovered $I_{sc}$ values of the C11A group cells are 38 ma after irradiation of $3x10^{15}$ e/cm$^2$. The value is significantly better than the comparable data for conventional n/p cells. Recovery of $I_{sc}$ in the C11B group reached values of 36 to 37 ma.

The cells of group C11D were lithium diffused at the slightly higher temperature of 375°C for 180 minutes. This diffusion schedule resulted in a higher concentration of lithium at the junction. These cells have about $5x10^{14}$ lithium atoms/cm$^3$. The C11A cells diffused at 325°C for 480 min.had only $3x10^{14}$ Li/cm$^3$. It is also noted that slope of the log capacitance versus log voltage is -0.26. This is the lowest value found in the current groups of cells under evaluation. The high lithium concentrations in group C11D are reflected in a slightly more rapid recovery after irradiation. The initial $I_{sc}$ values of the cells in groups C11A and C11D are comparable with those of conventional n/p solar cells. Figure 3 shows $I_{sc}$ recovery of the C11D cells after an irradiation of $3x10^{15}$ e/cm$^2$. The $I_{sc}$ value recovered to 38 ma. The cells of groups C11A, C11B, and C11D are interesting in that they have the lowest lithium concentrations of any quartz crucible silicon cell evaluated.

The remaining Centralab group, C11C, was fabricated from Lopex (low oxygen, low dislocation) silicon. In general, the performance of the group was very good. The cells were lithium diffused at 325°C for 480 minutes. The resulting lithium concentration in this group was $1.5x10^{14}$/cm$^3$. The

results of the $3x10^{14}$ e/cm$^2$ and $3x10^{15}$ e/cm$^2$ radiations are shown in Table II and in Figures 4 and 5. In both cases the $I_{sc}$ recovered to values greater than those of comparably irradiated n/p solar cells, as shown by the dashed lines on these graphs. Although the recovery kinetics are relatively slow in these cells, due to the lower lithium concentration, the irradiated cell performance is among the best received to date.

The cells from the C13 series, manufactured by Centralab, represent a JPL-designed matrix of lithium diffusion temperatures and times. The matrix is designed to investigate the optimum lithium diffusion and the reproducibility of the process. All the cells were fabricated from quartz crucible grown silicon with resistivities between 25 and 40 ohm-cm. The diffusion matrix is shown in Table IV. Also shown in the table are the mean donor concentrations at the junction of the cells of each group in the matrix. The voltage-capacitance relationship or range of relationships is also shown for each group. The donor concentrations were determined by means of capacitance. Since the phosphorus concentration is approximately $1.5x10^{14}$ atoms/cm$^3$, the lithium concentrations were estimated by subtracting the phosphorus concentration from the donor concentrations. Since the phosphorus concentration may go as high as $2x10^{14}$ atoms/cm$^3$ (i.e., 25 ohm-cm), some groups may contain cells with very low lithium concentrations. Specifically, these are the cells which received diffusions of 6 or 7 hours. It can also be observed that both higher temperatures and longer diffusion times result in greater variations in lithium concentration.

The mean donor concentrations of the various groups are plotted in Figure 6 as a function of diffusion time. It can be seen from the data in Figure 6 that the lithium concentrations at the junction are decreasing with time, in the time span

studied. Such a decreasing lithium concentration is inconsistent with diffusion from an infinite source. Since the donor concentration originally was equal to the phosphorus concentration, it was necessary for the donor concentration to rise from the original to a maximum before declining. This decrease in lithium concentration with diffusion time is characteristic of diffusion from a starved source. As the lithium source is exhausted, the surface concentration of the cells will decrease and concentrations at the junction will decrease. In the past, manufacturers of lithium solar cells have interrupted the lithium diffusion and removed the lithium source to produce starved source diffusion. This second diffusion has been referred to as a redistribution. The data in Figure 6 indicate that redistribution is not necessary. It is not clear what causes the exhaustion of the lithium source.

The before irradiation I-V characteristics of the C13 series cells were measured under tungsten illumination. The short circuit currents of these cells were analyzed in relation to the lithium concentration. These data are shown in Figures 7 through 11. In these figures, the short circuit current of the cell is plotted versus the donor concentration at the junction. The data for groups C13A and C13B are shown in Figure 7. In this case, there is very little variation of the lithium concentration and the $I_{sc}$ values fall in a fairly close grouping between 60 and 66 ma for the two square cm cells. In this case the $I_{sc}$ variation appears to be a result of variations in the recombination center concentrations present after manufacture.

In Figure 8 the results for groups C13C and C13D are shown. These cells show a tendency for the short circuit current to decrease with increasing donor concentration. In Figures 9 through 11, the tendency for

$I_{sc}$ to decrease with higher donor concentrations becomes a clear trend. The cell groups shown in Figures 9 through 11 are those diffused at the higher temperatures ($350^{o}C$, $360^{o}C$, and $370^{o}C$). It would appear that the suggested relationship is a valid one, but the wider variations in lithium concentration caused by higher temperature diffusions are necessary to observe the behavior.

The nature of the degradation process in solar cells is such that the minority carrier diffusion length of the cell is reduced as the reciprocal of the square root of the damaging particle fluence. This relationship assumes only that the damage sites are created linearly with increasing particle fluence and that all sites formed are retained during further irradiation. It also must be assumed that all damage sites of the same species which are generated will be equally effective. This means changes in the fill factor will not occur and changes in injection level are not produced by the irradiation. Despite these restrictions, it is found that the behavior of conventional solar cells is consistent with the above description. This behavior is illustrated by the dashed lines shown on Figure 12. Two lithium-doped p/n cells were irradiated to a total fluence of $3x10^{15}$ $e/cm^2$. The manner in which their diffusion length decreased with electron fluence is also shown in Figure 12. It is apparent that the lithium cells do not behave in the manner of conventional cells, because the slope of their degradation curves are significantly lower than those of the conventional cells.

This point is of particular interest in the determination of damage coefficients. The expression for the damage coefficient is:

$$\frac{1}{L^2} = \frac{1}{L_o}^2 + K \Phi$$

where

L = diffusion coefficient after irradiation

$L_o$ = diffusion coefficient before irradiation

$\Phi$ = electron fluence

K = the damage coefficient

The damage coefficient is meaningful only if the L and $\Phi$ relationship has a -1/2 slope, as shown by conventional cells. Since the lithium-doped cells have lower slopes, the calculated K values will be functions of the electron fluence rather than constants. Since this quantity is often used to compare the radiation hardness of solar cells, it would appear its value in lithium-doped cell evaluations would be limited.

Because of the manner in which solar cells operate, one empirically finds a direct relation between short circuit current and logarithum of the measured minority carrier diffusion length. We have verified this relationship, and the usual trend for high efficiency conventional cells is shown in Figure 13. The experimental data accumulated from two lithium-doped cells are also shown in Figure 13. It is obvious that the relationship for lithium-doped cells is significantly different from conventional cells. The most puzzling aspect of the difference is the high short circuit currents developed by the lithium-doped cells despite their relatively low minority carrier diffusion length. Cell C13D-1 is able to generate a $I_{sc}$ of 63 ma despite the fact that its diffusion length was only 60 $\mu$m. The explanation of this effect is not clear at this time. As a result of the non-linear behavior shown in Figure 12, the changes of short circuit current observed for lithium-doped cells during irradiation differ from those in conventional solar cells. Our extensive studies in the past have

established a consistent relationship between degraded short circuit current and electron fluence. It has always been found that cells degrade in $I_{sc}$ by 6.5 ma/cm$^2$ decade fluence. The rate has been found for all types of irradiation with all types of penetrating radiation. It can be seen from the data in Figure 14 that the lithium-doped cells degrade at a different rate than do the conventional cells. One possible cause of this behavior could be a diffusion length injection level dependence as previously reported in our proton irradiation work. Further work is necessary to verify this explanation.

Two cells of each C13 series group were irradiated with $3 \times 10^{14}$ e/cm$^2$ (1 MeV) and were allowed to recover at 60$^{o}$C. The changes in $I_{sc}$ for the C13 cells, so irradiated, are shown in Figures 15 through 24. These figures indicate that all the $I_{sc}$ values of all cells were degraded to the 30 to 36 ma range. The times necessary for half recovery to occur at 60$^{o}$C varied between 50 and 100 hours. The ultimate recovered $I_{sc}$ values were in the 47 to 55 ma range. It is clearly evident from the data in Figures 15 through 24 that the cells with lower donor concentrations at the junction, i.e., lower lithium donor concentrations, are degraded less during irradiation and also recover to higher $I_{sc}$ values. Examples of such behavior are cells C13B4 (Figure 16), C13D4 (Figure 18), and C13H4 (Figure 22). These cells have donor concentrations of $2.4 \times 10^{14}$/cm$^3$ at the junction. The lithium donor concentration is approximately $10^{14}$/cm$^3$ in the above three cells. The $I_{sc}$ values of these three cells were degraded to about 36 ma during irradiation and recovered to approximately 55 ma during recovery. Conversely, the results for cells C13E5, C13F5, and C13H5 represent the opposite extremes in the range of lithium donor concentrations. These cells were degraded in $I_{sc}$ to about 30 ma by irradiation and recovered to approximately 47 ma. The effect of the various lithium diffusions in the

matrix of Table IV is mainly to establish a particular range and distribution of lithium donor concentrations at the junction. There is no evidence to indicate any effect of lithium diffusion time and temperature other than that of determining the lithium distribution near the junction.

Three cells of each C13 series group were irradiated with $3x10^{15}$ e/cm$^2$ (1 MeV) and were allowed to recover at 60$^0$C. The most pronounced changes during recovery occur to the short circuit current. The open circuit voltages of nearly all cells in the C13 series were about 0.6V. After a $3x10^{15}$ e/cm$^2$ irradiation, the $V_{oc}$ was reduced to about 0.45 in all cases. Very little recovery is subsequently observed in this parameter. The changes in $I_{sc}$ for cells of the C13 series are shown in Figures 25 through 34. Several general observations can be made about these cells. With a few exceptions, the $3x10^{15}$ e/cm$^2$ irradiation reduced the $I_{sc}$ to 20 to 25 ma. In most cases, the time necessary for the $I_{sc}$ to reach the half recovery point was 100 to 200 hours at 60$^0$C. This time is somewhat longer than what was previously found in similar cells. Except for cells with low lithium concentration, most cells ultimately recover to $I_{sc}$ values of 35 to 38 ma. The most important factor in the extent of the recovery is the lithium concentration at the junction rather than the diffusion schedule. As previously noted, the shorter, low temperature diffusions produce the more consistent results. The donor concentration of each cell irradiated is noted on the respective figures. The lithium concentration at the junction can be determined by subtracting the approximate phosphorus concentration ($1.5x10^{14}$/cm$^3$) from the donor concentration.

B. Heliotek Cells

All Heliotek cells received for evaluation during the past quarter were fabricated from either floating zone or Lopex silicon and,

therefore, had lower oxygen concentrations than quartz crucible cells. There are two different experimental variables represented in these Heliotek cells. Two groups (H1A and H4A) were diffused at lower temperatures: 325°C lithium diffusion for 480 minutes. Group H2A was lithium diffused at 425°C for 90 minutes with a 120 minute redistribution cycle. This latter diffusion schedule has been used extensively in the past and can be regarded as a control. The capacitance measurements results from the H1A group, shown in Table II, indicate that very little or no lithium reached the junction. For this reason the irradiation recovery results shown in Figures 35 and 36 are very poor. Although recovery is observed after $3x10^{14}$ e/cm$^2$, the higher fluence of $3x10^{15}$ e/cm$^2$ exhausts the lithium and no recovery is observed. These results are in direct conflict with those for group H4A which had an identical history. The H4A cells had approximately $5x10^{14}$ lithium donors/cm$^3$ at the junction, and exhibited satisfactory recovery as shown in Figures 37 and 38. The recovered $I_{sc}$ values of the H4A cell would probably have been higher if the before irradiation $I_{sc}$ values had been higher than 46 ma. This condition is not necessarily a result of the lithium diffusion, as other cells with similar lithium concentrations have initial $I_{sc}$ values in excess of 60 ma. Despite this difficulty, the data indicated that cells of group H4A recover to $I_{sc}$ values of 40 ma after a fluence of $3x10^{15}$ e/cm$^2$. This is considerably higher than a comparable irradiated n/p solar cell.

The irradiation recovery results for the cells of group H2A are shown in Table II. As mentioned previously, this lithium diffusion schedule has previously been used many times to produce superior lithium cells. The results in Figures 39 and 40 confirm that such cells exhibit excellent $I_{sc}$ values when recovered from an irradiation. The results in the case of the $3x10^{15}$ e/cm$^2$ fluence are particularly interesting in that the recovered

$I_{sc}$ reached a value of 44 ma. The fact that these cells were fabricated from Lopex silicon as opposed to float zone silicon is not considered significant.

The remaining groups of Heliotek cells represent a series of experiments to determine the effectiveness of area coverage during the application of lithium diffusion source material to the back of the cell. Groups H5A1, H5A2, and H5A3, respectively, received 100%, 80%, and 50% back surface area coverage. The results of this experiment are very interesting for comparative analysis. The first point of interest is the measured lithium concentrations at the junctions of the various groups as seen in Table II. The cells with 100% coverage (H5A1) have approximately $6x10^{14}$ lithium donors/$cm^2$ at the junction. The groups which received less coverage (H5A2, H5A3) had roughly half the above lithium concentration. The results indicate quite clearly that decreased area coverage reduces the concentration of lithium at the junction. The relationship does not appear to be linear, since the cells with 80% coverage (H5A2) have lithium concentrations nearly as low as those with 50% (H5A3). It can be concluded that incomplete area coverage with the lithium source material significantly reduces the lithium concentration at the junction. It is also of interest to compare the cells of these groups to cells of other groups. The cells of group H2A were made with the same material and diffusion schedule, but presumably no control on area coverage. The data in Table II indicate the H2A cells had much lower lithium concentrations than any of the cells in H5 groups. It must be concluded that there are other unknown factors which extend strong influences on the concentration of lithium reaching the junction. One possible factor could be the chemical activity of the lithium in the source material.

The effects of various lithium source area coverages on radiation

response can be seen in Figures 41 through 46. The initial $I_{sc}$ values of these cells are all relatively low. The values average approximately 51 ma. This parameter influences radiation recovery behavior because the maximum recovered parameters can only approach and not exceed their initial values. Despite this problem, the cells of group H5A1 (100% coverage) recovered to a maximum $I_{sc}$ of 50 ma after an irradiation of $3x10^{14}$ e/cm and 39 ma after $3x10^{15}e/cm^2$. In both cases these values are above those of similarly irradiated conventional n/p solar cells. The H5A1 cells, irradiated with $3x10^{14}$ $e/cm^2$, show some redegradation of $I_{sc}$ after the maximum was reached. The radiation recovery of cells of group H5A2 (80% coverage) was not drastically altered by the reduced coverage. The cells of group H5A2 which were irradiated with $3x10^{14}$ $e/cm^3$ recovered to $I_{sc}$ values of 45 ma. The recovery probably would have exceeded the above value if the initial $I_{sc}$ value had been greater than 46 ma. The $3x10^{15}$ $e/cm^2$ irradiation of H5A2 cells allowed the $I_{sc}$ recovery to reach 39 ma after irradiation. This value is equal to that achieved in the group having 100% coverage (H5A1). This result is difficult to explain considering the lower lithium concentration and the studies of D.L. Kendall at Texas Instruments which indicated very little lateral spreading of lithium during diffusion. The results for cells of H5A3 (50% coverage) show comparable performance after $3x10^{14}$ $e/cm^2$ (Table II). In the case of the higher electron fluence on the H5A3 cell, the recovered $I_{sc}$ values were significantly reduced. It appears that incomplete coverage with diffusion source material does not reduce recovery behavior, except in extreme cases.

C. Electron Energy Dependence of Lithium-Doped Cell Recovery

Most of the studies of radiation behavior of lithium-doped cells have been done with a 1 MeV electron environment. With the exception of a

few studies with reactor neutrons and one early study with protons, there is a complete lack of much of the data needed to accurately predict behavior in space. One area in which more data are desirable is response of these cells to electrons with energies greater than 1 MeV. Through the courtesy of Dr. J. A. Naber of Gulf Radiation Technology, several lithium-doped cells were irradiated with 28 MeV electrons.

Because of the necessary delays between the irradiation at the Gulf facilities and analysis at TRW, cells made from quartz crucible grown silicon were selected because of their slow recovery rate at room temperature. This allowed the cells to be mailed to TRW before any post-irradiation recovery occurred. The cells used in this experiment were from the C11D series, manufactured by Centralab. These cells are considered to be typical of good lithium-doped cells and adequate 1 MeV electron data had previously been obtained. Cells were irradiated with $3x10^{14}$ and $3x10^{15}$ $e/cm^2$. The $I_{sc}$ recovered at $60^oC$ to 46 and 31 ma respectively for the two fluences (Figure 47). The degraded and recovered $I_{sc}$ values are shown in Figure 48 as a function of electron fluence. The previously accumulated 1 MeV data are also shown and typical 1 and 28 MeV data for a 10 ohm-cm n/p solar cell are also shown as dashed lines. The critical fluence, defined as that necessary to degrade a cell $I_{sc}$ to 19 $ma/cm^2$, is shown as a dotted line. It has been observed that all solar cells are degraded by penetrating radiation at a rate of about 6.5 $ma/cm^2$ under tungsten illumination for each decade of fluence added. It is apparent that the initially degraded $I_{sc}$ values of the lithium-doped cells decrease at a much smaller rate. In this case, the lower rate is probably due to annealing of defects which occurs during the irradiation. The curious effect of longer half recovery times with greater fluences may be an artifact of low degradation

rate. The dashed line on Figure 47 indicates that the half recovery time might have been much shorter if the degradation had occurred at the normal rate of 6.5 ma/cm$^2$- decade. After the 60$^0$C recovery, the $I_{sc}$ of the lithium-doped cells declines 13 ma per decade of fluence. The important point in Figure 48 is that, while at 1 MeV the lithium cells are slightly superior to the conventional n/p cell, at 28 MeV the lithium cell will withstand over 10 times the fluence before being degraded to the same $I_{sc}$ value of a similarly irradiated conventional cell.

The critical fluence levels were determined from the data in Figure 48 and used to plot Figure 49 for comparative study. In Figure 49 , the reciprocal of the critical fluence is plotted as of function of incident electron energy using previous TRW data for conventional p/n and n/p cells for reference. The upper dashed line represents the lithium-doped cells as irradiated. The lower dashed line represents the effective critical fluence values of the lithium cell after recovery. Since lower reciprocal fluences mean greater radiation hardness, it can be seen that, in higher energy electron environments, the lithium-doped cell provides a major increase in radiation resistance.

D. Incremental Irradiation

The space applications for lithium-doped solar cells involve electron fluences which are accumulated at extremely low rates. Although conventional n/p solar cell degradation is not influenced by rate effects, there are reasons to believe that the behavior of lithium-doped solar cells could be influenced differently when irradiated at widely varied rates. It is not practical to operate a particle accelerator at the necessary low flux for the required long periods of time. A long, low flux irradiation of lithium-doped solar cells is equivalent to a large number of

infinitesimally short irradiations separated by similar length recovery periods. Although this condition is equally difficult to produce, it can be approximated by a large number of short irradiations with intermediate recovery periods.

Although an incremental irradiation, as proposed above, may not give results equal to a long,low flux irradiation, any similarities or differences in results, as compared to those of a single fast irradiation, are evidence for or against the use of single irradiation techniques as an accelerated real time space environment test. To evaluate this technique, lithium-doped solar cells from group C13A were irradiated incrementally. Each of the ten increments of fluence was a $3x10^{13}$ e/cm$^2$ irradiation. A recovery period between increments of about seven days at 60$^o$C would be adequate for maximum recovery to occur; however, the limitations of time allowed only an average of 4 days at 60$^o$C for recovery intervals, and in some cases only 2 days at 60$^o$C were available between irradiations. The data for this study are presented in Figure 50. In addition to the incremental irradiation data, the figure contains the comparable data for a single fast irradiation of cells C13A-5 and -6. It can be seen from Figure 50 that the short circuit currents of cells C13A-7 and -8 recovered to at least 90% of their pre-irradiation value after each increment. After a total of 10 increments of irradiation, a fluence of $3x10^{14}$ e/cm$^2$ was accumulated. The final recovery period raised the $I_{sc}$ values of cells C13A-7 and -8 to 51.5 and 52.6 ma. Cells C13A-5 and -6 had $I_{sc}$ values of 53.0 and 54.0 ma after recovery from a single fast irradiation of the same fluence. Although the cells receiving the incremental irradiations showed slightly lower $I_{sc}$ values (after final recovery) than the single irradiation cell, the difference is not considered to be as large as normal differences

between individual cells.

The single irradiation cells had been stored several thousand hours at 60°C and had reached maximum recovery. If the incremental recovery periods had been longer or if the final recovery was extended, higher $I_{sc}$ values may have been reached. Considering the small $I_{sc}$ differences observed, the effect of long, low flux irradiations on cell output, as evidenced by incremental irradiations, is not significantly different from short, high flux irradiations. These cells will be discussed further in the solar simulator measurements section.

## E. Solar Simulator Measurements

The response of solar cells is such that the spectral nature of a light source, in addition to the intensity, greatly influences the electrical output. It is desirable to make all solar cell measurements under the illumination of an acceptable solar simulator light source. Because of the expense and inconvenience of operating such a source, the changes caused by fast particle irradiation of solar cells are often observed under tungsten illumination. In the irradiation studies of lithium-doped solar cells, most measurements previously reported were made under 100 mw/cm$^2$ 2800°K tungsten illumination. Such measurements are satisfactory for comparative studies of radiation hardness if the spectral responses do not differ greatly between cells over the course of irradiation and recovery. The tungsten light measurements indicate that the design of lithium-doped solar cells has been optimized to the extent that they merit consideration for spacecraft use; however, the spacecraft designer needs solar cell data in terms of 140 mw/cm$^2$ solar simulator illumination. For this reason several recovered cells of various groups and irradiations were evaluated under simulator illumination.

These measurements were made by Heliotek with an X25 solar simulator. The cell temperatures were 28°C. The data from these measurements are tabulated in Table V. The simulator data include $I_{sc}$, $V_{oc}$, and $P_{max}$. Data for maximum power of irradiated commercial 10 ohm-cm n/p solar cells as reported by Cherry and Statler are included in the table for comparative purposes.[9] All of the data are normalized for 1x2 cm cell areas. Cell temperatures for the Cherry and Statler data were 26°C and, therefore, a 1.2% decrease should be applied to their $P_{max}$ values when comparing them to those measured at 28°C.

At fluences of $3x10^{14}$ 1 MeV e/cm$^2$ cells C13A-5 and -6 have $P_{max}$ values greater than those of the commercial cells. Cells C13A-7 and -8 received the same fluence incrementally, but have significantly lower $P_{max}$ and $V_{oc}$ values than the commercial cells. The lower power output of cells C13A-7 and -8 was due to a decrease in curve factor in addition to the greater $V_{oc}$ decrease. Further work is necessary to determine if these changes were induced by the incremental irradiations.

At the higher electron fluences of $3x10^{15}$ 1 MeV e/cm$^2$, however, many of the lithium-doped cells have equal or inferior power output to comparably irradiated commercial cells. Cells C11D-3 and -6 and H2A6993 and 6994 had $P_{max}$ values greater than those of the commercial cells. In general this result confirms our previous finding that lithium-doped solar cells manufactured to an optimum design have superior radiation hardness. The data for C13A-2 show a particularly low power output after recovery. Further investigation indicated that this low power condition resulted from a decrease cell curve factor which occurred after maximum recovery. Capacitance measurements on C13A-2 indicated

that the lithium-donor concentration changes associated with recovery were no different from other cells in this group. It was suspected that the change was caused by a series resistance problem related to cell contacts. This cell, along with control samples, has been returned to the manufacturer for further analysis.

## III. KINETICS OF LITHIUM IN IRRADIATED SOLAR CELLS

During the past year, extensive capacitance studies were made on Heliotek and Centralab cells previously evaluated under 1 MeV electron irradiation. By using capacitance-voltage measurement techniques previously discussed in reports of this series, the donor concentration in the n-type base can be determined as a function of distance into the base. These studies can be made before irradiation, after irradiation, and after recovery. In this manner the changes in carrier concentration occurring during irradiation and recovery can be determined. These data can be of use in the construction of physical models of the damage and recovery processes and to provide information for the design of improved solar cells. The basic equations used in the analyses are:

$$N_d = \frac{S\ V\ C^2}{q\ \varepsilon}$$

where: $N_d$ = donor concentration
$V$ = voltage
$C$ = capacitance/unit area
$q$ = electronic charge, and
$\varepsilon$ = dielectric constant

$$W = \frac{\varepsilon}{C}$$

where: $W$ = width of space charge region

The factor S is related to the exponent of the $k=VC^n$ relationship for the cell.

### A. Removal Rates, Low Oxygen Cells

An example of capacitance-voltage measurement results is shown in Figure 51. These data were taken from Heliotek cell H1A-6903. The radiation evaluation of the solar cell parameters of the cell was shown in the previous section where it was noted that the cells of group H1A recovered from an irradiation of $3\times10^{14}$ e/cm$^2$, but not from

$3x10^{15}$ e/cm$^2$. The data in Figure 51 indicate the reason for the observed behavior. Previous experience has shown that the carrier removal rate during normal recovery must exceed that during the irradiation. Since the silicon used in these cells had a resistivity of greater than 20 ohm-cm, it can be assumed that a concentration of approximately $2x10^{14}$/cm$^3$ phosphorus donors was present. The data in Figure 51 show that the total donor concentration in the base of the cell exceeds the phosphorus concentration by only a small amount. Since the removal rate during recovery is lower than that during irradiation, the recovery process was limited by the lack of lithium. This low lithium concentration caused the recovery process to proceed at a very low rate (half time 200 hours) after an electron fluence of $3x10^{14}$ e/cm$^2$. This lack of lithium became more apparent when cells of this type failed to show any recovery after an irradiation of $3x10^{15}$ e/cm$^2$. The low lithium concentration in this group is a result of manufacturing factors other than the 480 min lithium diffusion at 325$^{o}$C, because this schedule is used with good results in other cases.

The results of a similar analysis on cell H4A-7595 are shown in Figure 52. Cells of the H4A group received the same lithium diffusion as those of H1A. The radiation evaluation reported in the cell evaluation section indicated excellent recovery, but low short circuit currents as received. The data in Figure 52 are a marked contrast to those in Figure 51. The lithium concentrations before irradiation of cell H3A-7595 are several times those of the phosphorus (approximately $2x10^{14}$/cm$^3$). The removal rates during both irradiation and recovery were between 0.1 and 0.2 cm$^{-1}$. These quantities apparently are enough to allow full recovery after exposure to electron fluences of $3x10^{15}$ e/cm$^2$.

The data shown in Figure 53 are from a similar capacitance study of cell H2A-6993, which was irradiated with $3x10^{15}$ e/cm$^2$. The H2A group was

fabricated from Lopex silicon. Since the recovery characteristics of these cells were outstanding, the lithium distributions are of particular interest. The before irradiation lithium concentrations are somewhat lower than those of cell H4A-7595, but much higher than those of cell H1A-6903. The removal rate during the irradiation of $3x10^{15}$ e/cm$^2$ is roughly equal to that of cell H4A-7595, but the removal rate during recovery is significantly higher (0.2 to 0.3 cm$^{-1}$). It would appear that higher removal rates during recovery promote more complete recovery, and that for low oxygen cells (FZ, Lopex) the removal during a normal recovery should exceed that during irradiation by at least 1.5 times.

The next group of cells studied were from the H5A series. These cells were made by Heliotek to investigate the effect upon cells caused by incomplete coverage with lithium diffusion source material. All of these cells were made with Lopex silicon. Cell H5A1-7164 data are shown in Figure 54. This cell received 100% diffusion source coverage. The data for a cell which received only 50% coverage (H53-7169) are shown in Figure 55. Cell H5A1-7164 exhibited excellent recovery after irradiation with $3x10^{15}$ e/cm$^2$. The data in Figure 54 indicate that the lithium concentrations are several times greater than those of the phosphorus (approximately $2x10^{14}$/cm$^3$), and the removal rate during recovery is roughly three times that observed during irradiation. The data in Figure 55, for the cell with a 50% area diffusion source, indicate significantly lower lithium concentrations compared to the 100% coverage cell, but the lithium concentration is still much greater than that of the phosphorus. The removal rates for both cells are plotted in Figure 56. The first point of interest is that the removal rates during irradiation are nearly identical for both cells. A significant difference is observed in the removal rate during recovery. In the cell with 100%

diffusion source coverage,the removal rates during recovery exceed those during irradiation by at least three times. In contrast, in the cell with 50% coverage, the rate during recovery is only 25% larger than that observed during irradiation. It was previously observed that the $I_{SC}$ recovered to only 30 ma in cell H5A3-7169(50%). Since the $I_{SC}$ recovery of cell H5A1-7164 (100%) was excellent, the data in Figure 56 support the previous observation that a condition necessary for good recovery of cell parameters in low oxygen cells is that the recovery removal rate must exceed that during irradiation by 1.5 or more times.

A capacitance study was done on Centralab cells from the C11C group. These cells were fabricated from Lopex silicon, and showed excellent initial and recovery characteristics. The phosphorus concentration of the silicon was approximately $6x10^{13}/cm^3$. The before irradiation data shown in Figure 57 indicate a lower donor concentration compared to other cells which have exhibited good recovery. Cell C11C-7 and C11C-3 were irradiated with $3x10^{14}$ and $3x10^{15}$ $e/cm^2$ electrons respectively. It can be seen after recovery from an irradiation of $3x10^{15}$ $e/cm^2$ that the donor concentration is approaching the phosphorus concentration. This indicates near exhaustion of lithium donors. The removal rates, during irradiation and recovery, were calculated for these cells and are plotted in Figure 58 as a function of barrier width. The removal rates are of interest in this case because of the two different electron fluences used. Although there was some difference in lithium concentration between the two cells, the differences in removal can be considered to be largely due to differences in fluence. One might expect that the removal rates would be relatively independent of electron fluence, if the behavior is based upon discrete solid state

reactions in which one atomistic species reacts stoichiometrically with another. The fact that,during satisfactory recoveries from similar fluences,the removal rate during recovery has been observed to vary between 1.5 to 4 times that observed during irradiation indicates that no discrete quantity of lithium appears to react with the radiation products.

The data in Figure 58 indicate that in C11C cells the removal rates during irradiation and recovery from a $3x10^{14}$ e/cm$^2$ fluence are significantly greater than those resulting from a $3x10^{15}$ e/cm$^2$ fluence. Not only are the removal rates lower with the higher fluence, but the ratio of the rates during recovery and irradiation decrease from 4 to 2 when the fluence is increased from $3x10^{14}$ to $3x10^{15}$ e/cm$^2$. It is obvious that the models which we have proposed in the past must be modified to account for the widely varying removal rates which we have observed in cells made from low oxygen silicon.

B. Removal Rates, High Oxygen Cells

Our analysis of lithium distributions also included cells made from silicon grown from quartz crucibles. Our previous studies have shown that the very small removal rate observed during irradiation of this type of cell can be explained by the production Si-A centers (oxygen-vacancy pairs) with an introduction rate of about 0.2 cm$^{-1}$. The two cells presented in Figure 59 had previously exhibited excellent recovery when irradiated with $3x10^{15}$ e/cm$^2$. The data in Figure 59 indicate a very low removal rate during irradiation of both cells. This is because the concentrations of Si-A centers produced are barely detectable in these donor concentrations. Much larger changes in donor concentration occur during the recovery phase. The removal rates during recovery are plotted as a function of barrier width in Figure 60. To further study possible relationships, the removal rate

data from Figure 60 are replotted in Figure 61 as a function of lithium concentration present at the particular barrier width position after irradiation. In addition, similar data from a cell (H14-4921) analyzed during our previous year's work are added to Figure 61. It can be seen from the data of the three cells shown in Figure 61 that the removal rate during recovery is directly proportional to the concentration of lithium present at that point in the cell.

Since our previous work has shown that Si-A centers are introduced uniformly throughout the active n-type area of the cell, it must be concluded that the amount of lithium which reacts with the radiation-produced defects is not directly related to the concentration of Si-A centers. The earlier proposed models involved the reaction of one or possibly two lithium donor atoms with a Si-A center. It is clear that this model will require considerable modification. It is possible that precipitation rather than ion pairing may be the basis of the recovery reaction. It has already been proposed that the O-V vacancy pair is the nucleation site for the precipitation of lithium in silicon and germanium.[10] In such a process the quantity of lithium donors reacting during recovery would be independent of the number of radiation defects, and the ratio of lithium donors reacting during recovery to the number of radiation defects could vary considerably.

The study was extended to include cells irradiated with low electron fluences. Cells of the C13 group were used in this work. The differences between these cells and those of C11A and D are not considered significant enough to introduce other variables in addition to electron fluence and lithium donor concentration. Plots of donor concentration versus barrier width for cells C13A-6 and C13E-4 are shown in Figures 62 and 63. As noted, the difference before and after irradiation was not detectable. The change

in lithium donor concentration during recovery as a function of barrier width was tabulated from the data in Figures 62 and 63. These data are plotted versus the original lithium donor concentration in Figure 64. There appears to be a linear relationship between the loss of lithium donors and the original lithium concentration, similar to that observed in Figure 61. The constant relating of the two variables, however, is 0.35 in the case of the $3x10^{14}$ e/cm$^2$ fluence. For a $3x10^{15}$ e/cm$^2$ fluence, the data in Figure 61 indicate a value of 0.75 for this dimensionless ratio.

Study of the ratio between initial lithium donor concentration and the change in lithium donor concentration during recovery can provide an important insight into the nature processes. The above ratio or recovery ratio can be normalized to the electron fluence to provide some measure of the number of lithium donors which react with each radiation defect. The results are as follows:

at $3x10^{14}$ e/cm$^2$

$$\frac{\Delta[Li]_R/[Li]_o}{\Phi} = \frac{0.35}{3x10^{14}} = 11.7x10^{-16}$$

at $3x10^{15}$ e/cm$^2$

$$= \frac{0.75}{3x10^{15}} = 2.34x10^{-16}$$

The above figures indicate that 5 times as many lithium donors react per defect during recovery from a $3x10^{14}$ e/cm$^2$ fluence as from a $3x10^{15}$ e/cm$^2$ fluence. Although fewer lithium donors react per radiation defect, at the higher fluences, our other work indicates that the fractional recovery, as measured by short circuit recovery, is the same at both fluences. Since the same state of recovery can be reached, despite a much lower

number of lithium donors per radiation defect, the physical model must reflect a wide possible variation in the number of lithium donors reacting during the recovery phase.

An additional study was made to determine the relationship between minority carrier diffusion length changes and lithium donor concentration changes during recovery. Using previously described capacitance versus voltage methods, the donor concentrations at various distances into the n-type base were determined before and after irradiation and during the recovery process. The results of such a study of cell C13A-1 are shown in Figure 65. After 600 hours the recovery process, as indicated by the $I_{SC}$, is nearly complete and the changes in donor concentration have diminished. To allow a more systematic study of the lithium donor changes, the data for specific barrier widths were reduced to lithium donor concentration and normalized to that present immediately after an irradiation with $3x10^{15}$ e/cm$^2$. These data are shown as a function of time after irradiation, at three different points in the cell in Figure 66.

The mathematical form of the change in lithium concentration with time could indicate information regarding the nature of the recovery process. The data in Figure 66 are plotted in semilog form to detect any relationship between the logarithum of the lithium concentration and the time elapsed. Such relationships may indicate first order chemical kinetics or some aspects of the precipitation of a second phase. The data in Figure 66 indicate that the lithium concentration decreases in a nearly straight line form until half of the lithium donors have reacted. The rate of reaction appears to slow to zero as the lithium concentration approaches about 25% of its original value. A similar analysis was made on cell C13D-1 after an irradiation of $3x10^{15}$ e/cm$^2$. These results are shown in Figures 67 and 68. Although

the lithium concentrations in cell C13D-1 are higher than those in cell C13A-1, the results are very similar. The linearity of lithium decrease during the first portion of the decline could not be confirmed because the reaction proceeded more rapidly.

It was established earlier than an irradiation of $3x10^{15}$ e/cm$^2$ produced a uniform concentration of defects (probably Si-A centers) of $6x10^{14}$ in a lithium-doped cell made from quartz crucible silicon. Our recent work has indicated that such an irradiation will cause at least 70% of lithium present to react with the defects. Using cell C13D-1 as an example, this means that near the zero bias position of the n-type side of the space charge region (2 μm) about $6x10^{14}$ cm$^{-3}$ lithium donors react during the recovery. This amounts to a one-to-one relation between defects and reacting lithium donors. At a distance of 3 μm deeper in the n-type region, about $3x10^{15}$ cm$^{-3}$ lithium donors react during recovery. At this point, the concentration of lithium donors reacting during the recovery period is 5 times that of the radiation defects detected. It would be highly desirable to extend these measurements to deeper areas of the n-type base. After the $3x10^{15}$ e/cm$^2$ irradiation of cell C13D-1, the measured diffusion length of the cell was 4.3 μm. The data in Figure 67 indicate that immediately after the irradiation, the capacitance-voltage measurement investigates the lithium concentration of the entire active portion of the n-type base. During the recovery phase, the measured diffusion length increased to 17.5 μm. The distance is currently beyond the limits of the capacitance technique. If the original concentration of donors before irradiation is found by extrapolation to 17.5 μm, about $2x10^{16}$ cm$^{-3}$ lithium donors are present. If 75% of these react during recovery phase, 50 lithium donor ion cores react for each radiation defect detected. Such behavior is

clearly beyond explanation by models previously proposed.

Minority carrier diffusion length measurements were determined for cells C13A-1 and C13D-1 during the recovery. The concentration of recombination centers is inversely related to the minority carrier lifetime. For this reason, diffusion length measurements of solar cells can easily be reduced to a parameter which reflects the fraction of radiation introduced recombination centers which remain unannealed during the recovery. The parameter is as follows:

$$\frac{\frac{1}{L^2} - \frac{1}{L_o^2}}{\frac{1}{L_r^2} - \frac{1}{L_o^2}}$$

where: $L$ = diffusion length as a function of time

$L_o$ = diffusion length before irradiation

$L_r$ = diffusion length after irradiation

In Figures 66 and 68 the above parameter is plotted versus time after recovery for cells C13A-1 and C13D-1. The form of these recovery curves does not appear to be well defined by the data. It is clear that the time necessary for half recovery, based upon diffusion length measurements, is close to the time at which the original lithium donor concentration decreased by half. While these data do not conclusively prove that the recovery of diffusion length and the reaction of lithium donor are directly related, the fact that they occur in the same time scheme strongly suggests a relationship.

Several observations on the recovery process can be used to construct a model of this process. The observations are as follows:

1. The change in lithium-donor concentration during recovery varies widely and is rarely equal to the recombination center concentration.

2. The change in lithium-donor concentration during recovery is often much greater than recombination center concentration.

3. The change in lithium-donor concentration during recovery is not linear with the fluence of high energy particles.

4. The change in lithium donor concentration during recovery is proportional to the initial lithium donor concentration.

The above facts require the modification of the previously proposed ion pairing model for recovery. The model which appears to be most consistent with the experimental facts is the precipitation of the supersaturated solid solution of lithium in silicon. The role of the radiation-produced recombination centers (i.e., Si-A center, etc.) is to form the nucleation centers upon which the lithium donors can begin the formation of a second phase. Complete precipitation of all lithium donors is prevented by the presence of oxygen which promotes the formation of lithium-oxygen donors.

C. Capacitance Measurements

Early in the study of lithium-doped solar cells it was noted by TRW and RCA that the concentration of lithium donors was not uniform throughout the base of the device. In general, the concentration of lithium donors tends to increase in a somewhat linear manner with increasing distance from the space charge region. These observations were made through capacitance measurements of solar cells, made as a function of voltage. The linear gradient junction has received considerable attention in the device literature. It is well known that in such junctions the product of voltage and third power of the capacitance is a constant. Although many lithium cells approximated this behavior, it was observed that most did not follow it precisely. Some cells deviated to the extent of fourth power behavior.

The distribution of lithium donors near the junction is the result of the approach of a diffusion front. One can derive a relationship

between the concentration of lithium donors and gradient of lithium donors at the junction determined by capacitance measurements. This relationship is shown on Figures 69 and 70 in the form of dashed lines. The long-short dashed line represents the case in which the space charge region expands equally on both edges. The other dashed line represents the case where the space charge region is constrained at one edge. Experimental data from several lithium-doped solar cells made from low oxygen silicon are shown in Figure 69. Similar data are shown in Figure 70 for high oxygen cells. Since the gradient is rarely constant, it was necessary to determine the gradient near the junction. In both figures the experimental data appear to follow the theoretical 2/3 power slope at some position intermediate between the two space charge region conditions.

For the above reasons,any relationship which is drawn between lithium donor concentration and some cell parameters can also be related to the gradient of lithium donors. Since the determination of the gradient requires several capacitance measurements, the averaging effect makes it inherently more accurate than a donor concentration which requires only two capacitance measurements. For this reason better relationships, between device parameters and the gradient, may be possible than with lithium donor concentration.

The data from the high oxygen cells were used to make a plot of the parameter "n" versus the gradient of lithium donor concentration at the junction. The "n" parameter is defined as the exponent in the $k=VC^n$ relationship. These data are shown in Figure 71. It appears that higher "n" parameters are associated with higher gradients. If the "n" value is equal to 3.0, the base region has a linear gradient of lithium donor concentration. IF the "n" value is equal to 4.0, the lithium donor concentration increases in a quadratic or parabolic manner. Examination of the

donor concentration versus barrier width data presented in earlier sections indicates a tendency for cells with high "n" values to show an increasing slope in the vicinity of the junction.

D. Lithium Counterdoped n/p Solar Cells

In this initial effort it was observed that when such lithium counterdoped structures were irradiated, a significant room temperature recovery of minority carrier diffusion length occurred. To realize the full importance of this observation it is necessary to review some basic information. The introduction of lithium into solar cells for the purpose of radiation hardness was basically a modification of the previously existing p/n solar cell. The p/n solar cell was known to be of inferior radiation hardness to the n/p solar cell. When lithium was added to the p/n solar cell in an optimum manner, a finite increase in the hardness of this type of cell was observed. The increased hardness made the lithium doped p/n cell superior to the n/p cell. If the benefit of lithium doping can be applied to the n/p cell, it is reasonable to expect that a similar increase in hardness could be added to the originally superior characteristics of the n/p cell.

Our first attempt to produce a lithium counterdoped device involved wafers of 2 ohm-cm, p-type, floating zone silicon purchased from Wacker Chemical Corp. These wafers were shallow diffused with phosphorus to form a n/p structure. Lithium was then diffused into the device from the back side, using temperatures, times, and techniques identical to those used for p/n cells. Contacts were applied and the minority carrier diffusion lengths were monitored using 1 MeV electrons. Such a diode was irradiated with 1 MeV electrons and allowed to recover at room temperature. These data are shown in Figure 72. It can be seen that when the irradiation was

interrupted at $10^{15}$, $3x10^{15}$ and $10^{16}$ e/cm$^2$, a significant recovery of the diffusion length was observed. A similar series of devices was fabricated from Lopex p-type silicon supplied by Texas Instruments. The degradation and subsequent recovery of these diodes is shown in Figure 73. Minority carrier diffusion lengths were measured on the Lopex-silicon lithium counterdoped n/p diode, which was irradiated with $3x10^{15}$ 1 MeV electrons/cm$^2$. This irradiation reduced the diffusion length of the diode from 77.5 to 39 microns. The diffusion length increased during 500 hours of storage to 64 microns. Comparable diffusion lengths for a similarly irradiated conventional n/p solar cell and lithium-doped p/n solar cell are also shown in the figure. The recovered diffusion length values are deceptively high because the lithium counterdoping raised the p-type base resistivity from 12 ohm-cm to well over 100 ohm-cm. Regardless of the exact resistivity, it was confirmed that the base of the cell was definitely p-type, and hence it can be concluded that the presence of lithium in irradiated p-type silicon promotes reactions which cause the degraded device diffusion length to increase during room temperature storage. Methods for control of degree of counterdoping have been developed. At present, we can foresee no problem which could prevent the incorporation of lithium counterdoping into the conventional n/p solar cell. Lithium counterdoping would require minor changes such as lower resistivity starting material (1 rather than 10 ohm-cm) and possibly low oxygen silicon.

We have processed several wafers of 3 ohm-cm Lopex p-type silicon which have been phosphorus diffused and lithium counterdoped to a resistivity of approximately 10 ohm-cm in the p-type base region. These 1x2 cm structures were processed to include conventional contacts and an antireflection layer by Peter Iles at Centralab. These cells are somewhat

lower in efficiency than conventional n/p cells because of a deeper phosphorus diffusion. A radiation evaluation was done on these cells. Figure 74 illustrates the changes in solar cell parameters which occurred after an irradiation with $3x10^{14}$ e/cm$^2$. The $I_{SC}$ was degraded from 52 to 43 ma during irradiation. After 400 hours at room temperature, the $I_{SC}$ had recovered to 48 ma and was stable. It was also noted that the lithium diffusion had the effect of widening the n-type layer and making a deeper junction. It is possible that some of the changes observed may have been due to lithium reactions in the front layer. Further evaluation is necessary to clarify extent and nature of the changes which we have observed.

## IV. CONCLUSIONS

The evaluation of lithium-doped solar cells did not reveal any major increases in radiation hardness over previously evaluated lithium-doped cells. Several significant improvements were observed during the past year. The before irradiation electrical outputs were improved. All cells of Centralab group C13 had $V_{oc}$ values of approximately 0.60V. This and other improvements make the power outputs of unirradiated lithium-doped solar cells equal to better or better than conventional n/p solar cells. This improvement in starting efficiencies has made it possible for lithium-doped solar cells to recover from lower electron fluences ($3x10^{14}$ e/cm$^2$) to power outputs superior to those of similarly irradiated conventional cells. Cells recovering from $3x10^{15}$ e/cm$^2$ irradiations also had power outputs in excess of similarly irradiated conventional cells; however, the same results were reported at this fluence level during the previous year of this study.

The use of lithium diffusion schedules without a redistribution cycle was extensively studied. It appears that the redistribution step is not necessary to produce superior cells,when low diffusion temperatures are used. Other variables such as boron diffusion source and lithium source area coverage were not significant factors in the cells evaluated. There appears to be a fairly wide range of lithium diffusion schedules which will produce good solar cells. The 8 hour diffusion at 325$^{o}$C appears to have most consistently produced good results, but other factors such as the activity of lithium in the source must be considered.

A study of lithium-doped solar cell behavior was made under 28 MeV electron irradiation. The results indicated that lithium-doped solar cells,

which have recovered from 28 MeV electron irradiations, are effectively degraded at only one tenth the rate of similarly irradiated conventional n/p solar cells.

Cells from groups which exhibited superior recovery, were evaluated in the recovered condition under a solar simulator. The simulator data confirm the conclusions reached by measurements with tungsten illumination.

The theoretical model for the degradation mechanism in lithium-doped solar cells was covered in Part I. of this final report. It was concluded that, in cells made from high oxygen silicon, oxygen-vacancy pairs (i.e., Si-A centers) were formed during the irradiation and degraded the cell diffusion length. In cells made from low oxygen silicon, lithium-vacancy pairs are formed in addition to the oxygen-vacancy pairs. Although some differences have been reported,[11,12] the work of many other investigators has confirmed this damage model.[13-18] The experimental evidence accumulated during the past year indicates that lithium donors do not simply pair with the radiation defects. The data can only be explained by a model in which the radiation defects act as nuclei for the precipitation of the lithium donors in solution in silicon. Complete precipitation is prevented by the presence of oxygen in the silicon which promotes the formation of stable lithium-oxygen donor pairs.[10]

## V. NEW TECHNOLOGY

There is no new technology reported in this paper.

## VI. PAPERS AND PUBLICATIONS GENERATED

### Presented

Title: "Role of Lithium in Irradiated Solar Cells"

Meeting: International Colloquium on Solar Cells, Toulouse, France, 6 July 1970.

Title: "Role of Lithium in Irradiated Solar Cell Behavior"

Meeting: Eight Photovoltaic Specialists Conference, Seattle, Washington, 11 August 1970.

### Submitted

Title: "Role of Lithium in Irradiated Solar Cell Behavior"

Journal: Advanced Energy Conversion

### Published

Title: "Effect of Electron Irradiation on Lithium Doped Silicon"

Journal: International Journal of Physics and Chemistry of Solids Vol. 31, p. 2405, 1970

## REFERENCES


1. V.S. Vavilov, "Radiation Damage in Semiconductors", p. 115, Academic Press, N.Y. (1964).

2. J.J. Wysocki, IEEE Trans. on Nuclear Science NS-13,6,168 (1966).

3. R.G. Downing, et al, TRW Final Report 10971-6002-RO-00, Contract NAS5-10322, 25 May 1968.

4. R.G. Downing, et al, TRW Final Report 10971-6014-RO-00, Contract 952251, 27 May 1969.

5. R.G. Downing, et al, TRW Interim Final Report 13154-6011-RO-00, JPL Contract 952554, 19 June 1970.

6. G.J. Brucker, et al, RCA Final Report AED R-3440, JPL Contract 952249, 21 April 1969.

7. G.J. Brucker, et al, RCA Final Report, Contract NAS5-10239, 8 March 1968.

8. G.J. Brucker, et al, RCA Report AED R-3601F, JPL Contract 952555, 10 July 1970.

9. W.C. Cherry and Richard L. Statler, Preprint X-716-68-204, Goddard Space Flight Center (1968).

10. J.W. Ferman, J. Appl. Phys. 39, 8, 3771 (1968).

11. G.J. Brucker, Phys. Rev. 183 712 (1969).

12. B. Goldstein, Physical Review B, Vol. 2, 4110, 1970.

13. I.V. Kryukova and V.S. Vavilov, Soviet Physics-Semiconductors, 2, 9, 1098 (1969).

14. C.A.J. Ammerlaan, J. Appl. Phys. 39, 6023 (1968).

15. J. Pigneret, Thesis, University of Lyon (1968).

16. D. Bielle-Daspet, et al, Proceedings of the International Colloquium on Solar Cells, Toulouse, Gordon and Breach, New York, 1970.

17. J.R. Carter, Jr., J. Phys. Chem. Solids 31, 2405 (1970).

18. W.H. Kool, et al, J. App. Phys. Vol. 42, 2024 (1971).

| BASE MATERIAL | | | LITHIUM INTRODUCTION | | |
|---|---|---|---|---|---|
| Cell Group | Mat'l Type | Resistivity Ω-cm | Diffusion Schedule °C/Min/Min | Average Li. Conc. @ Junction $Cm^{-3}$ | Remarks |
| C11A | Cruc | 45 | 325/480/0 | $3.1x10^{14}$ | $BCl_3$ Tackon |
| C11B | Cruc | 45 | 325/480/0 | $1.5x10^{14}$ | $BBr_3$ Diffused |
| C11C | Lopex | 75 | 325/480/0 | $1.5x10^{14}$ | $BCl_3$ Tackon |
| C11D | Cruc | 45 | 375/180/0 | $5.1x10^{14}$ | $BCl_3$ Tackon |
| C13A | Cruc | 25 - 40 | 330/240/0 | $2.5 x10^{14}$ | |
| C13B | Cruc | 25 - 40 | 330/360/0 | $1.6 x10^{14}$ | |
| C13C | Cruc | 25 - 40 | 340/180/0 | $3.3 x10^{14}$ | |
| C13D | Cruc | 25 - 40 | 340/420/0 | $2.1 x10^{14}$ | |
| C13E | Cruc | 25 - 40 | 350/300/0 | $3.1 x10^{14}$ | |
| C13F | Cruc | 25 - 40 | 350/300/0 | $3.3 x10^{14}$ | |
| C13G | Cruc | 25 - 40 | 360/180/0 | $5.0 x10^{14}$ | |
| C13H | Cruc | 25 - 40 | 360/420/0 | $2.2 x10^{14}$ | |
| C13I | Cruc | 25 - 40 | 370/240/0 | $4.3 x10^{14}$ | |
| C13J | Cruc | 25 - 40 | 370/360/0 | $1.7 x10^{14}$ | |
| H1A | F.Z. | 20 | 325/480/0 | 0 | (1st set of low temp.) |
| H2A | Lopex | 20 | 425/90/120 | $1.6x10^{14}$ | |
| H4A | F.Z. | 20 | 325/480/0 | $5.2x10^{14}$ | (2nd set of low temp.) |
| H5A1 | Lopex | 20 | 425/90/120 | $5.7x10^{14}$ | 100% Li-REAR |
| H5A2 | Lopex | 20 | 425/90/120 | $3.6x10^{14}$ | 80% Li-REAR |
| H5A3 | Lopex | 20 | 425/90/120 | $3.1x10^{14}$ | 50% Li-REAR |

TABLE I - LITHIUM SOLAR CELL MANUFACTURING PARAMETERS

| Cell Group | Diffusion Schedule °C/Min/Min | $N_{Li}$ $cm^{-3}$ | Average C vs V Slope | Electron Fluence $e/cm^2$, 1 MeV | Initial Level $I_{SC}$, mA | Damaged Level $I_{SC}$, mA | Recovered Level $I_{SC}$, mA | Time (hrs.) to 1/2 Recovery Pt. @ 25°C |
|---|---|---|---|---|---|---|---|---|
| C11C | 325/480/0 | $1.1x10^{14}$ | -.37 | $3x10^{14}$ | 60.3 | 34 | 54 | 50 |
| H1A | 325/480/0 | 0 | -.47 | $3x10^{14}$ | 58 | 33 | 47 | 200 |
| H2A | 425/90/120 | $.4x10^{14}$ | -.32 | $3x10^{14}$ | 51 | 31 | 48 | 5 |
| H4A | 325/480/0 | $4.9x10^{14}$ | -.35 | $3x10^{14}$ | 47 | 27 | 46 | 3 |
| H5A1 | 425/90/120 | $4.2x10^{14}$ | -.34 | $3x10^{14}$ | 52.5 | 27 | 50 | 3 |
| H5A2 | 425/90/120 | $2.8x10^{14}$ | -.34 | $3x10^{14}$ | 46.5 | 27 | 45.5 | 3 |
| H5A3 | 425/90/120 | $2.3x10^{14}$ | -.36 | $3x10^{14}$ | 52.0 | 27 | 47 | 3 1/2 |
| C11C | 325/480/0 | $1.9x10^{14}$ | -.34 | $3x10^{15}$ | 58.5 | 24.3 | 42 | 50 |
| H1A | 325/480/0 | 0 | -.47 | $3x10^{15}$ | 56 | 24 | 25 | |
| H2A | 425/90/120 | $2.7x10^{14}$ | -.30 | $3x10^{15}$ | 56 | 22 | 44 | 15 |
| H4A | 325/480/0 | $5.6x10^{14}$ | -.33 | $3x10^{15}$ | 46 | 19.5 | 40 | 14 |
| H5A1 | 425/90/120 | $8.5x10^{14}$ | -.32 | $3x10^{15}$ | 47.5 | 17.2 | 39 | 50 |
| H5A2 | 425/90/120 | $4.4x10^{14}$ | -.35 | $3x10^{15}$ | 51 | 19 | 39 | 25 |
| H5A3 | 425/90/120 | $3.8x10^{14}$ | -.36 | $3x10^{15}$ | 53. | 18 | 33 | 15-100 |

TABLE II - FLOAT ZONE SILICON CELL RECOVERY CHARACTERISTICS

| Cell Group | Diffusion Schedule $^{o}C$/Hrs. | $N_{Li}$ $cm^{-3}$ | Average C vs V Slope | Electron Fluence $e/cm^2/MeV$ | Initial Level $I_{sc}$, ma | Damaged Level $I_{SC}$, ma | Recovered Level $I_{sc}$, ma |
|---|---|---|---|---|---|---|---|
| C11A | 325/8 | $3.1 \times 10^{14}$ | -.28 | $3 \times 10^{15}$ | 64.2 | 22.0 | 39.5 |
| C11B | 325/8 | $1.5 \times 10^{14}$ | -.32 | $3 \times 10^{15}$ | 53.3 | 24.9 | 36.5 |
| C11D | 375/3 | $5.1 \times 10^{14}$ | -.26 | $3 \times 10^{15}$ | 61.5 | 20.7 | 38.0 |
| C13A | 330/4 | $2.5 \times 10^{14}$ | -.29 | $3 \times 10^{15}$ | 64.5 | 22.5 | 39.0 |
| | | | | $3 \times 10^{14}$ | 64.0 | 33.8 | 53.0 |
| C13B | 330/6 | $1.6 \times 10^{14}$ | -.29 | $3 \times 10^{15}$ | 61.8 | 22.7 | 37.0 |
| | | | | $3 \times 10^{14}$ | 61.8 | 35.7 | 51.8 |
| C13C | 340/3 | $3.3 \times 10^{14}$ | -.28 | $3 \times 10^{15}$ | 64.0 | 21.4 | 39.4 |
| | | | | $3 \times 10^{14}$ | 62.5 | 30.0 | 50.2 |
| C13D | 340/7 | $2.1 \times 10^{14}$ | -.29 | $3 \times 10^{15}$ | 63.8 | 22.5 | 37.8 |
| | | | | $3 \times 10^{14}$ | 65.0 | 35.8 | 50.5 |
| C13E | 350/5 | $3.1 \times 10^{14}$ | -.28 | $3 \times 10^{15}$ | 64.2 | 24.5 | 35.0 |
| | | | | $3 \times 10^{14}$ | 59.0 | 30.1 | 47.2 |
| C13F | 350/5 | $3.3 \times 10^{14}$ | -.28 | $3 \times 10^{15}$ | 61.5 | 22.0 | 36.0 |
| | | | | $3 \times 10^{14}$ | 59.8 | 29.8 | 49.0 |
| C13G | 360/3 | $5.0 \times 10^{14}$ | -.26 | $3 \times 10^{15}$ | 57.0 | 19.5 | 36.5 |
| | | | | $3 \times 10^{14}$ | 61.5 | 29.5 | 48.0 |
| C13H | 360/7 | $2.2 \times 10^{14}$ | -.31 | $3 \times 10^{15}$ | 63.5 | 26.0 | 35.0 |
| | | | | $3 \times 10^{14}$ | 61.5 | 30.0 | 49.0 |
| C13I | 370/4 | $4.3 \times 10^{14}$ | -.29 | $3 \times 10^{15}$ | 61.0 | 23.0 | 35.0 |
| | | | | $3 \times 10^{14}$ | 58.0 | 30.5 | 47.8 |
| C13J | 370/6 | $1.7 \times 10^{14}$ | -.31 | $3 \times 10^{15}$ | 60.5 | 24.0 | 34.0 |
| | | | | $3 \times 10^{14}$ | 62.8 | 37.8 | 47.0 |

TABLE III- CRUCIBLE LITHIUM SOLAR CELL RECOVERY CHARACTERISTICS, $60^{o}C$ RECOVERY

| Time / Temperature | 3 Hrs. | 4 Hrs. | 5 Hrs. | 6 Hrs. | 7 Hrs. |
|---|---|---|---|---|---|
| 330°C | | C13A<br>$4.6 \times 10^{14}$<br>$4.0 \times 10^{14}$<br>$3.4 \times 10^{14}$<br>$k = VC^{3.4}$ | | C13B<br>$4.2 \times 10^{14}$<br>$3.1 \times 10^{14}$<br>$2.4 \times 10^{14}$<br>$k = VC^{3.5}$ | |
| 340°C | C13C<br>$5.2 \times 10^{14}$<br>$4.8 \times 10^{14}$<br>$4.0 \times 10^{14}$<br>$k = VC^{3.6}$ | | | | C13D<br>$5.6 \times 10^{14}$<br>$3.6 \times 10^{14}$<br>$1.8 \times 10^{14}$<br>$k=VC^{3.2}$ , $k = VC^{3.7}$ |
| 350°C | | | C13E<br>$6.2 \times 10^{14}$<br>$4.6 \times 10^{14}$<br>$2.9 \times 10^{14}$<br>$k=VC^{3.5}$, $k=VC^{3.7}$<br>C13F<br>$6.1 \times 10^{14}$<br>$4.8 \times 10^{14}$<br>$3.4 \times 10^{14}$<br>$k=VC^{3.3}$ , $k=VC^{3.7}$ | | |
| 360°C | C13G<br>$7.8 \times 10^{14}$<br>$6.5 \times 10^{14}$<br>$5.1 \times 10^{14}$<br>$k=VC^{3.6}$, $k=VC^{3.7}$ | | | | C13H<br>$5.8 \times 10^{14}$<br>$3.7 \times 10^{14}$<br>$2.1 \times 10^{14}$<br>$k=VC^{2.9}$ , $k=VC^{3.6}$ |
| 370°C | | C13I<br>$7.5 \times 10^{14}$<br>$5.8 \times 10^{14}$<br>$3.2 \times 10^{14}$<br>$k=VC^{3.2}$, $k=VC^{3.8}$ | | C13J<br>$4.4 \times 10^{14}$<br>$3.2 \times 10^{14}$<br>$2.2 \times 10^{14}$<br>$k=VC^{2.9}$ , $k=VC^{3.3}$ | |

Table IV Lithium Diffusion Matrix C13 Series; Maximum, Mean and Minimum Donor Concentration at Junction;Voltage - Capacitance Relationship

TABLE V

SOLAR SIMULATOR MEASUREMENTS

| Cell | Fluence $e/cm^2$ | Energy MeV | Tungsten | | Solar Simulator | | |
|---|---|---|---|---|---|---|---|
| | | | Isc(ma) | Voc(V) | Isc(ma) | Voc(V) | Pm(mw) |
| C11C7 | $3x10^{14}$ | 1 | 55.0 | 0.545 | 66.3 | 0.555 | 24.5 |
| C11C9 | $3x10^{14}$ | 1 | 56.7 | 0.515 | 66.3 | 0.522 | 23.8 |
| C11C3 | $3x10^{15}$ | 1 | 45.1 | 0.445 | 60.1 | 0.461 | 17.0 |
| C11C5 | $3x10^{15}$ | 1 | 45.3 | 0.445 | 59.8 | 0.462 | 17.3 |
| C11D3 | $3x10^{15}$ | 1 | 38.4 | 0.502 | 57.2 | 0.516 | 20.4 |
| C11D6 | $3x10^{15}$ | 1 | 38.1 | 0.505 | 56.7 | 0.518 | 21.2 |
| C11D8 | $3x10^{15}$ | 28 | 32.3 | 0.452 | 50.7 | 0.470 | 15.7 |
| C11D10 | $3x10^{15}$ | 28 | 31.0 | 0.450 | 48.0 | 0.475 | 15.1 |
| C13A1 | $3x10^{15}$ | 1 | 39.2 | 0.460 | 54.5 | 0.475 | 16.0 |
| C13A2 | $3x10^{15}$ | 1 | 39.0 | 0.455 | 46.4 | 0.467 | 6.2 |
| C13A3 | $3x10^{15}$ | 1 | 39.4 | 0.457 | 55.3 | 0.481 | 18.1 |
| C13A5 | $3x10^{14}$ | 1 | 52.1 | 0.540 | 66.0 | 0.560 | 26.2 |
| C13A6 | $3x10^{14}$ | 1 | 53.9 | 0.541 | 64.1 | 0.562 | 25.7 |
| C13A7 | $3x10^{14}$ | 1 | 52.7 | 0.516 | 65.6 | 0.539 | 19.0 |
| C13A8 | $3x10^{14}$ | 1 | 51.2 | 0.516 | 62.4 | 0.538 | 20.4 |
| C13B3 | $3x10^{15}$ | 1 | 39.0 | 0.443 | 55.5 | 0.467 | 15.0 |
| C13C1 | $3x10^{15}$ | 1 | 40.1 | 0.475 | 55.5 | 0.497 | 16.6 |
| H2A6993 | $3x10^{15}$ | 1 | 44.8 | 0.480 | 61.1 | 0.495 | 20.0 |
| H2A6994 | $3x10^{15}$ | 1 | 44.1 | 0.500 | 60.4 | 0.515 | 21.4 |
| H4A7595 | $3x10^{15}$ | 1 | 38.8 | 0.482 | 54.6 | 0.500 | 19.0 |
| H4A7612 | $3x10^{15}$ | 1 | 39.8 | 0.477 | 55.3 | 0.490 | 18.6 |
| Commercial* 10Ω-cm n/p | $3x10^{14}$ | 1 | | | | | 23.0-25.0 |
| Commercial* 10Ω-cm n/p | $3x10^{15}$ | 1 | | | | | 17.4-19.6 |

*W.R. Cherry & R.L. Statler NASA X716-68-204

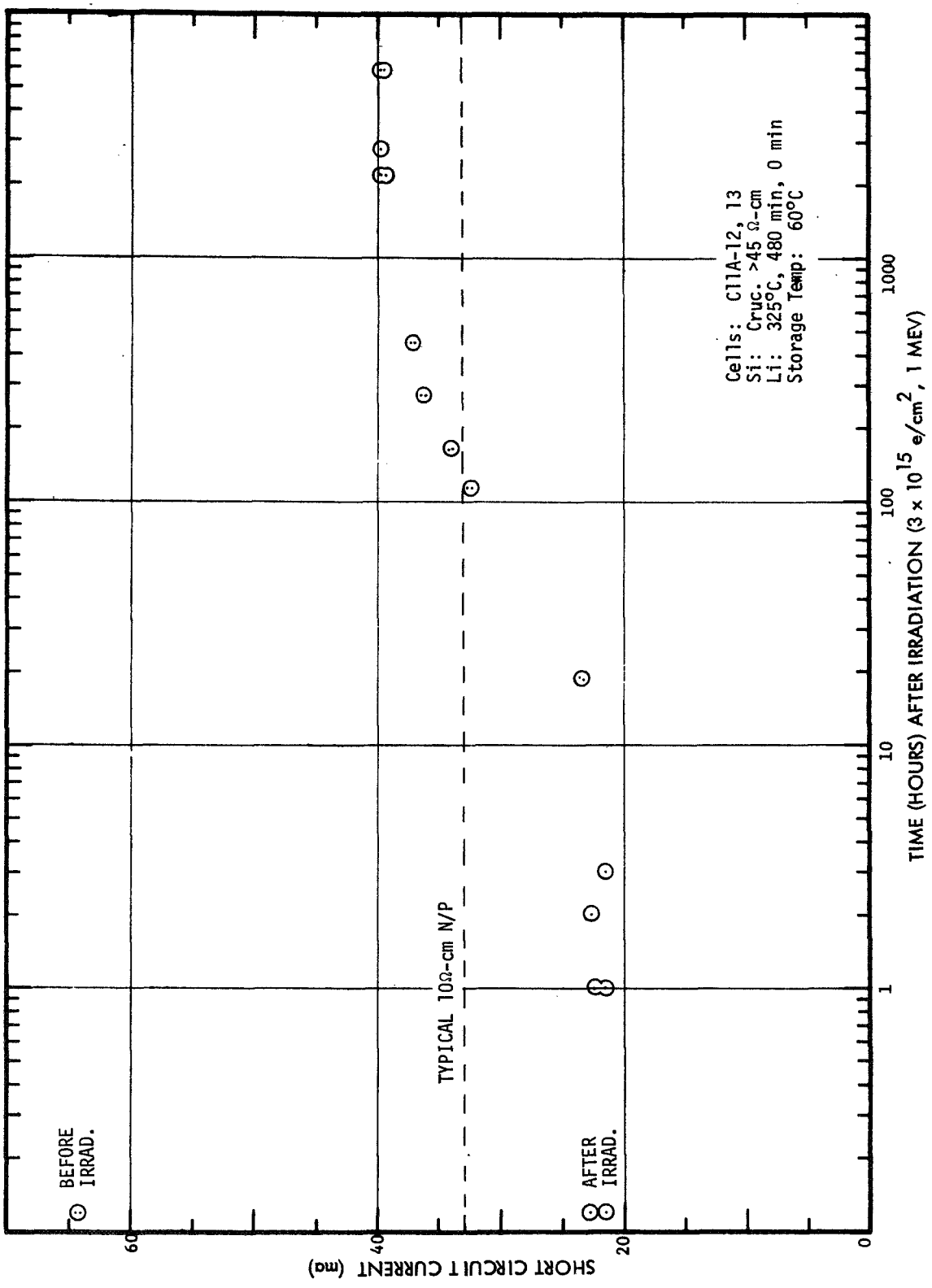


FIGURE 1 - RECOVERY OF GROUP C11A SOLAR CELLS, $3x10^{15}e/cm^2$

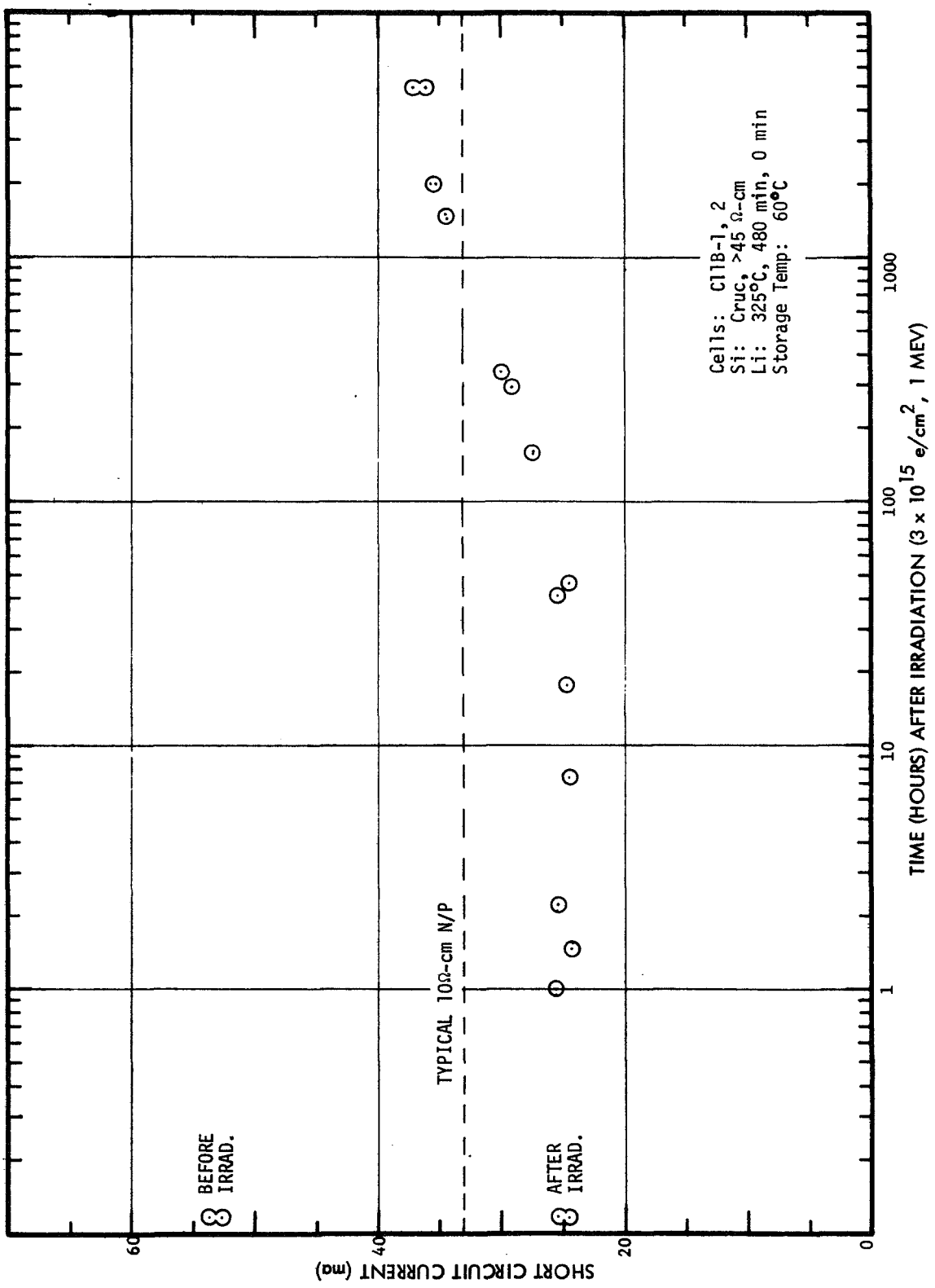


FIGURE 2 - RECOVERY OF GROUP C11B SOLAR CELLS, $3 \times 10^{15} e/cm^2$

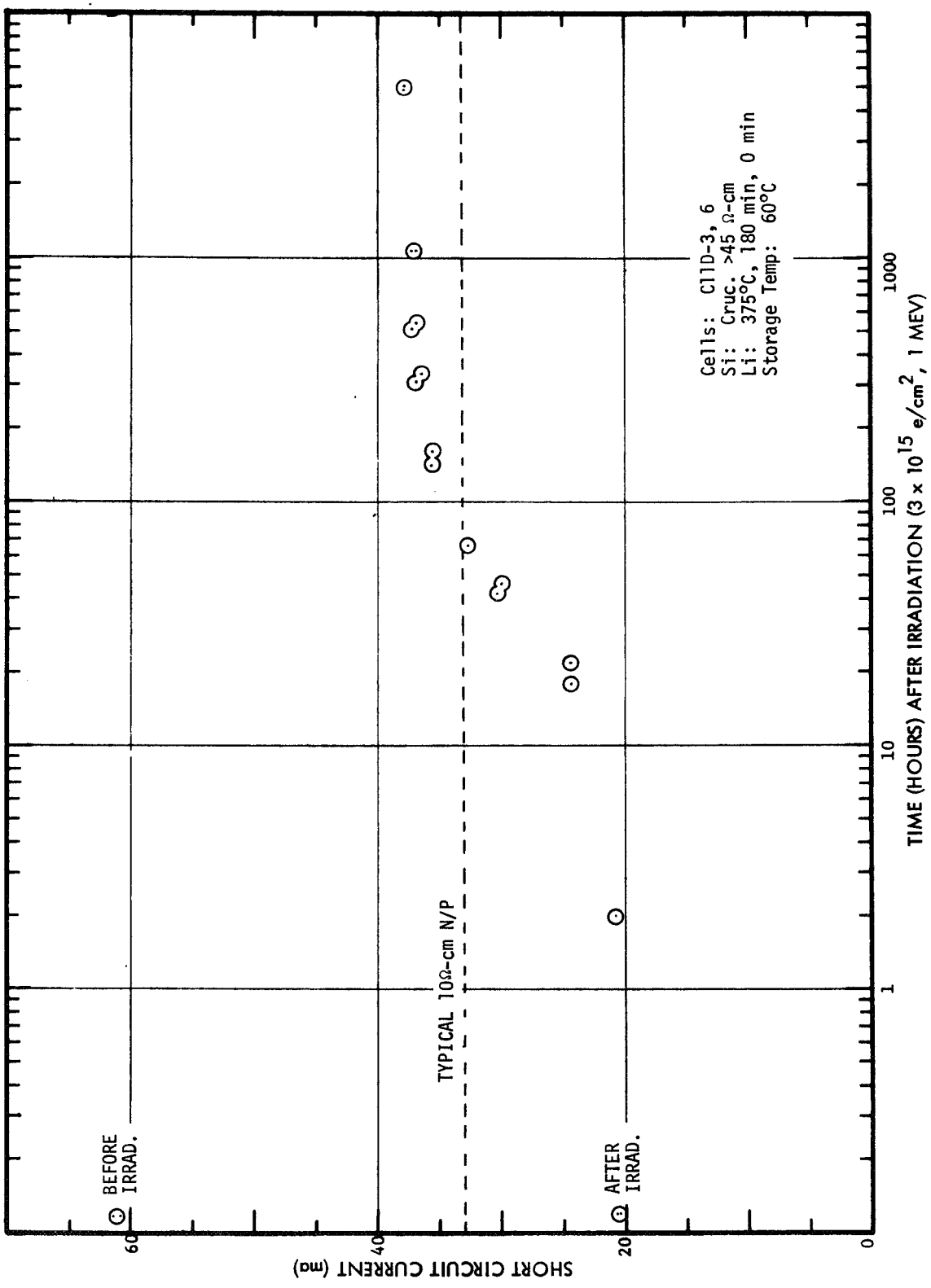


FIGURE 3 - RECOVERY OF GROUP C11D SOLAR CELLS, $3x10^{15}e/cm^2$

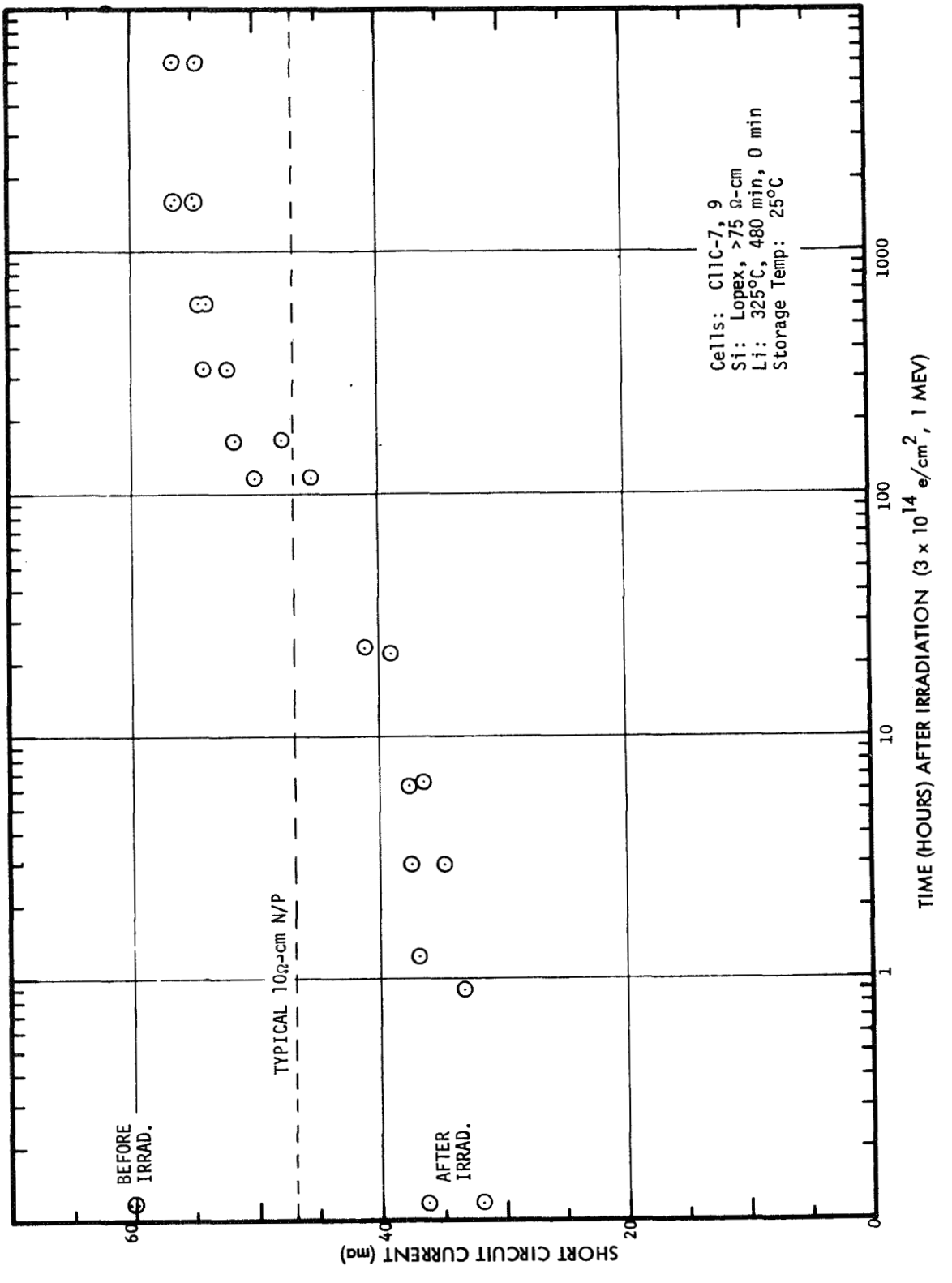


FIGURE 4 - RECOVERY OF GROUP C11C SOLAR CELLS, $3x10^{14}e/cm^2$

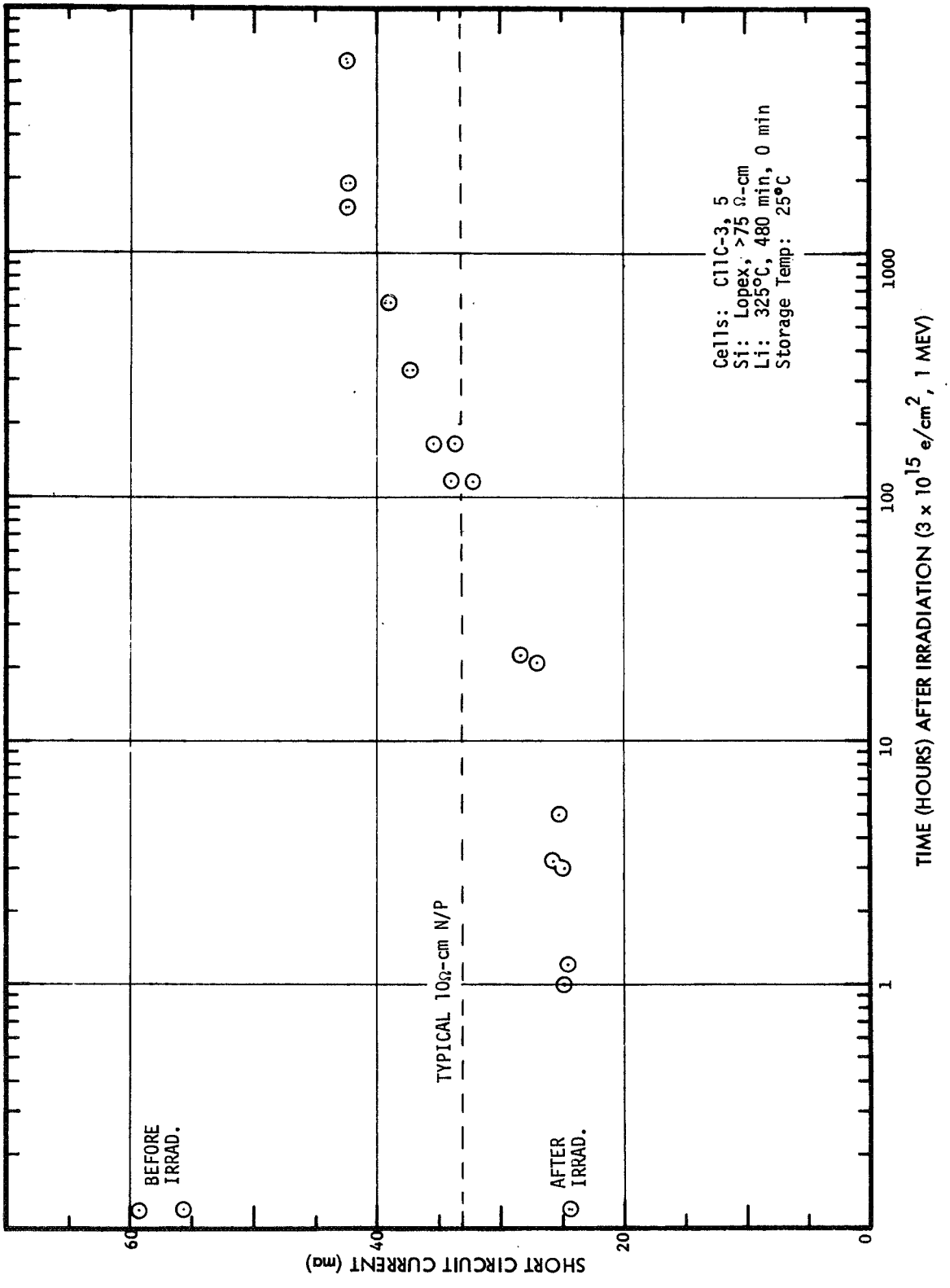


FIGURE 5 - RECOVERY OF GROUP C11C SOLAR CELLS, $3x10^{15}e/cm^2$

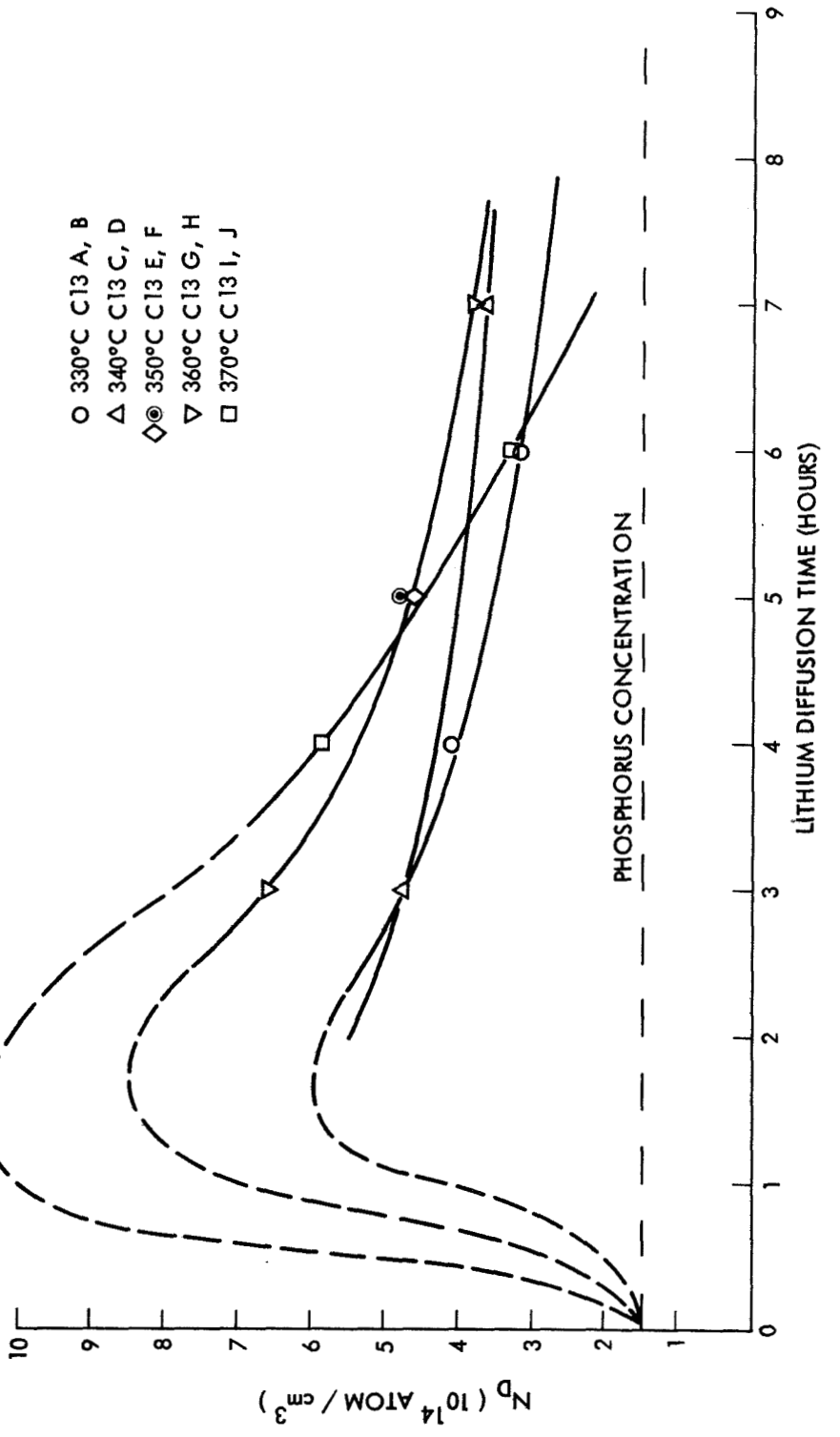


Figure 6. Donor Concentration (vs) Diffusion Time

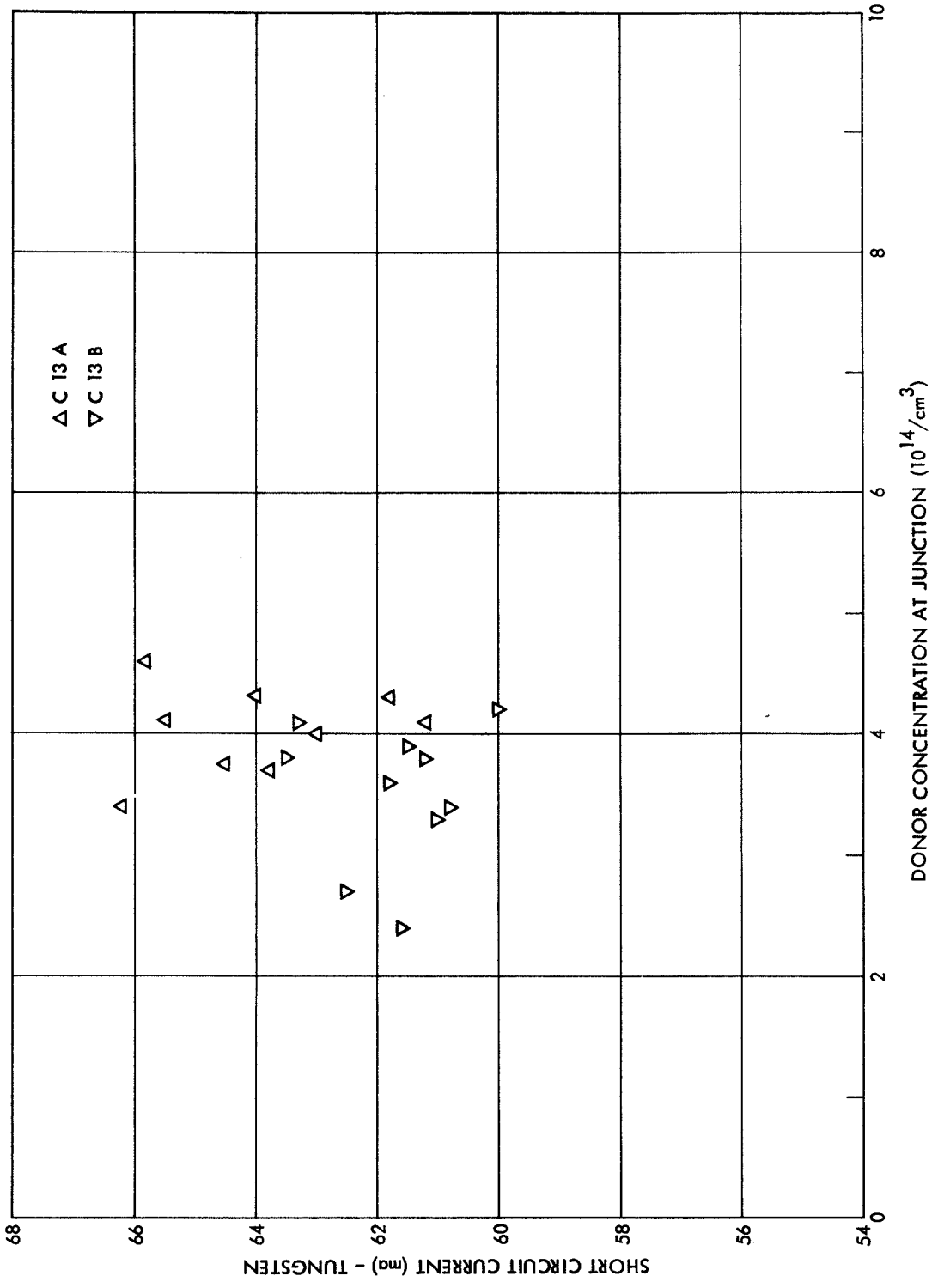


Figure 7. Short Circuit Current (vs) Donor Concentration, C13A, C13B.

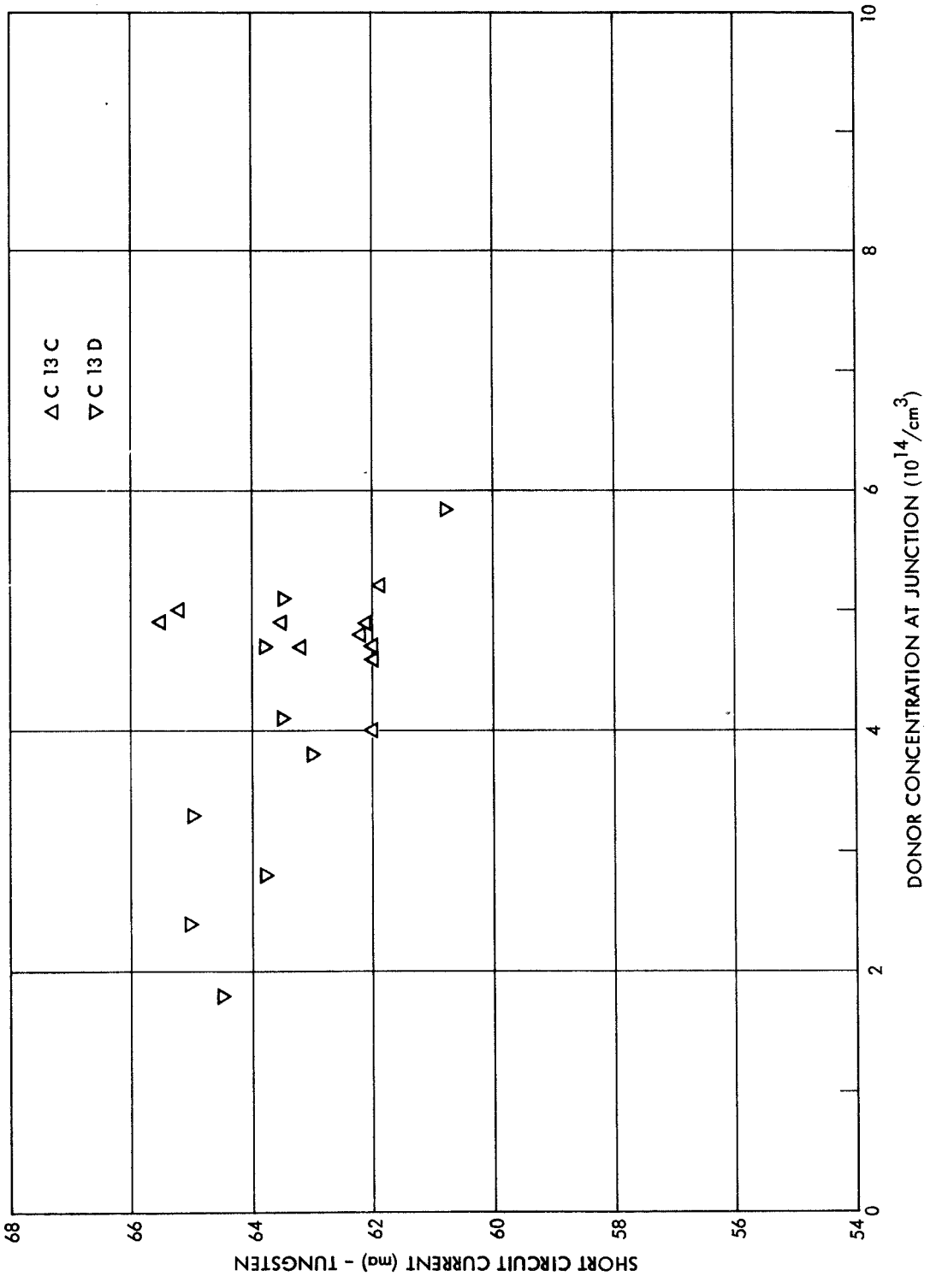


Figure 8. Short Circuit Current (vs) Donor Concentration, C13C, C13D.

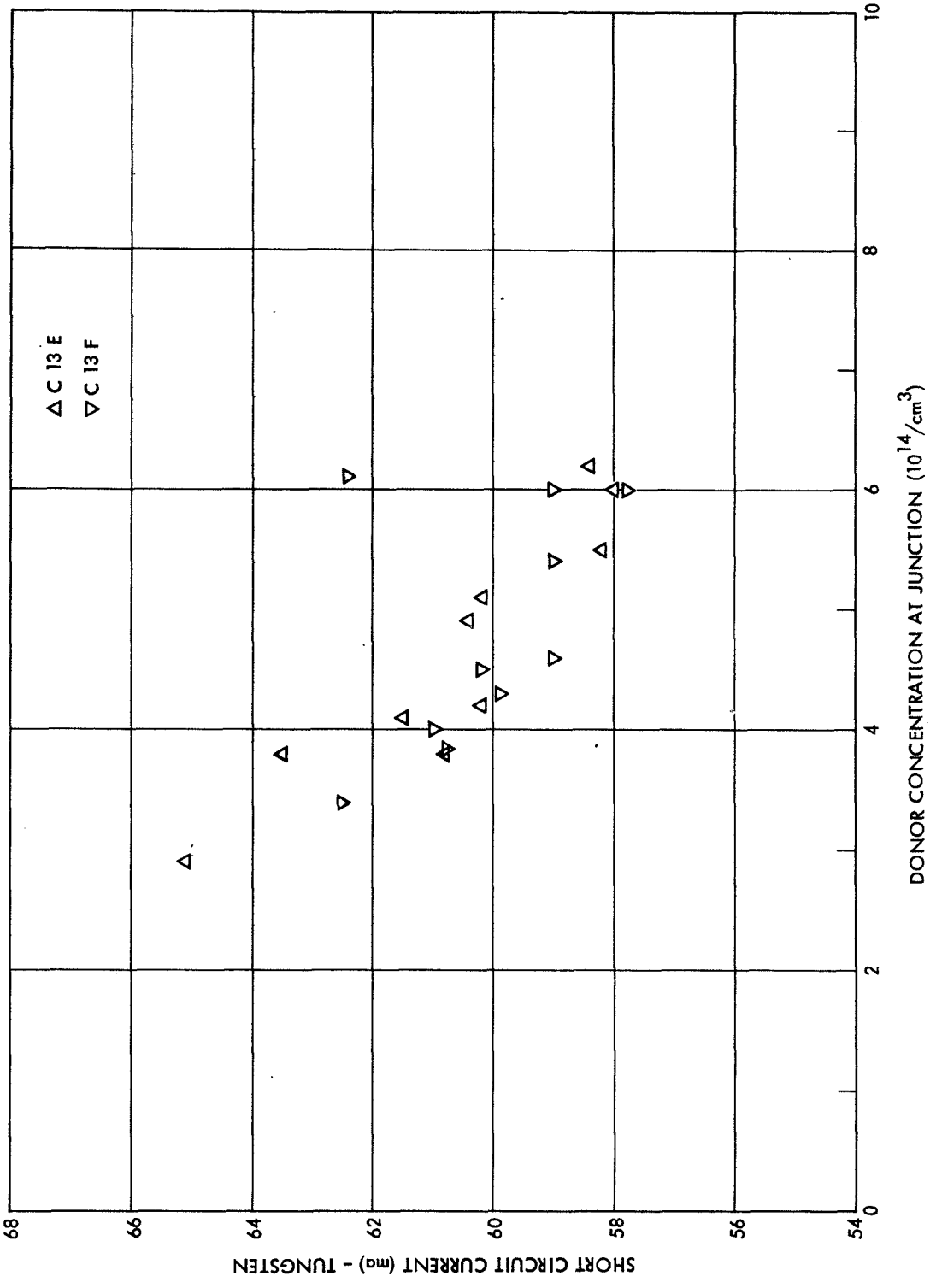


Figure 9. Short Circuit Current (vs) Donor Concentration, C13E, C13F

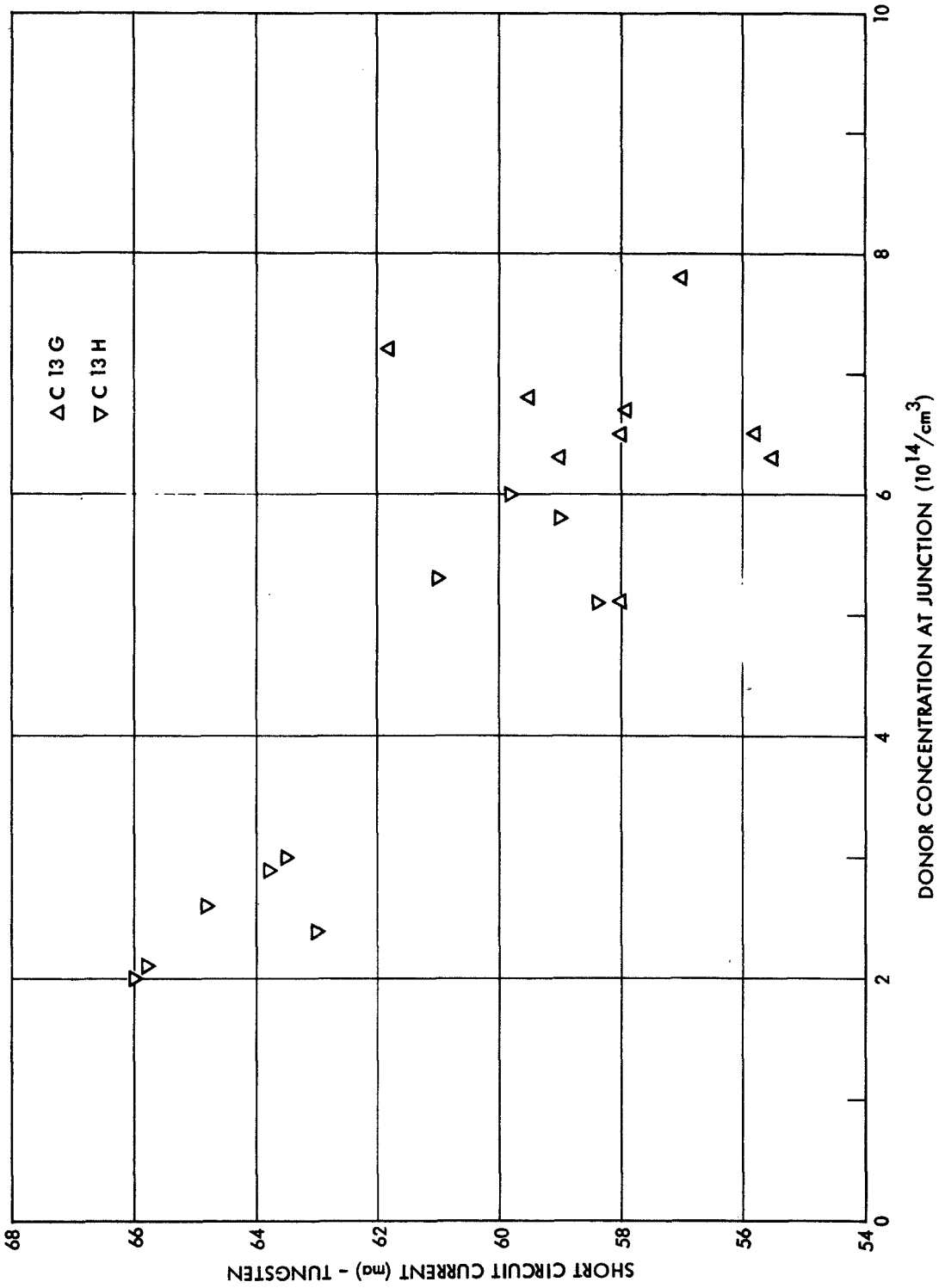


Figure 10. Short Circuit Current (vs) Donor Concentration, C13G, C13H.

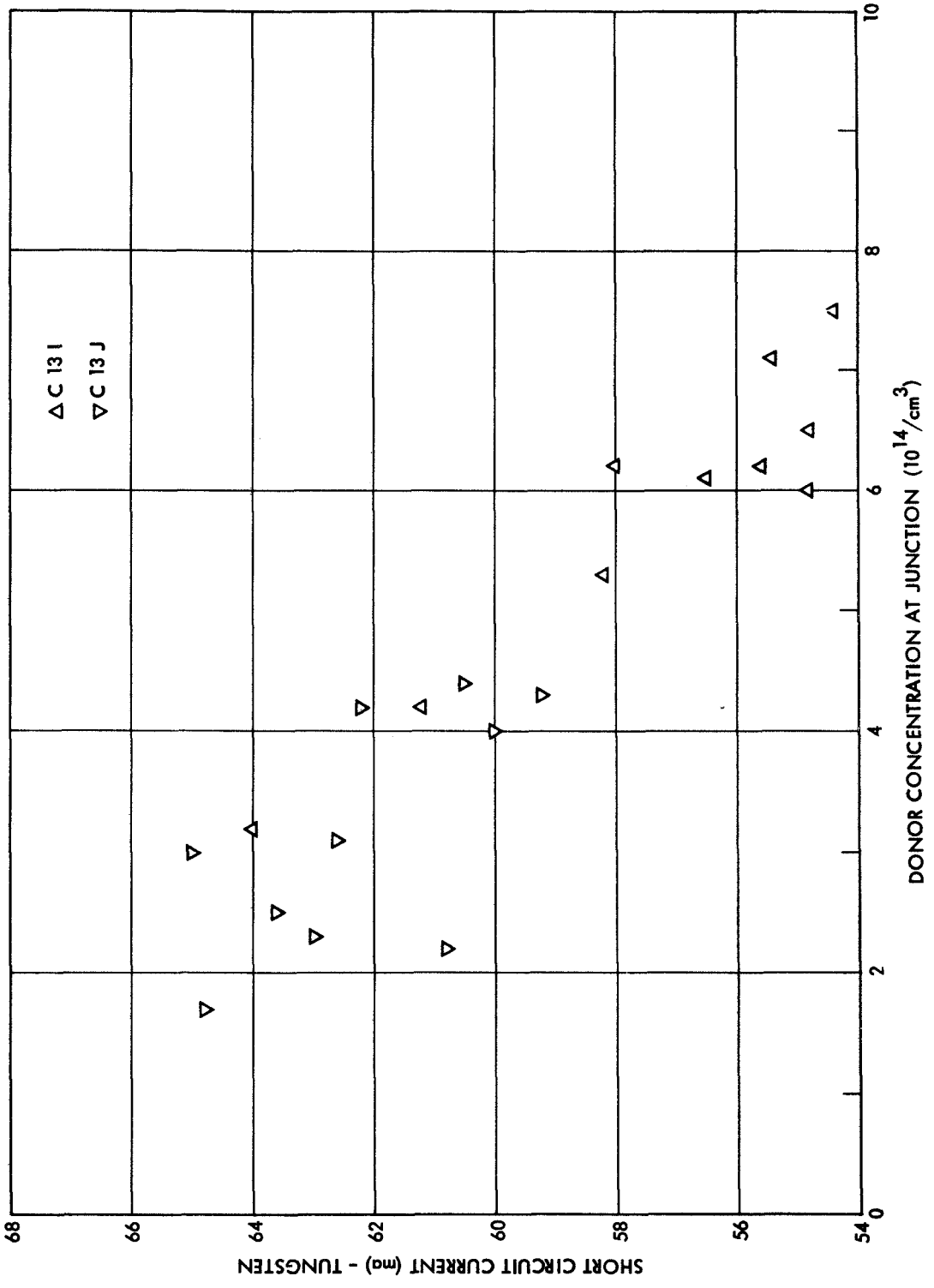


Figure11. Short Circuit Current (vs) Donor Concentration, C13I, C13J.

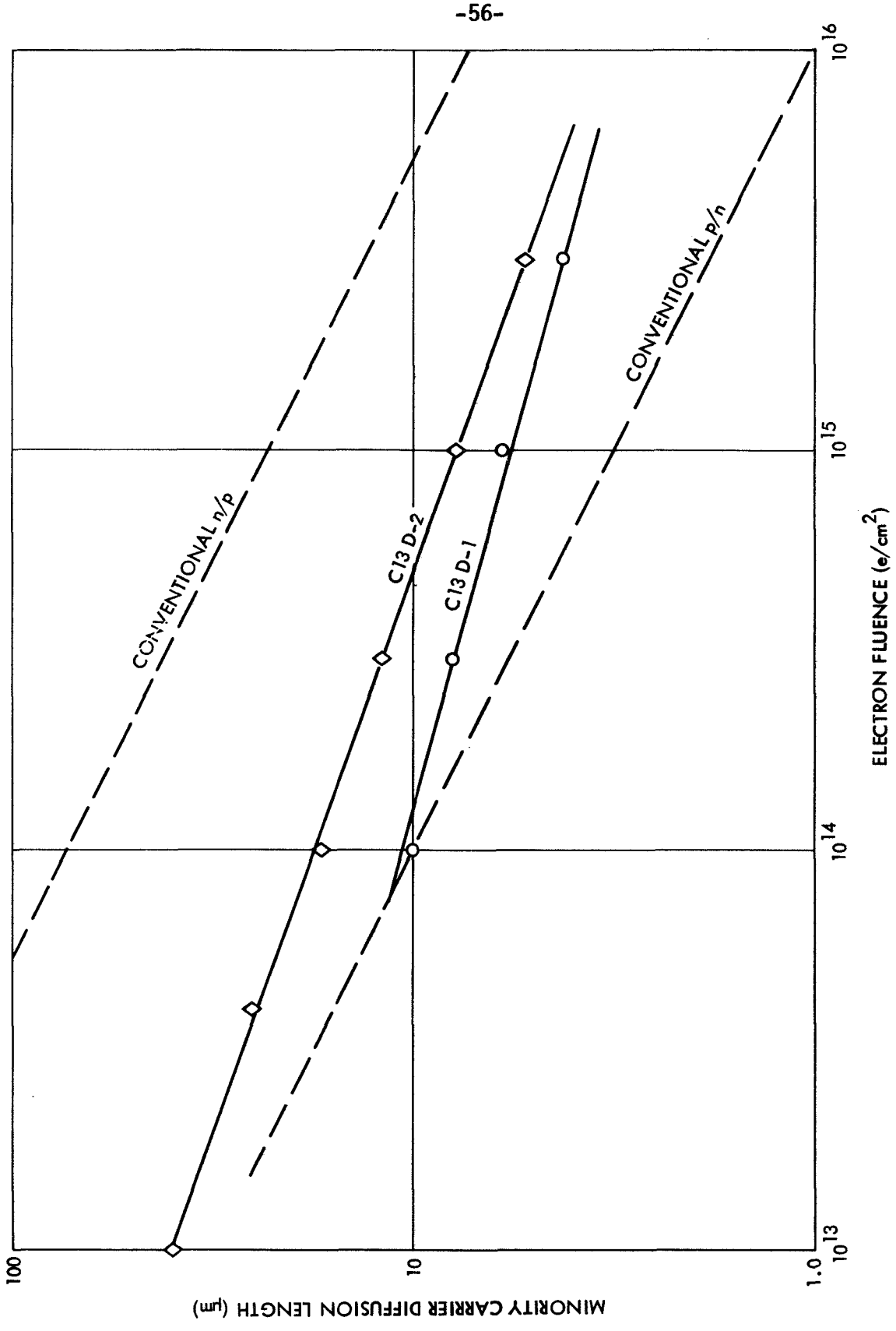


Figure12, Diffusion Length (vs) Electron Fluence

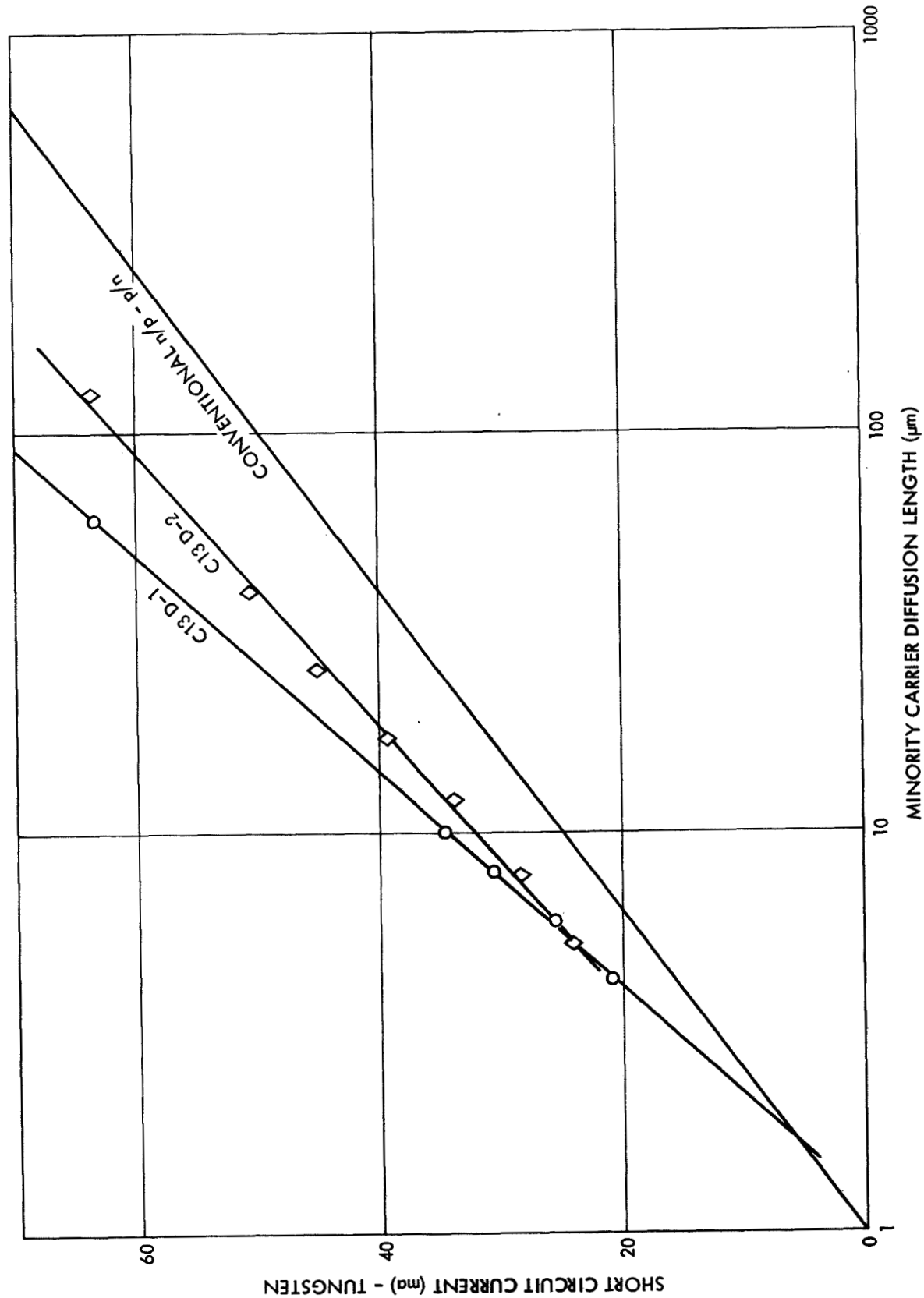


Figure 13. Short Circuit Current (vs) Diffusion Length

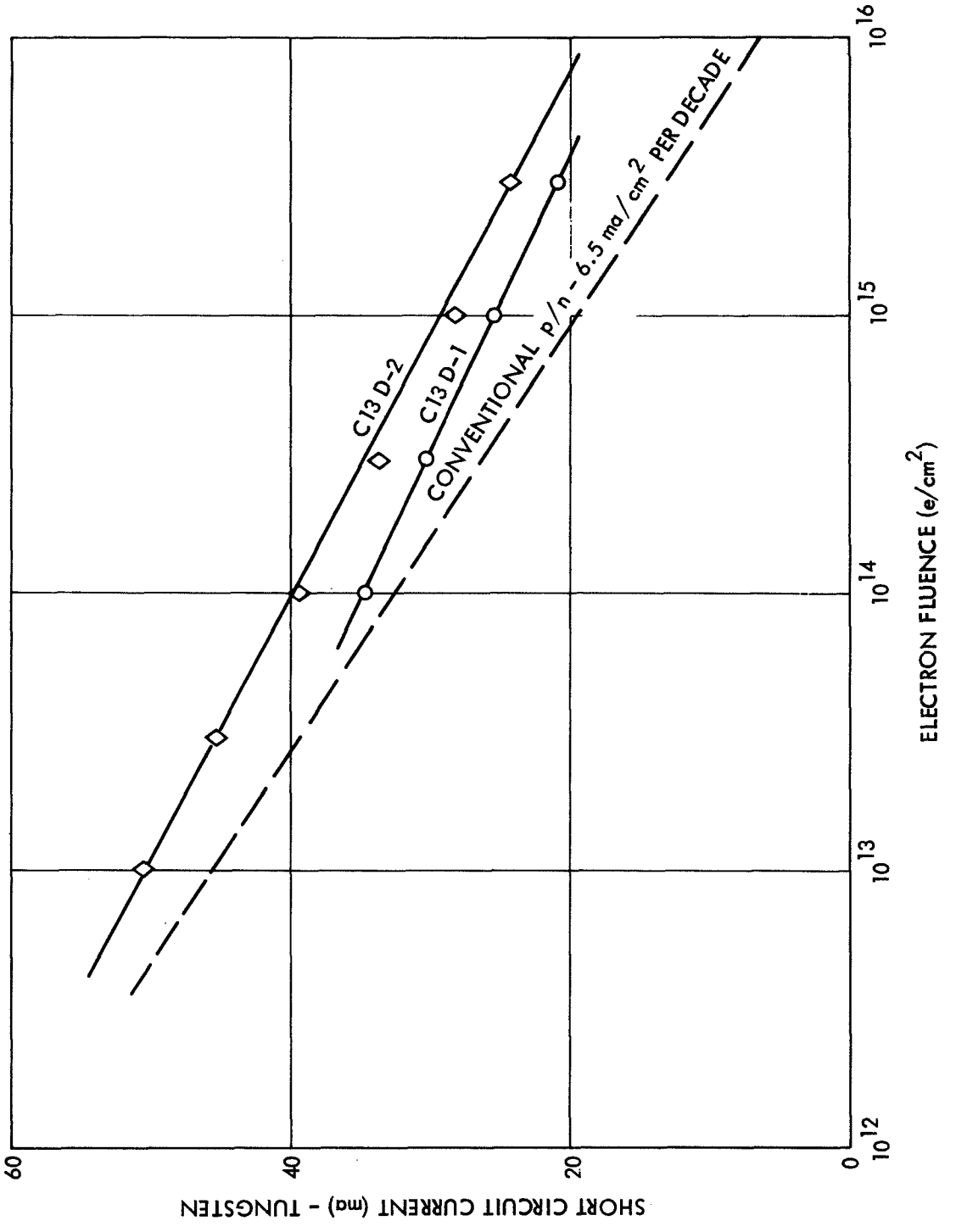


Figure 14. Short Circuit Current (vs) Electron Fluence

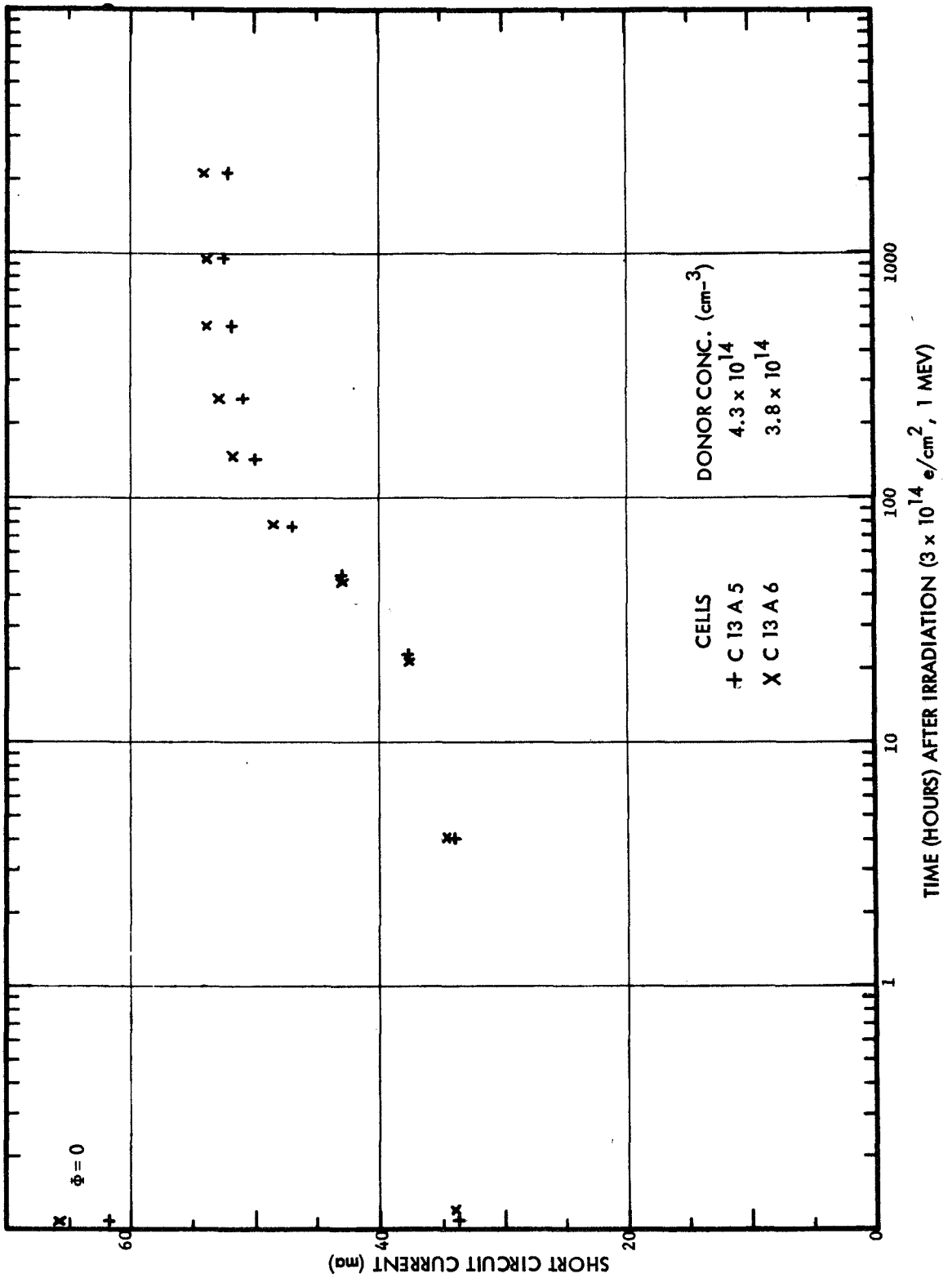


FIGURE 15. SHORT CIRCUIT CURRENT RECOVERY, Q.C. CELLS, AT 60°C

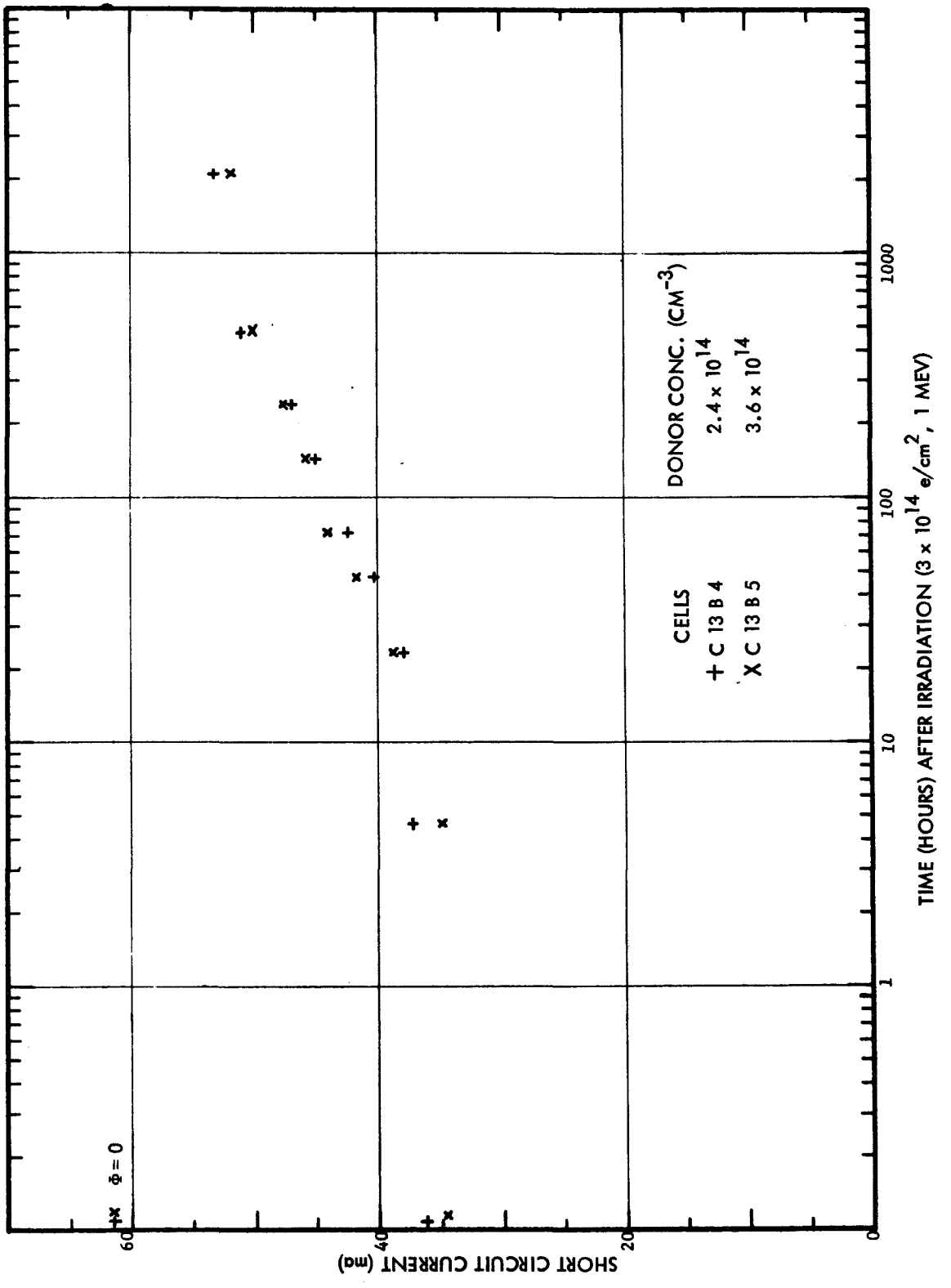


FIGURE 16. SHORT CIRCUIT CURRENT RECOVERY, Q.C. CELLS, AT 60°C

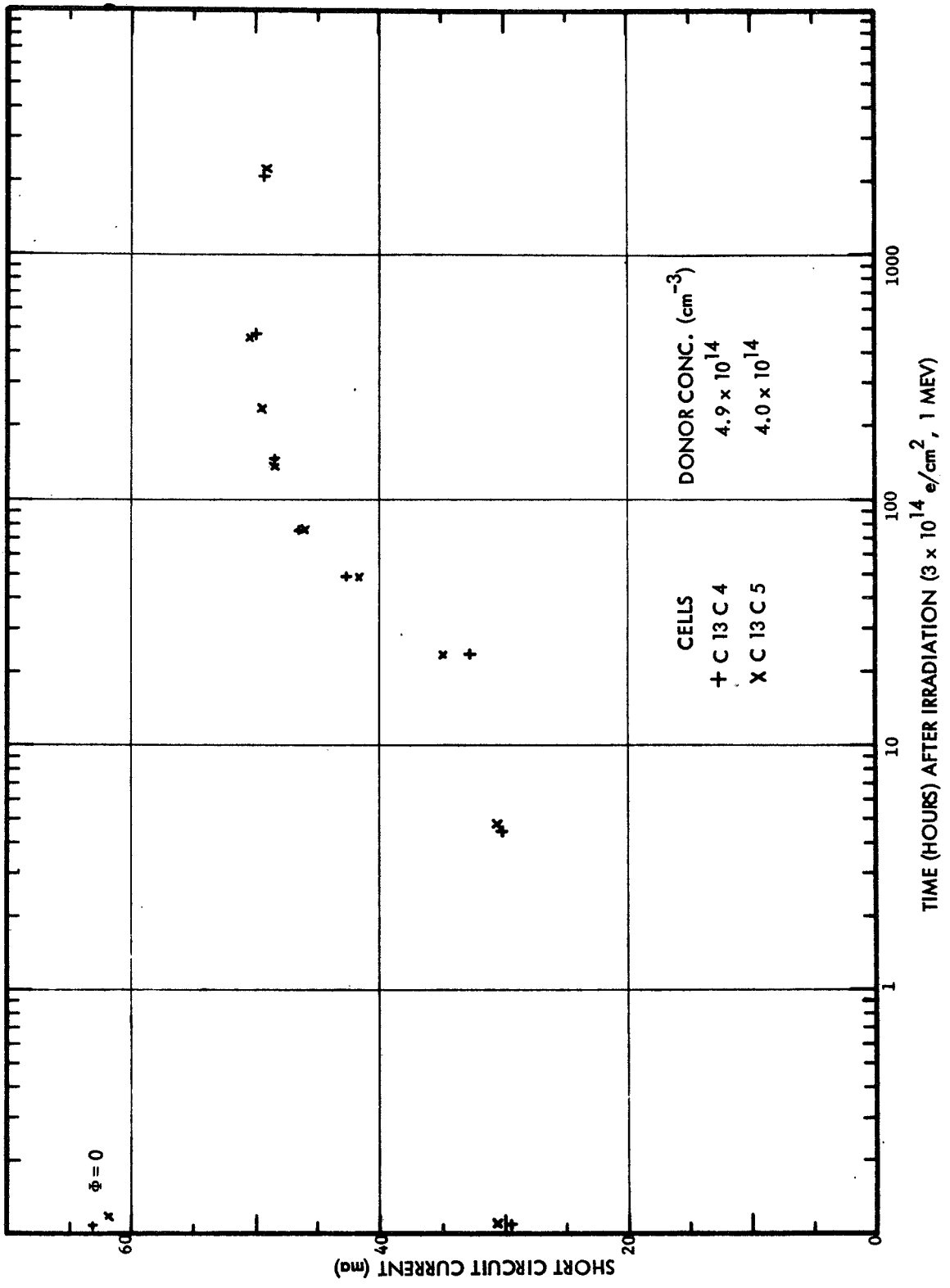


FIGURE 17. SHORT CIRCUIT CURRENT RECOVERY, Q.C. CELLS, AT 60°C

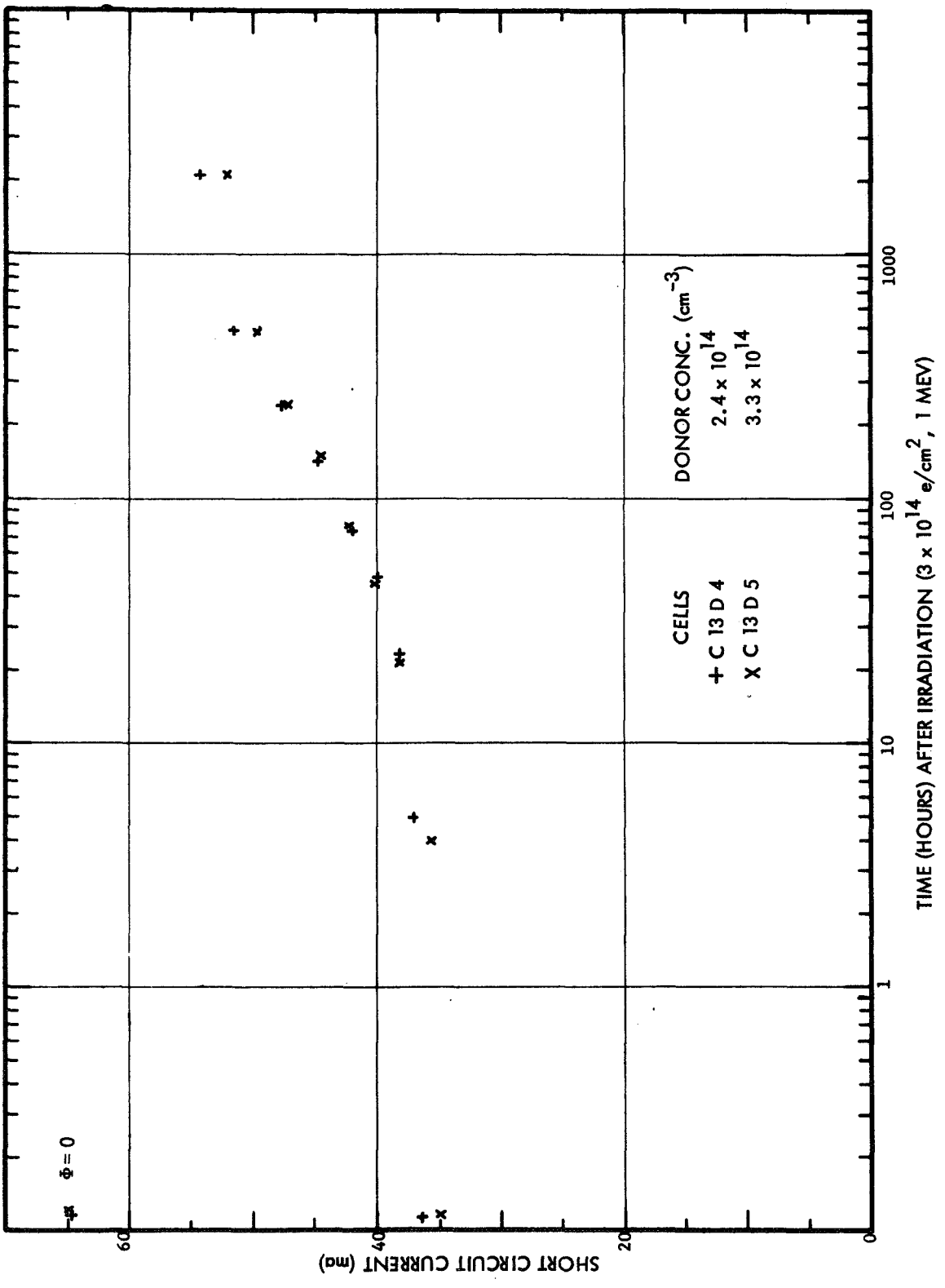


FIGURE 18. SHORT CIRCUIT CURRENT RECOVERY, Q.C. CELLS, AT 60°C

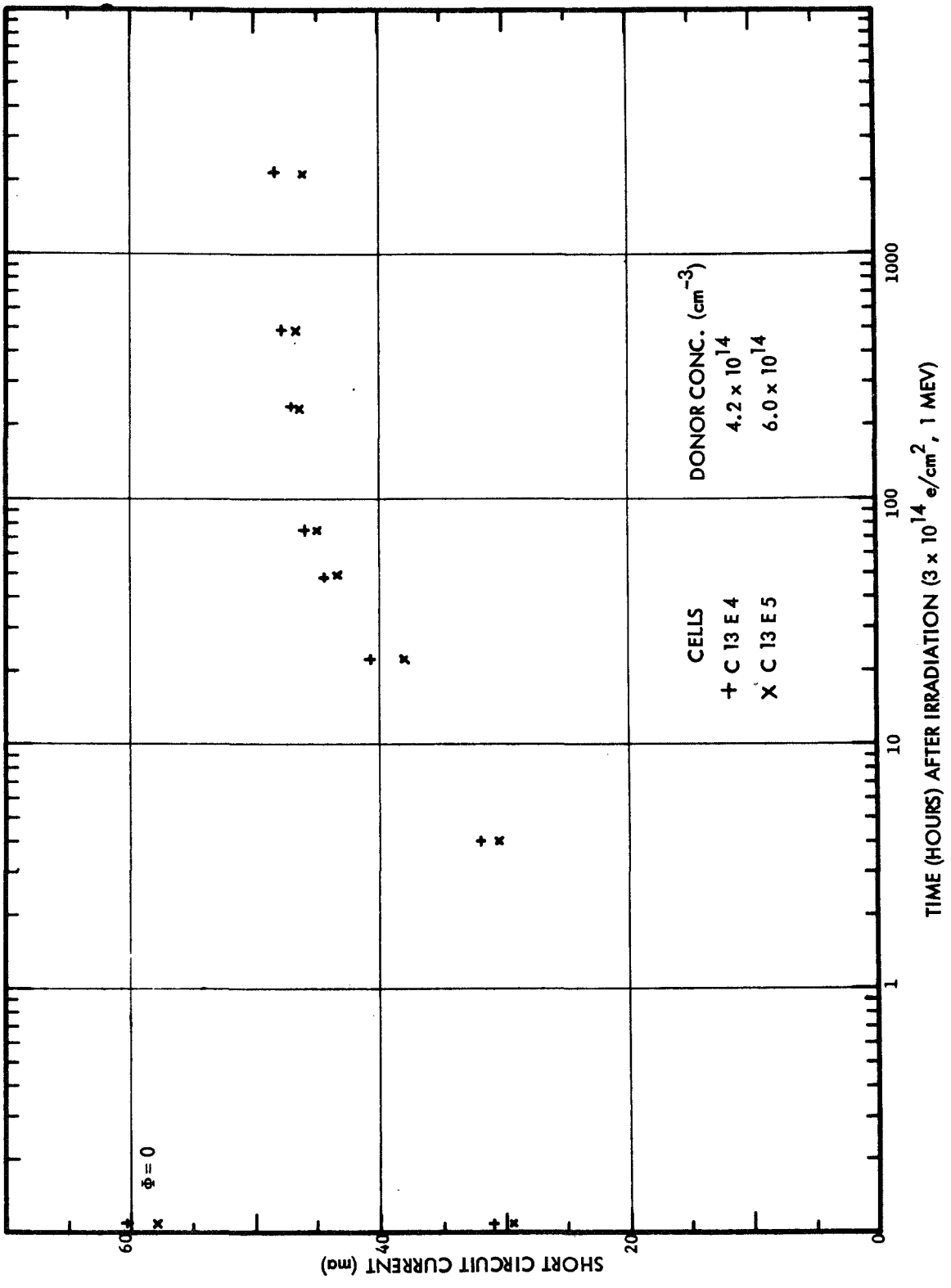


FIGURE 19. SHORT CIRCUIT CURRENT RECOVERY, Q.C. CELLS, AT 60°C

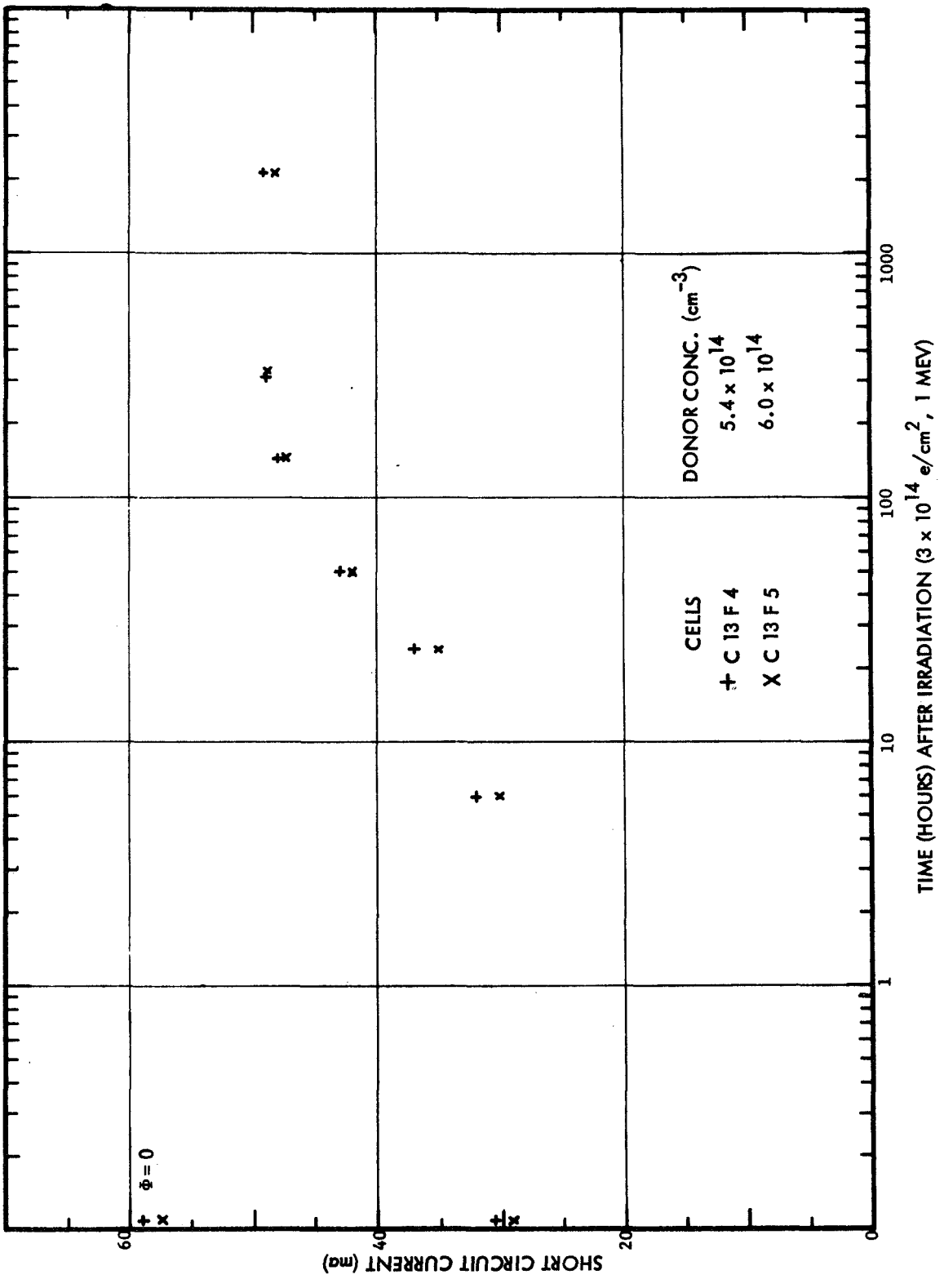


FIGURE 20. SHORT CIRCUIT CURRENT RECOVERY, Q.C. CELLS, AT 60°C

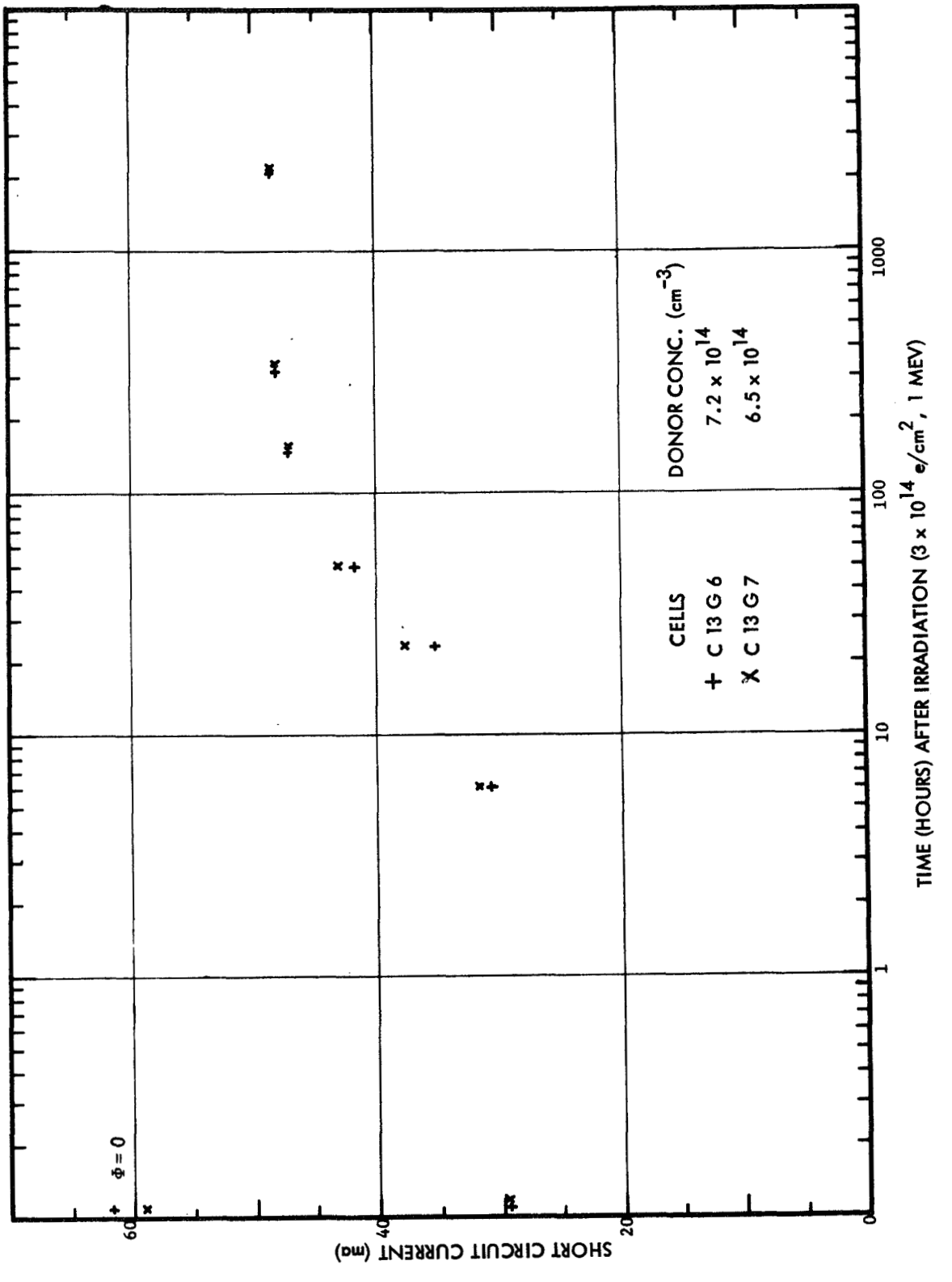


FIGURE 21. SHORT CIRCUIT CURRENT RECOVERY, Q.C. CELLS, AT 60°C

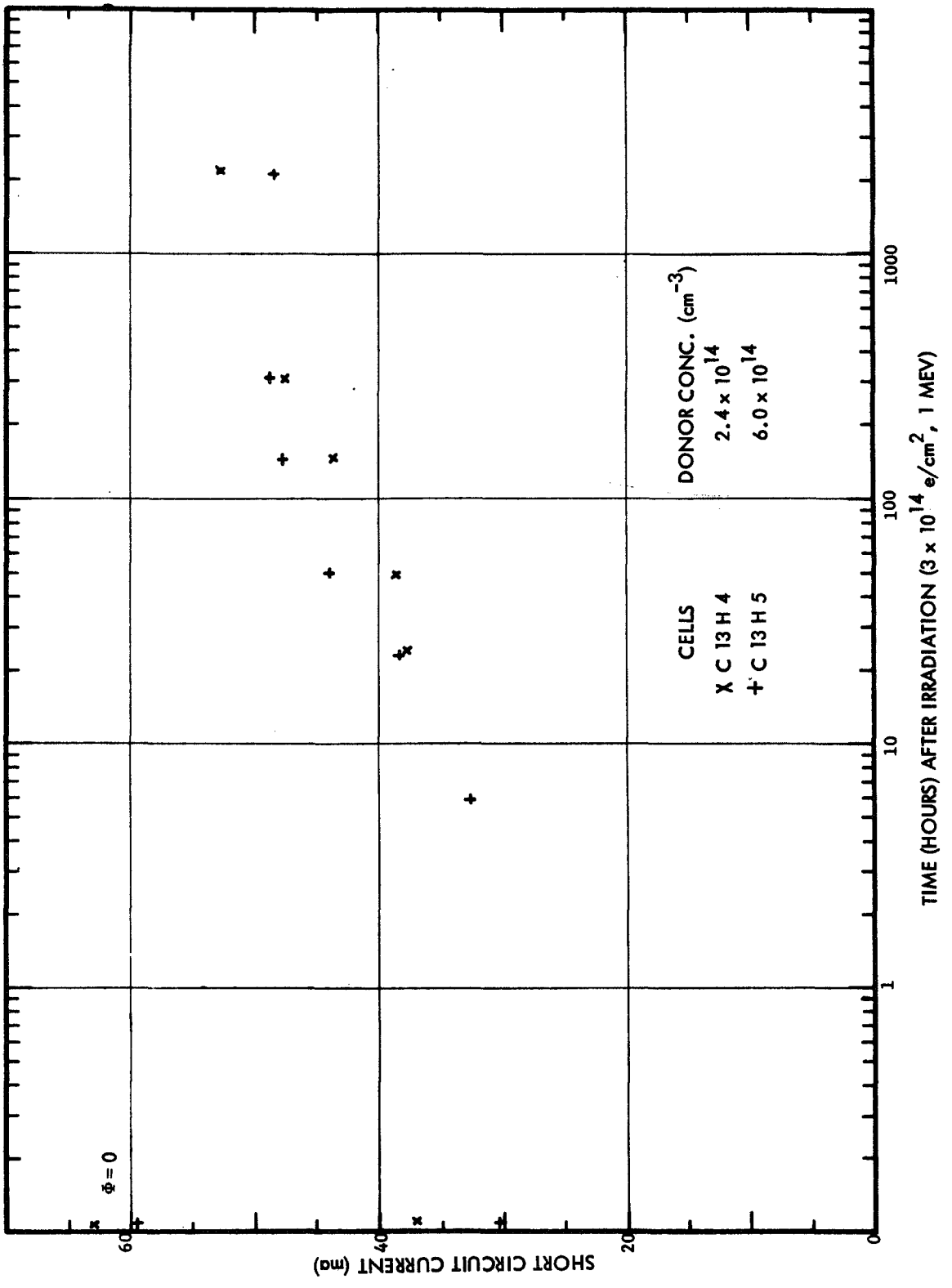


FIGURE 22. SHORT CIRCUIT CURRENT RECOVERY, Q.C. CELLS, AT 60°C

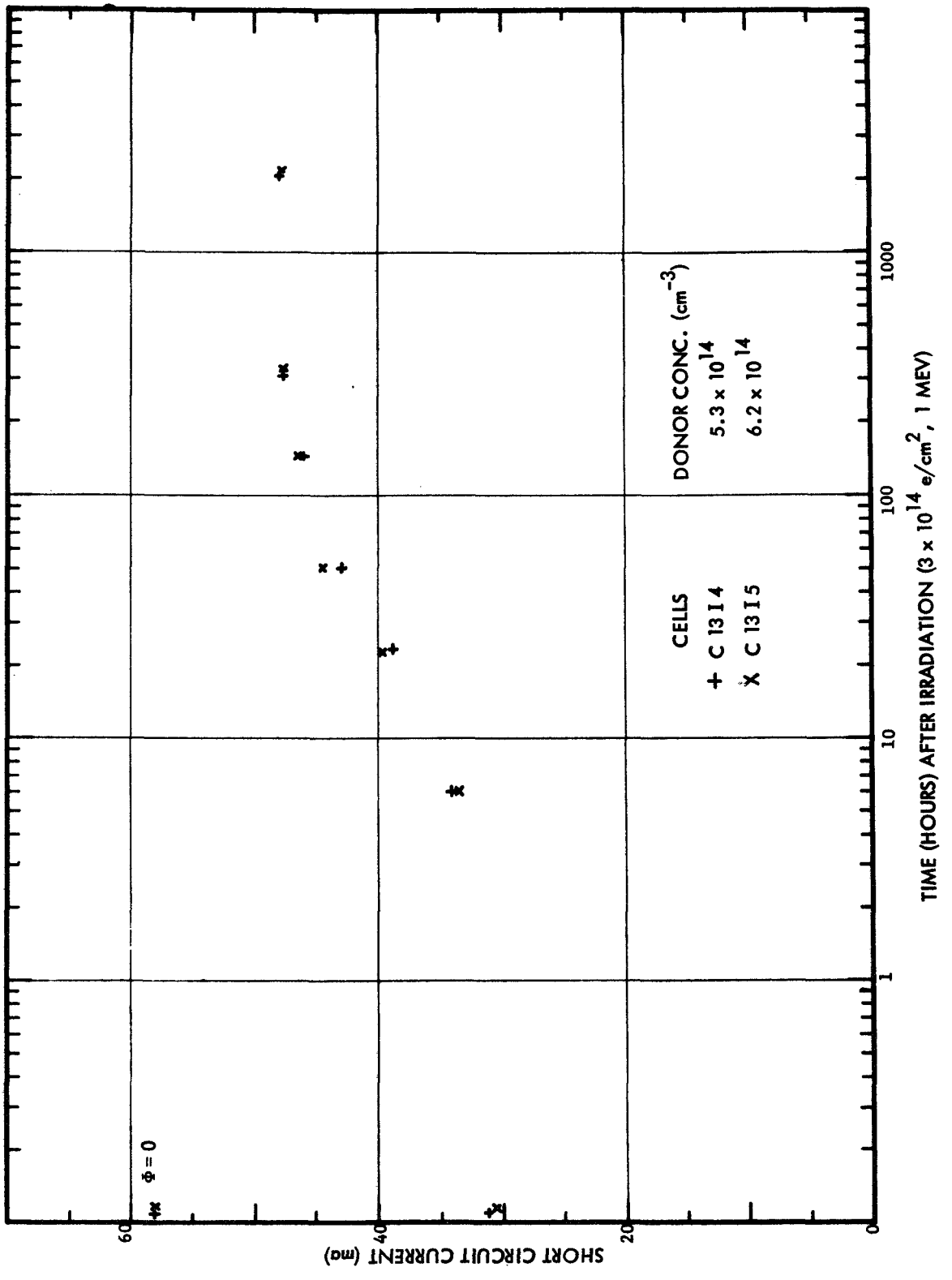


FIGURE 23. SHORT CIRCUIT CURRENT RECOVERY, Q.C. CELLS, AT 60°C

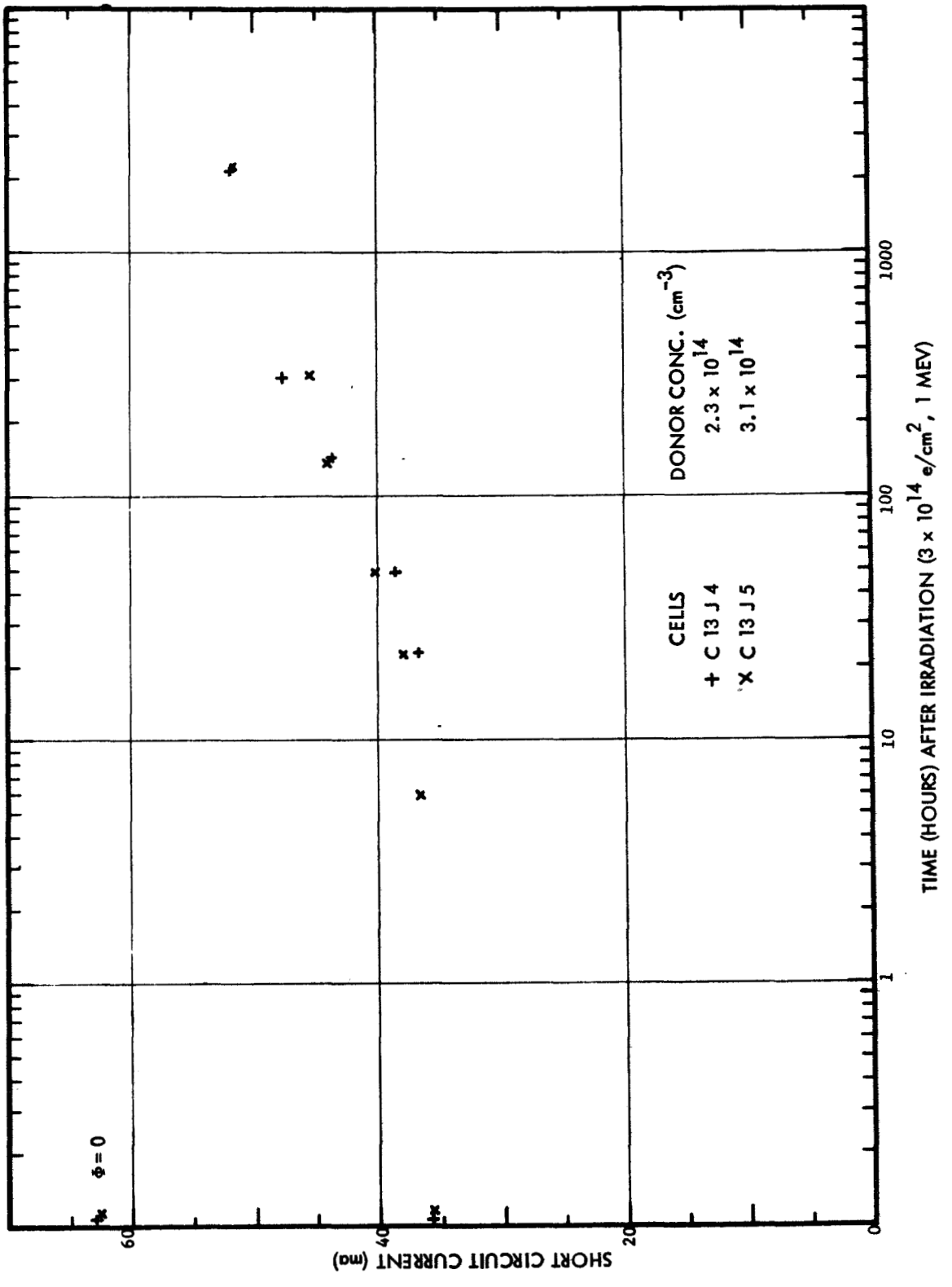


FIGURE 24. SHORT CIRCUIT CURRENT RECOVERY, Q.C. CELLS, AT 60°C

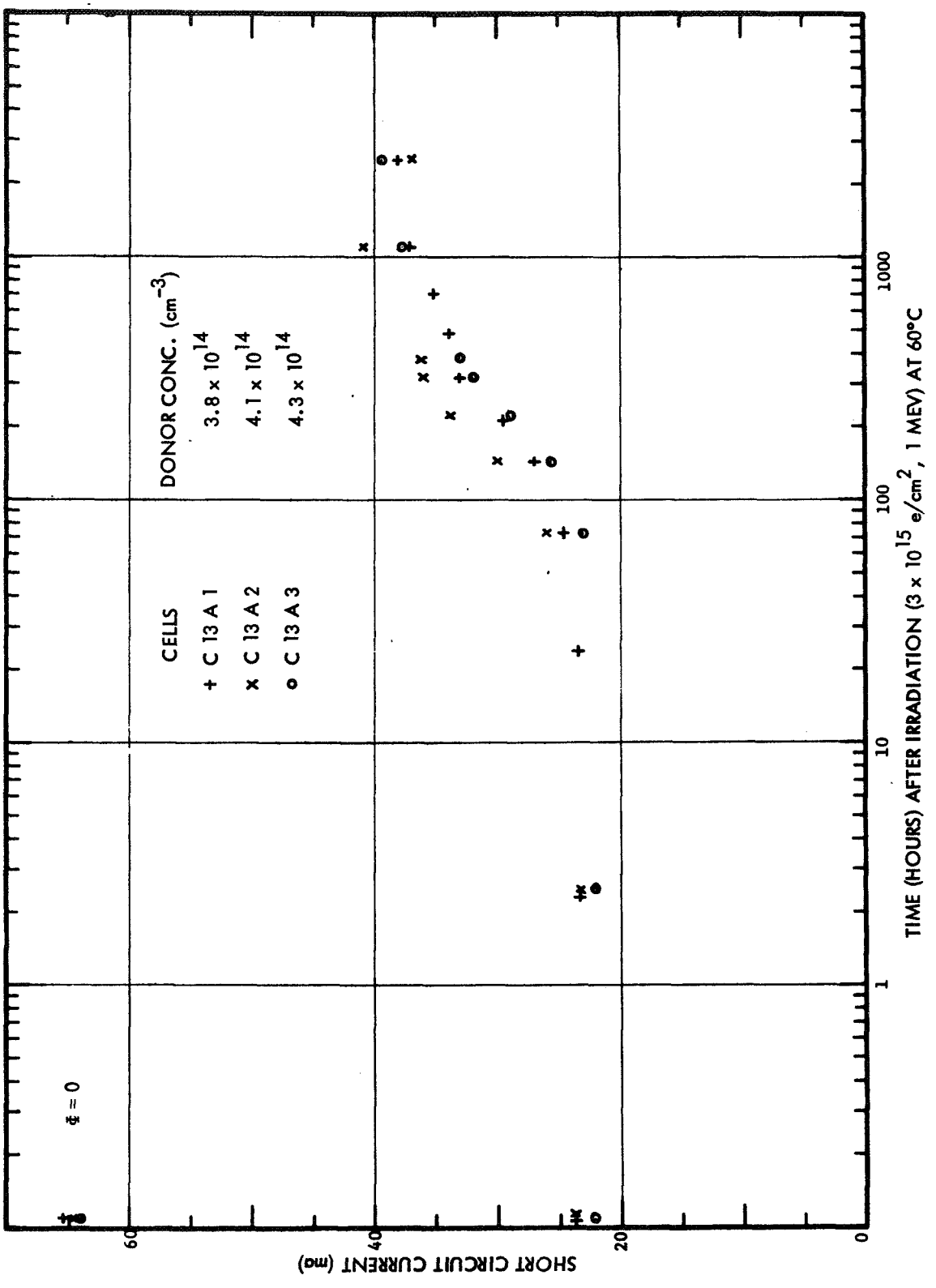


Figure 25. Short Circuit Current During Recovery, Q.C. Cells

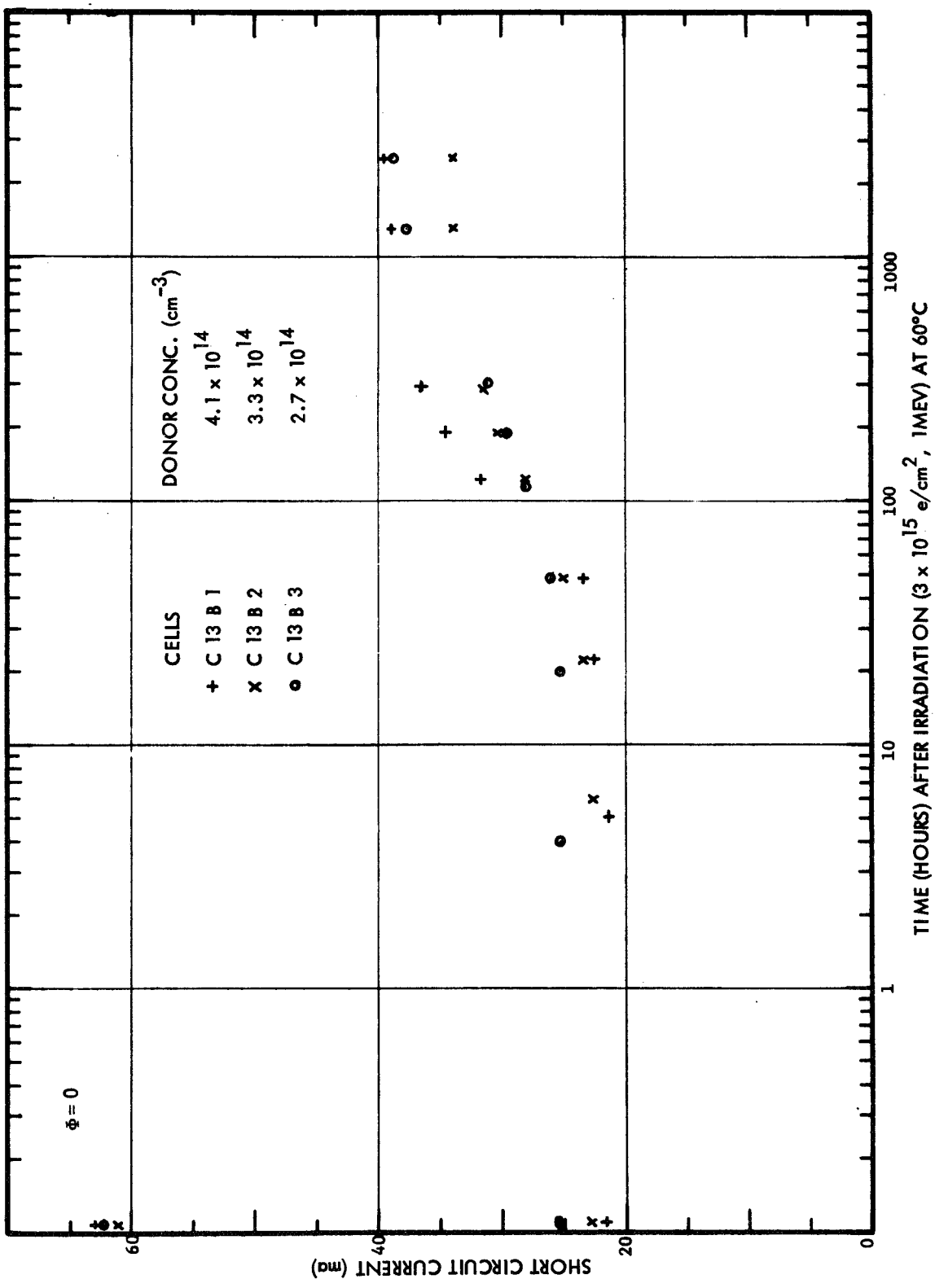


Figure 26. Short Circuit Current During Recovery, Q.C. Cells

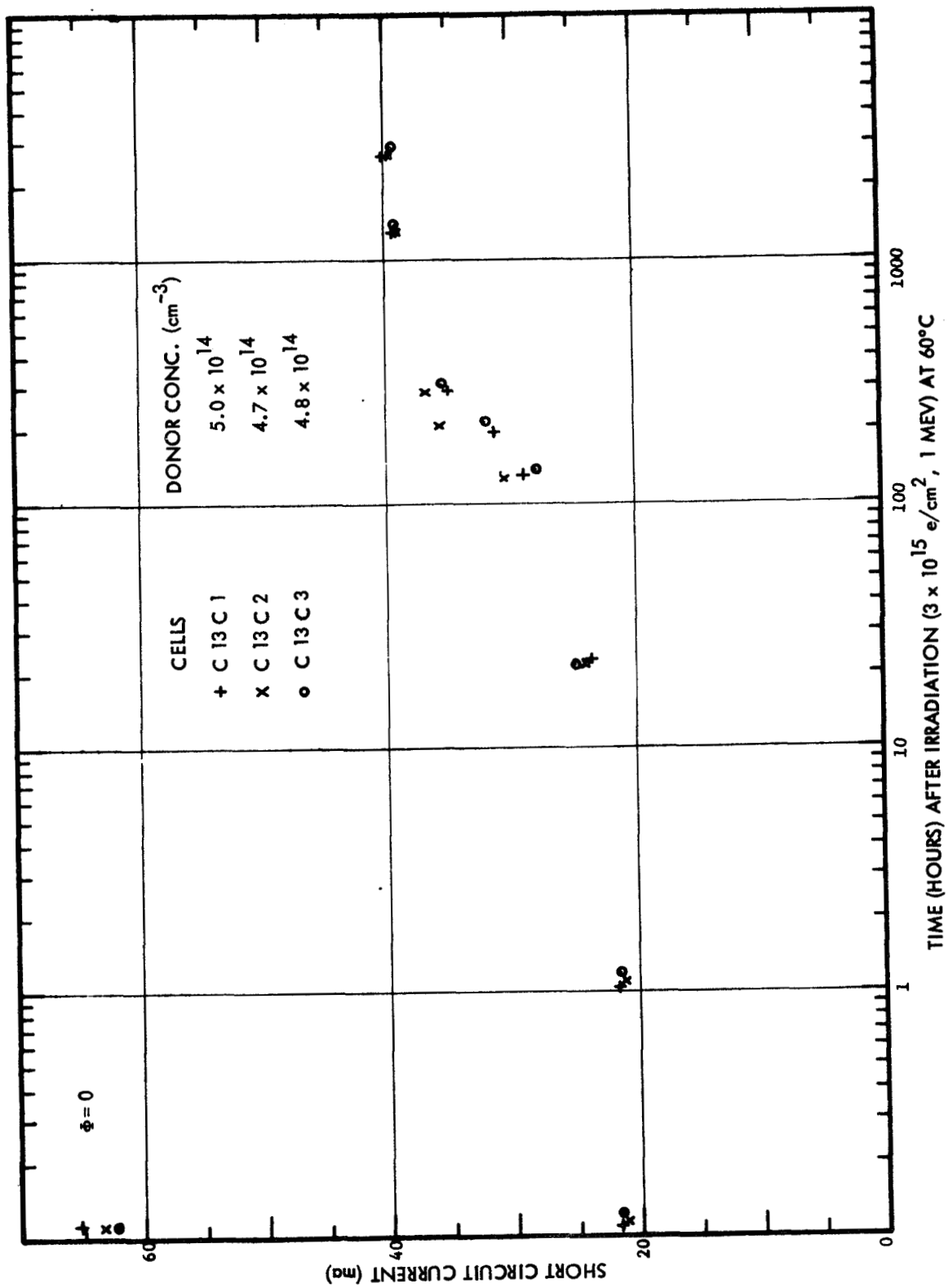


Figure 27. Short Circuit Current During Recovery, Q.C. Cells

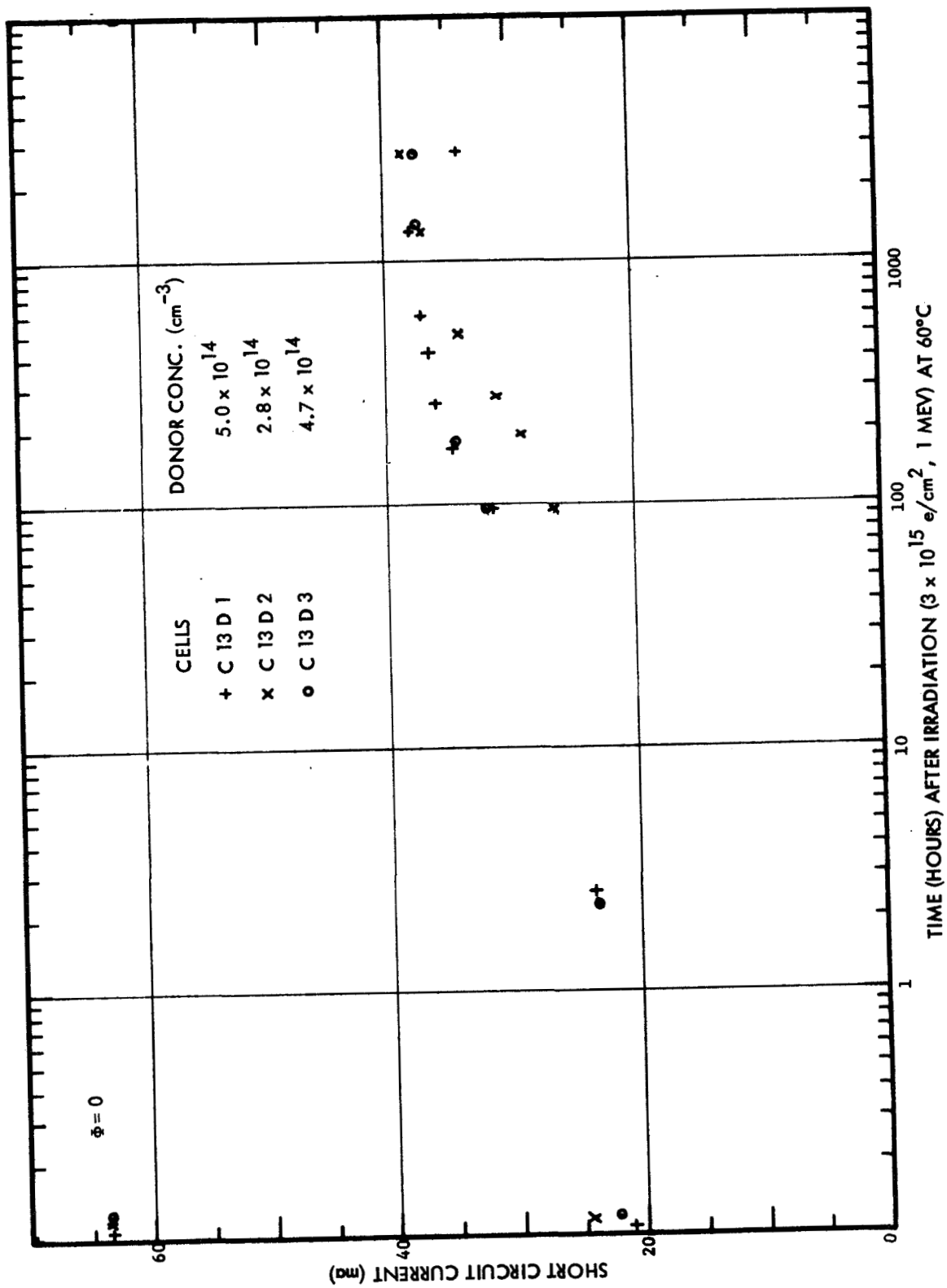


Figure 28. Short Circuit Current During Recovery, Q.C. Cells

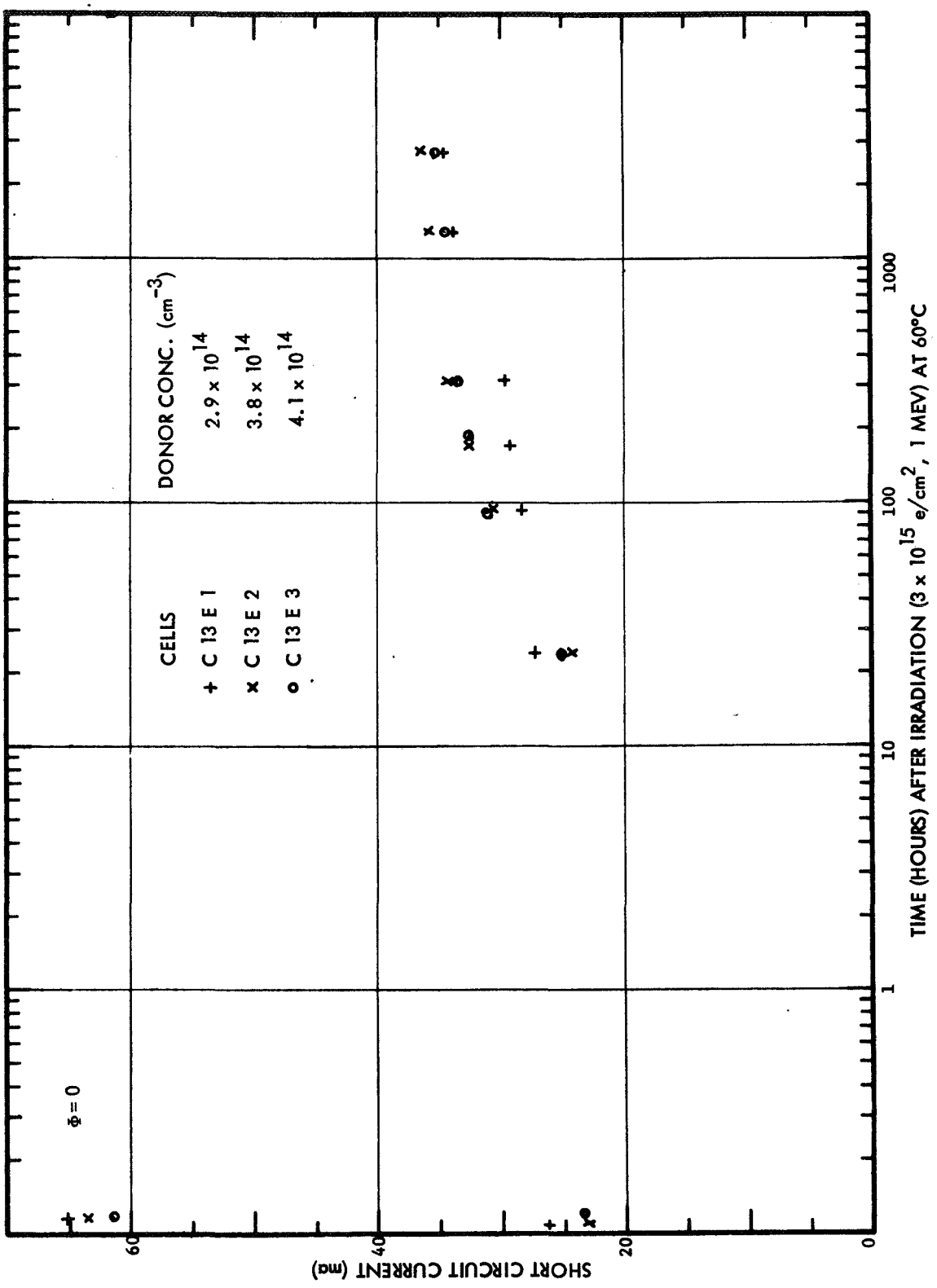


Figure 29. Short Circuit Current During Recovery, Q.C. Cells

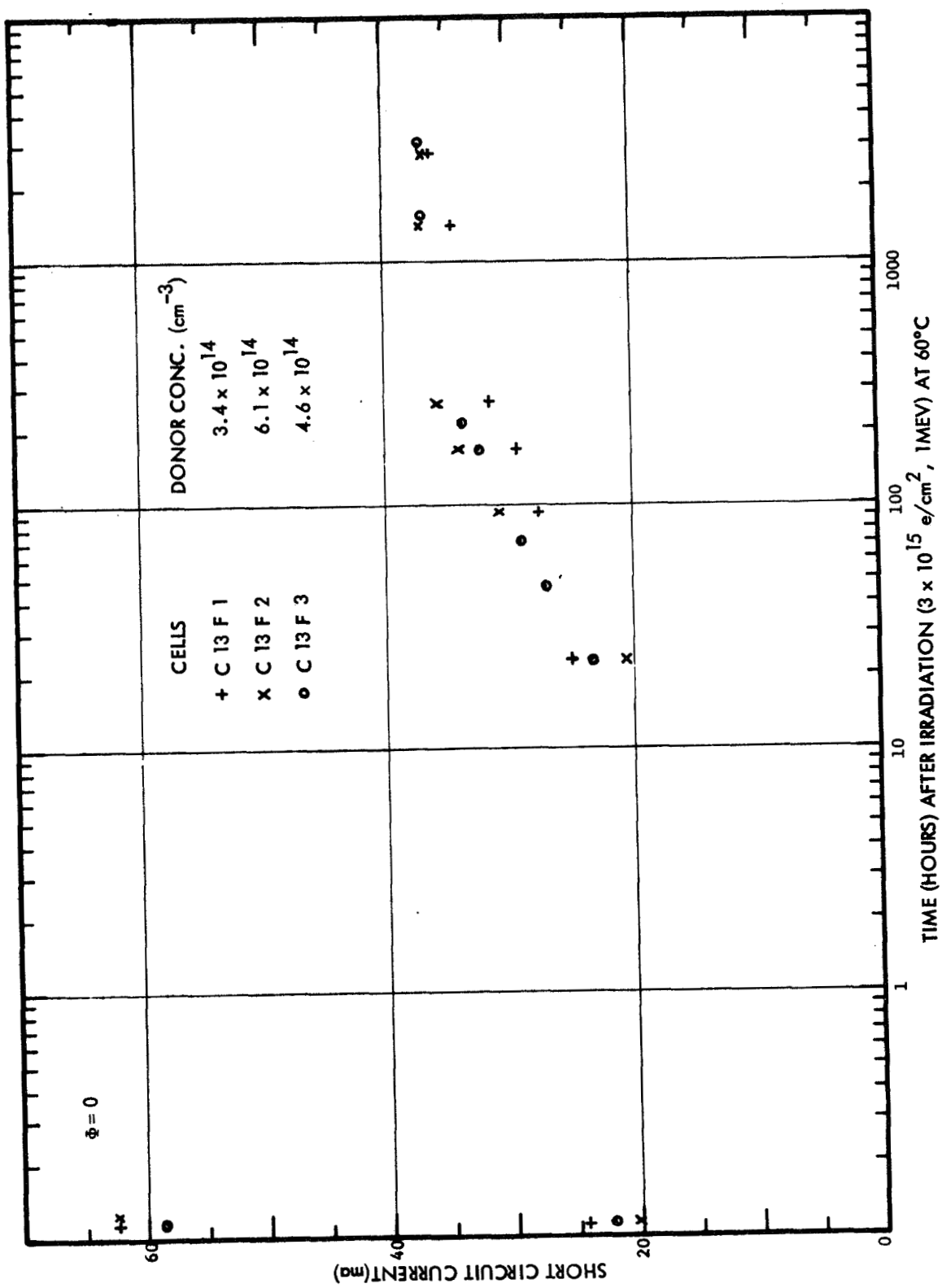


Figure 30. Short Circuit Current During Recovery, Q.C. Cells

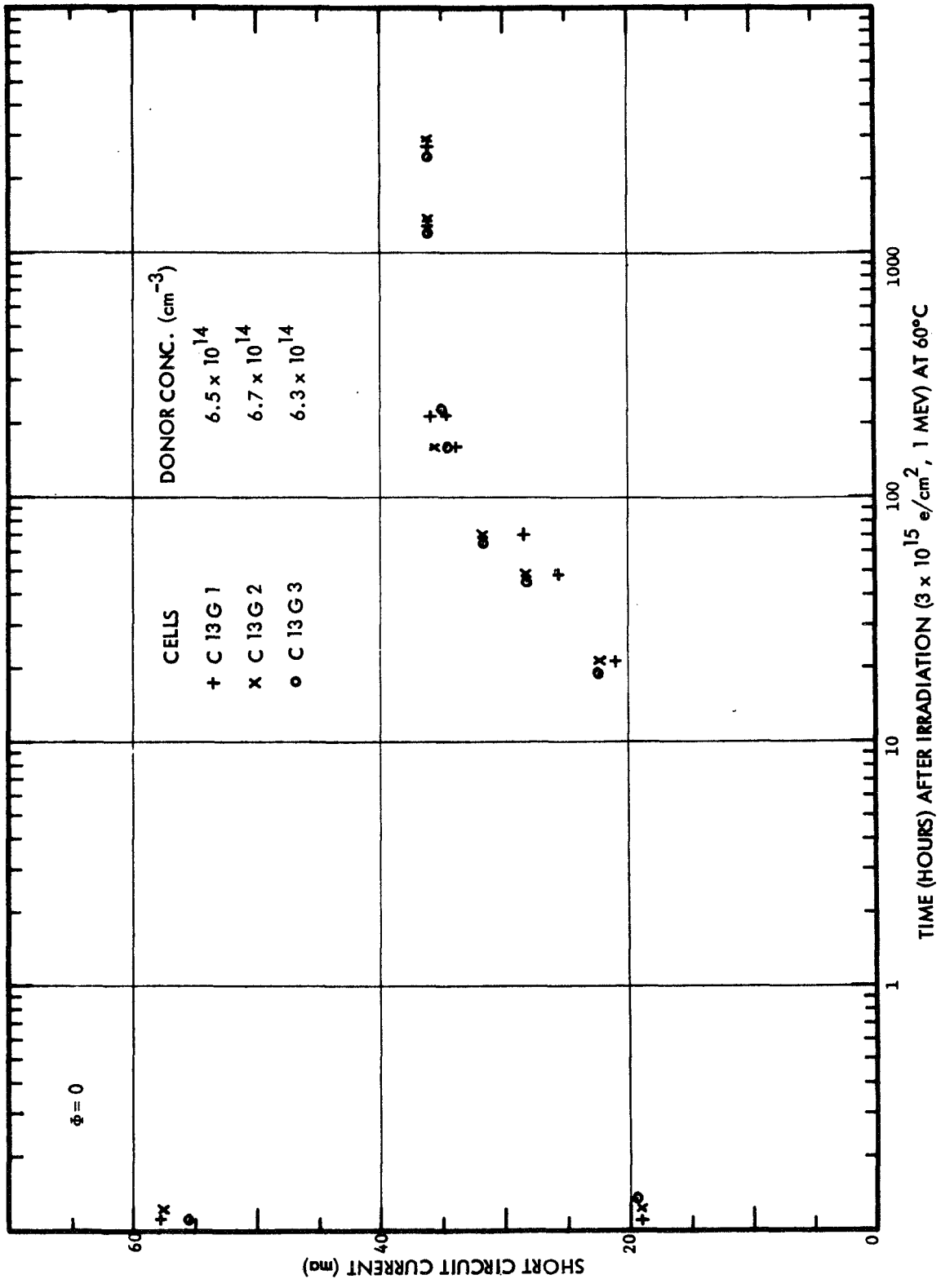


Figure 31. Short Circuit Current During Recovery, Q.C. Cells

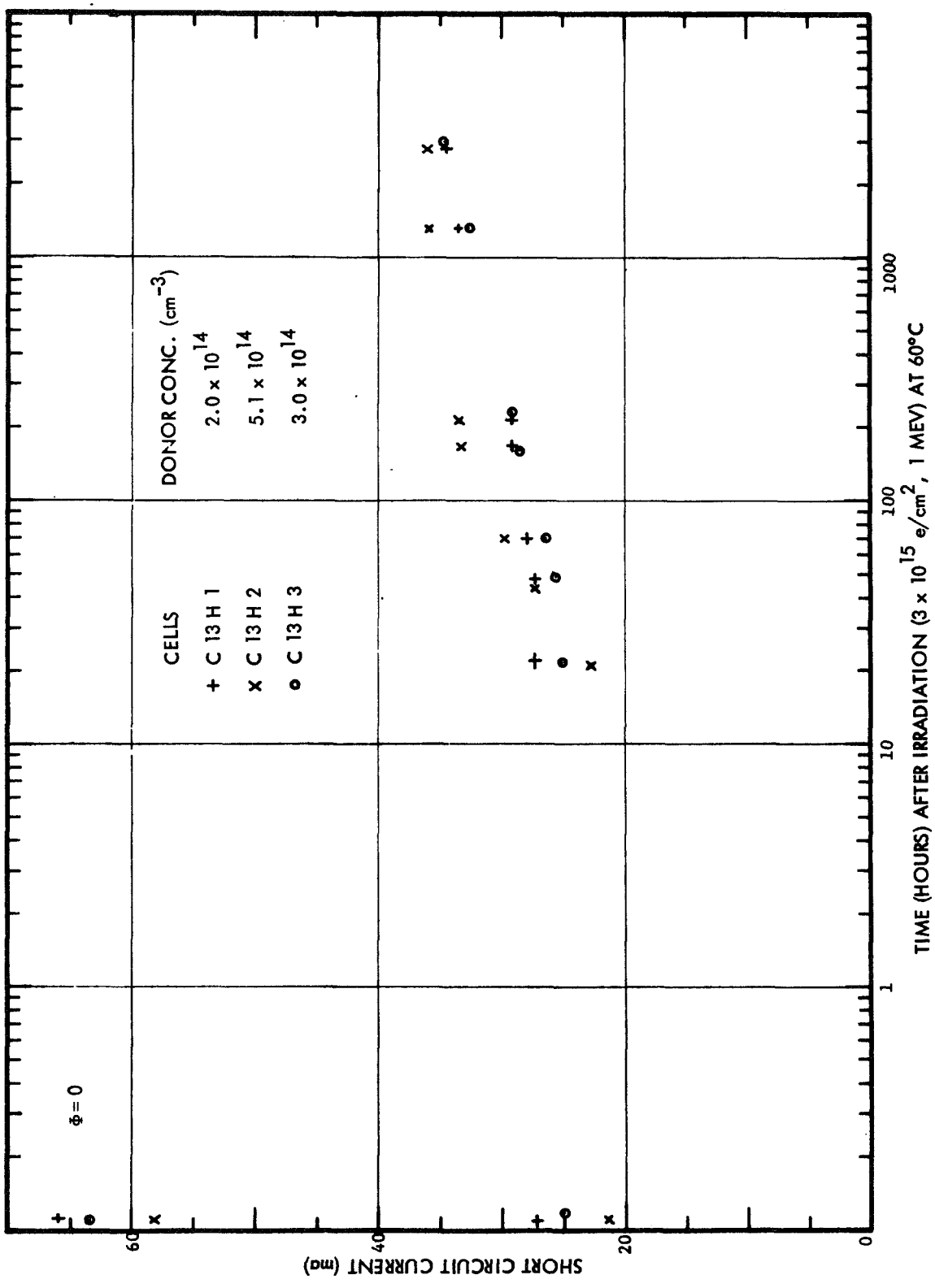


Figure 32. Short Circuit Current During Recovery, Q.C. Cells

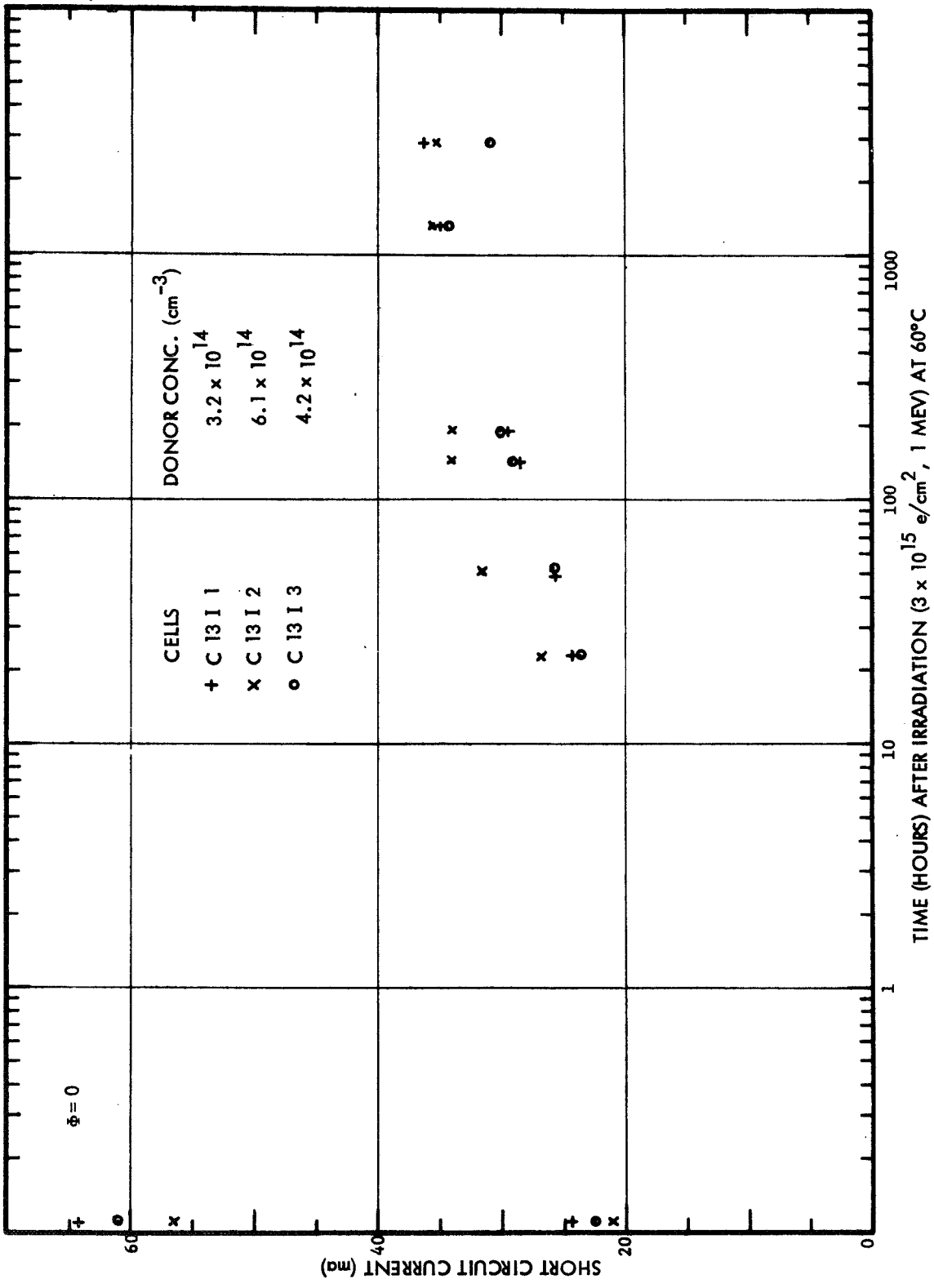


Figure 33. Short Circuit Current During Recovery, Q.C. Cells

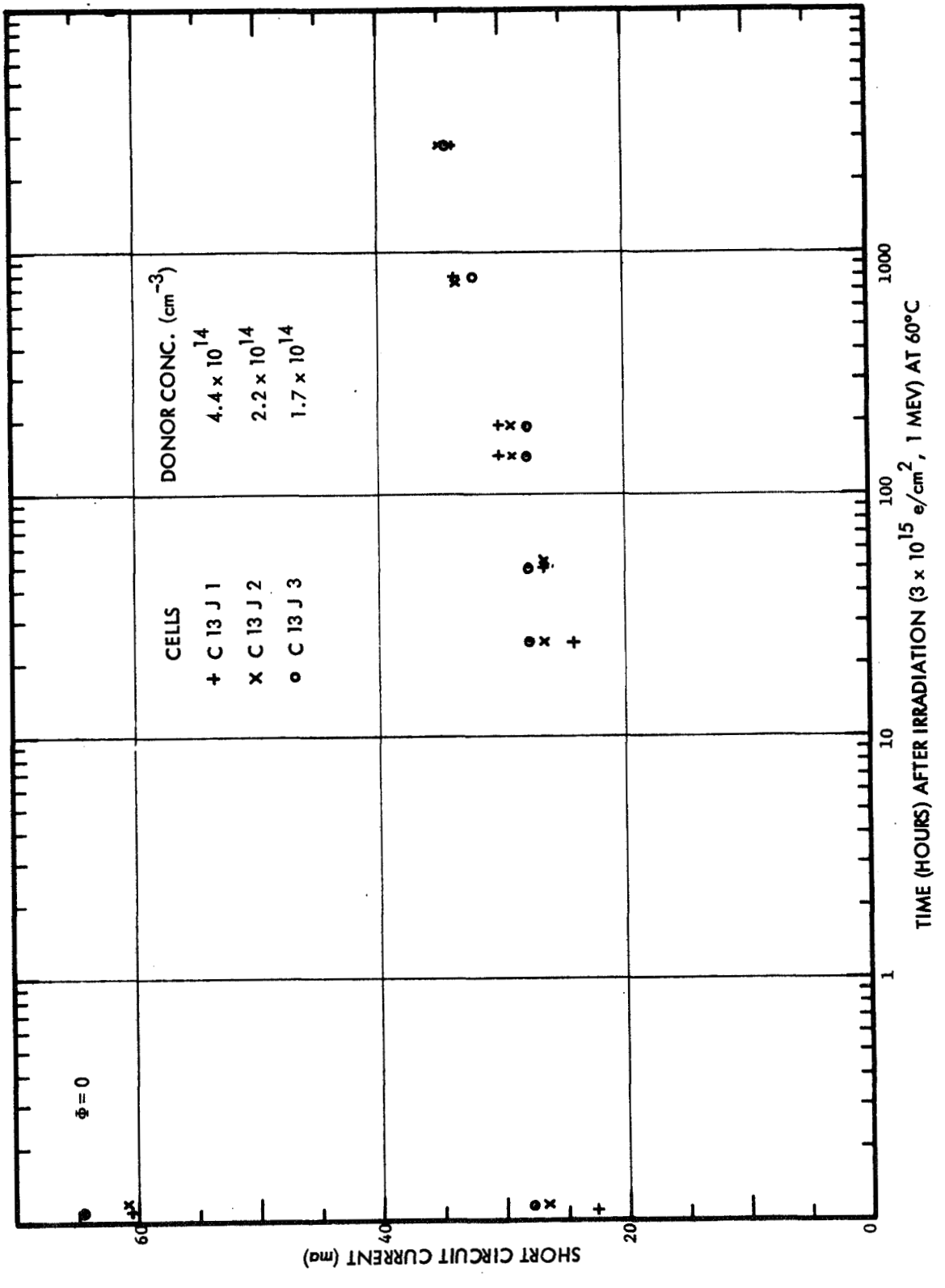


Figure 34. Short Circuit Current During Recovery, Q.C. Cells

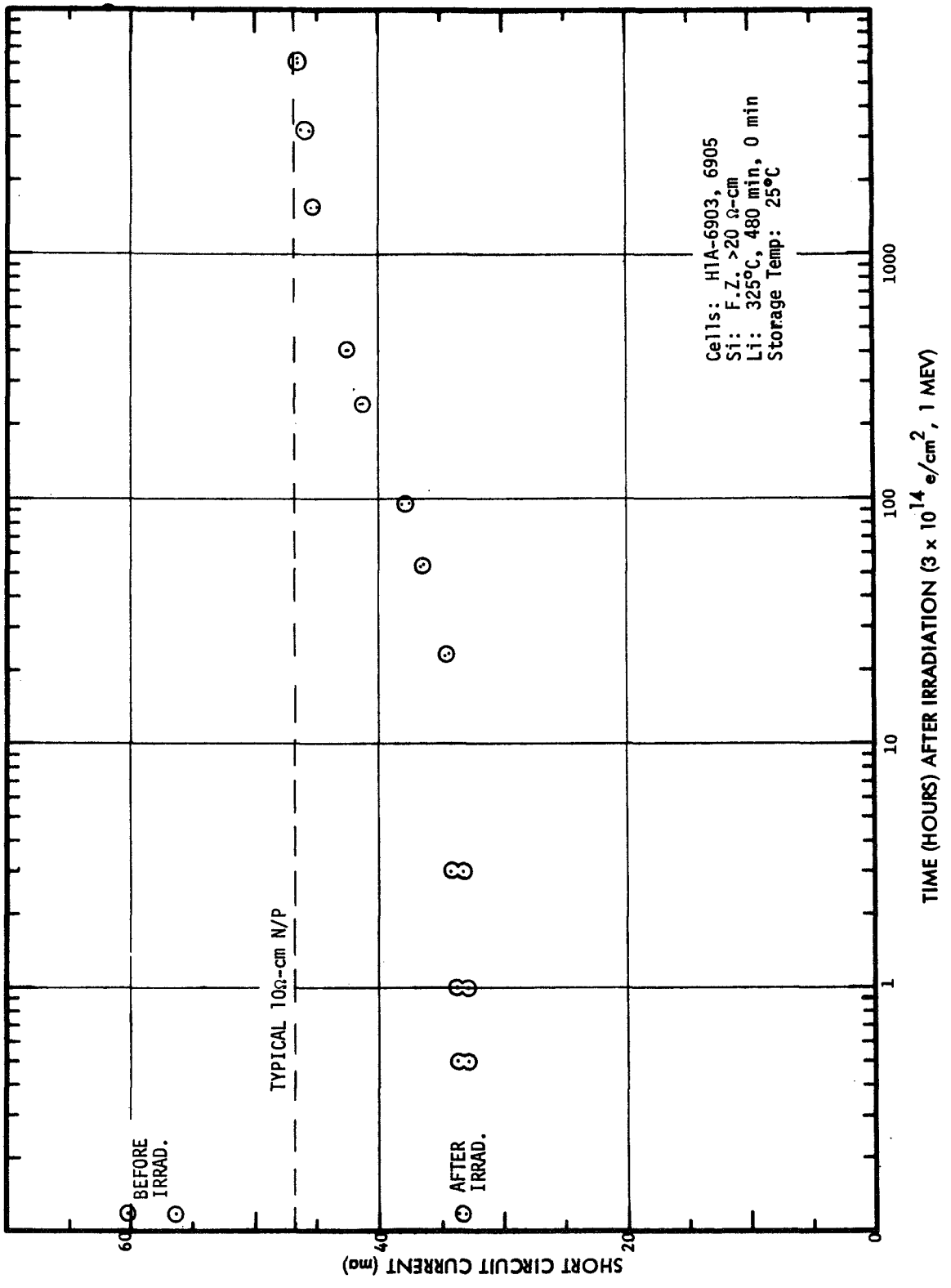


FIGURE 35. RECOVERY OF GROUP H1A SOLAR CELLS, $3 \times 10^{14} e/cm^2$

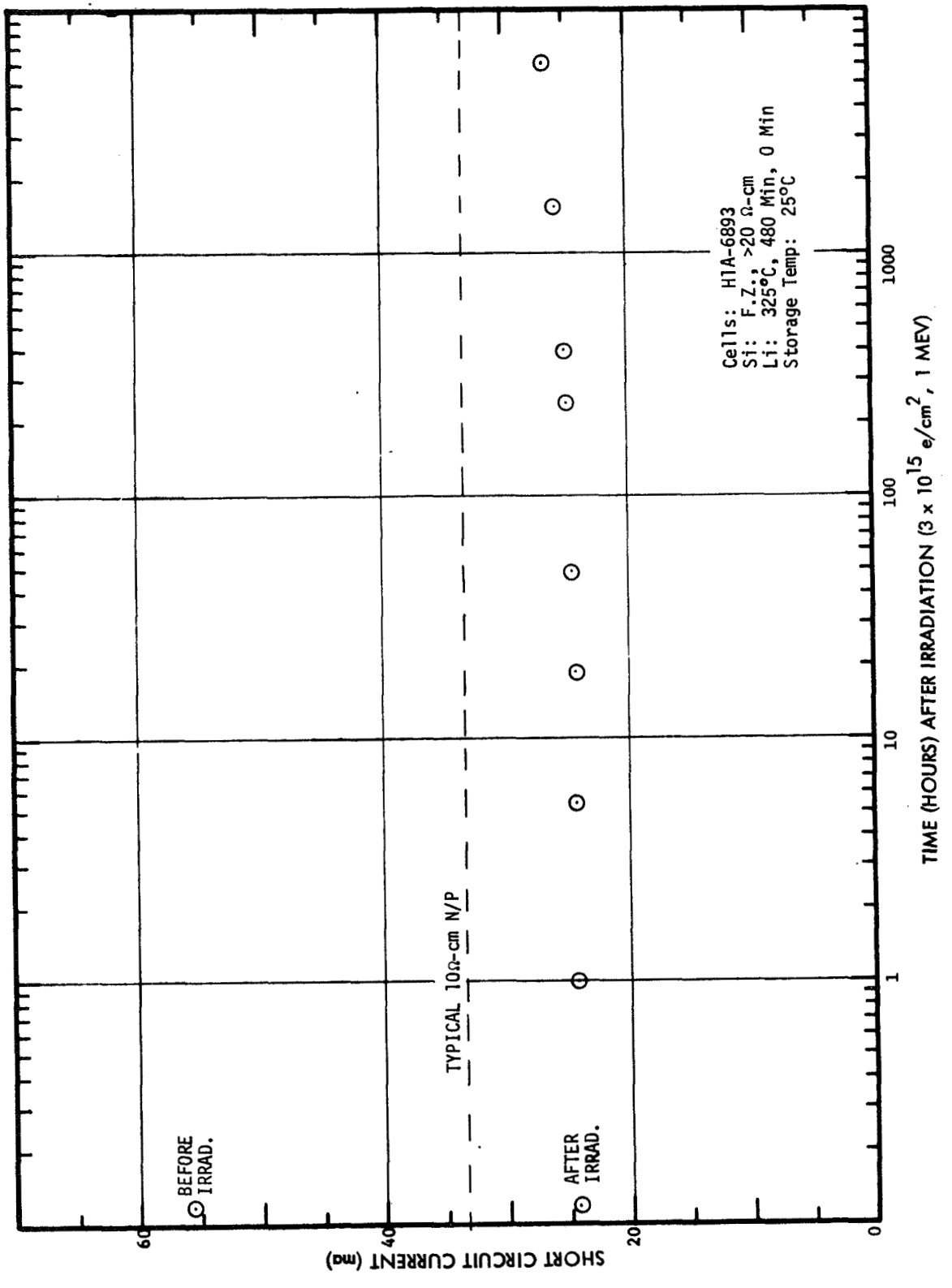


FIGURE 36. RECOVERY OF GROUP H1A SOLAR CELLS, $3x10^{15}e/cm^2$

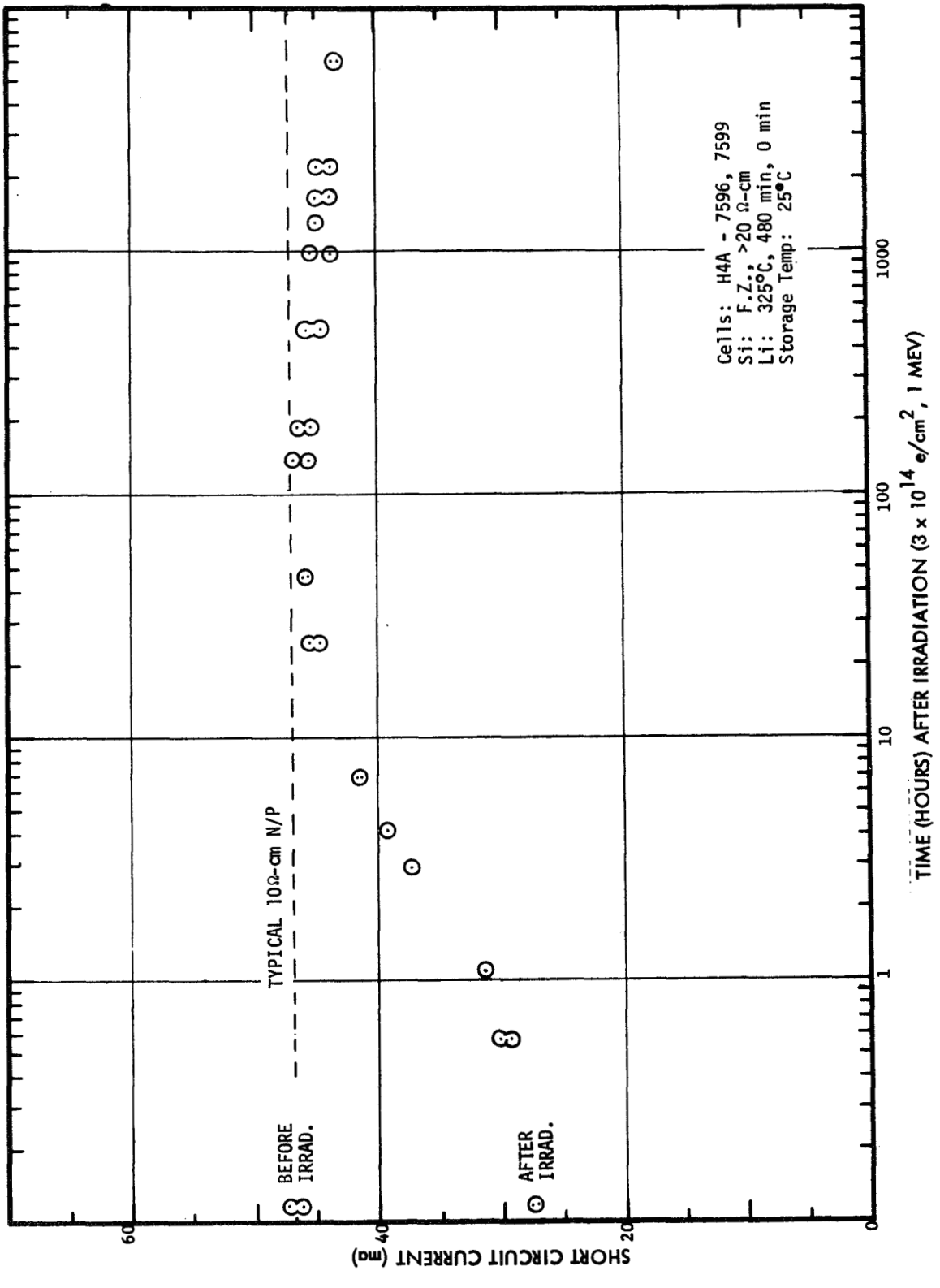


FIGURE 37. RECOVERY OF GROUP H4A SOLAR CELLS, $3 \times 10^{14} e/cm^2$

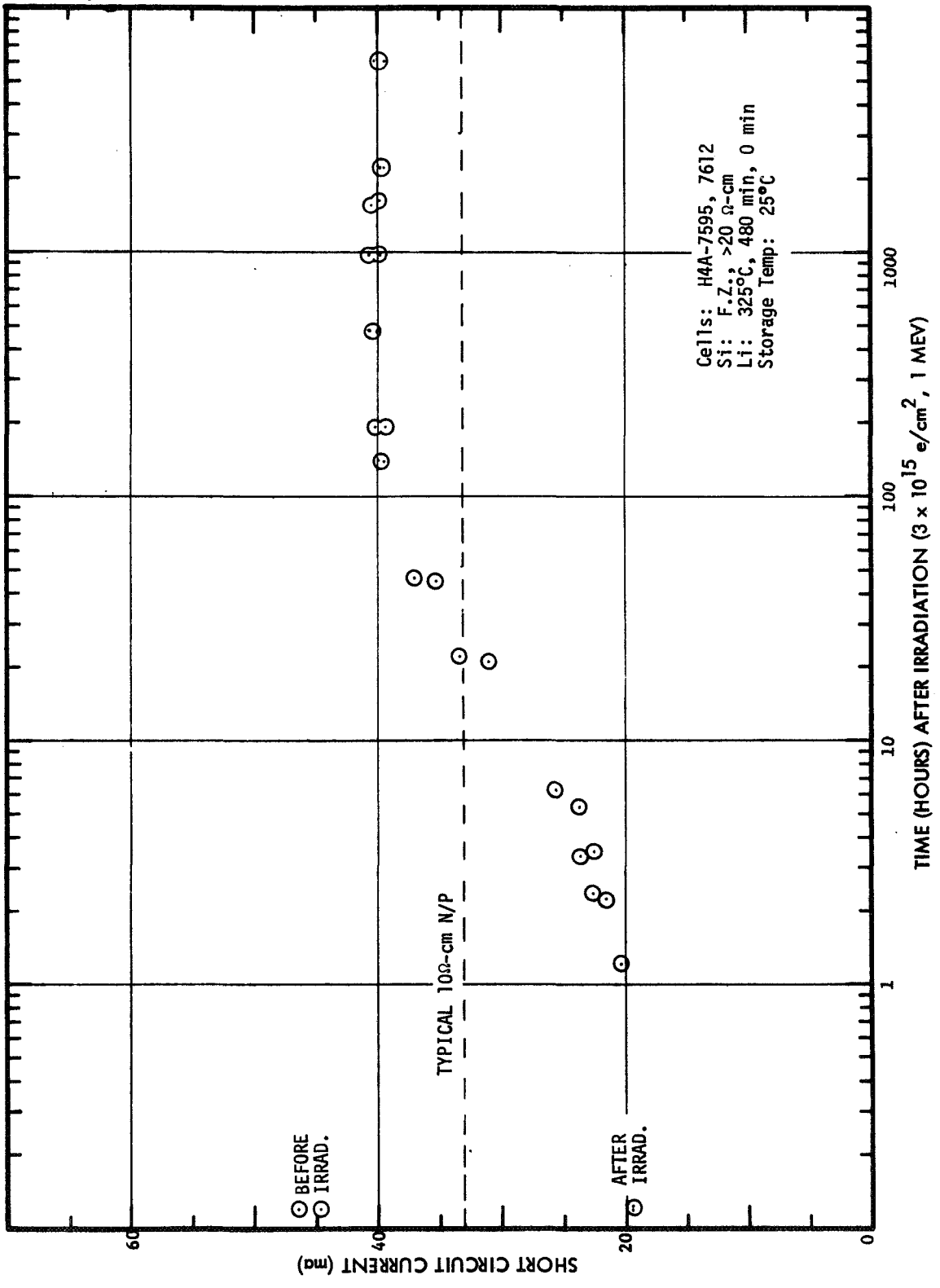


FIGURE 38. RECOVERY OF GROUP H4A SOLAR CELLS, $3 \times 10^{15} e/cm^2$

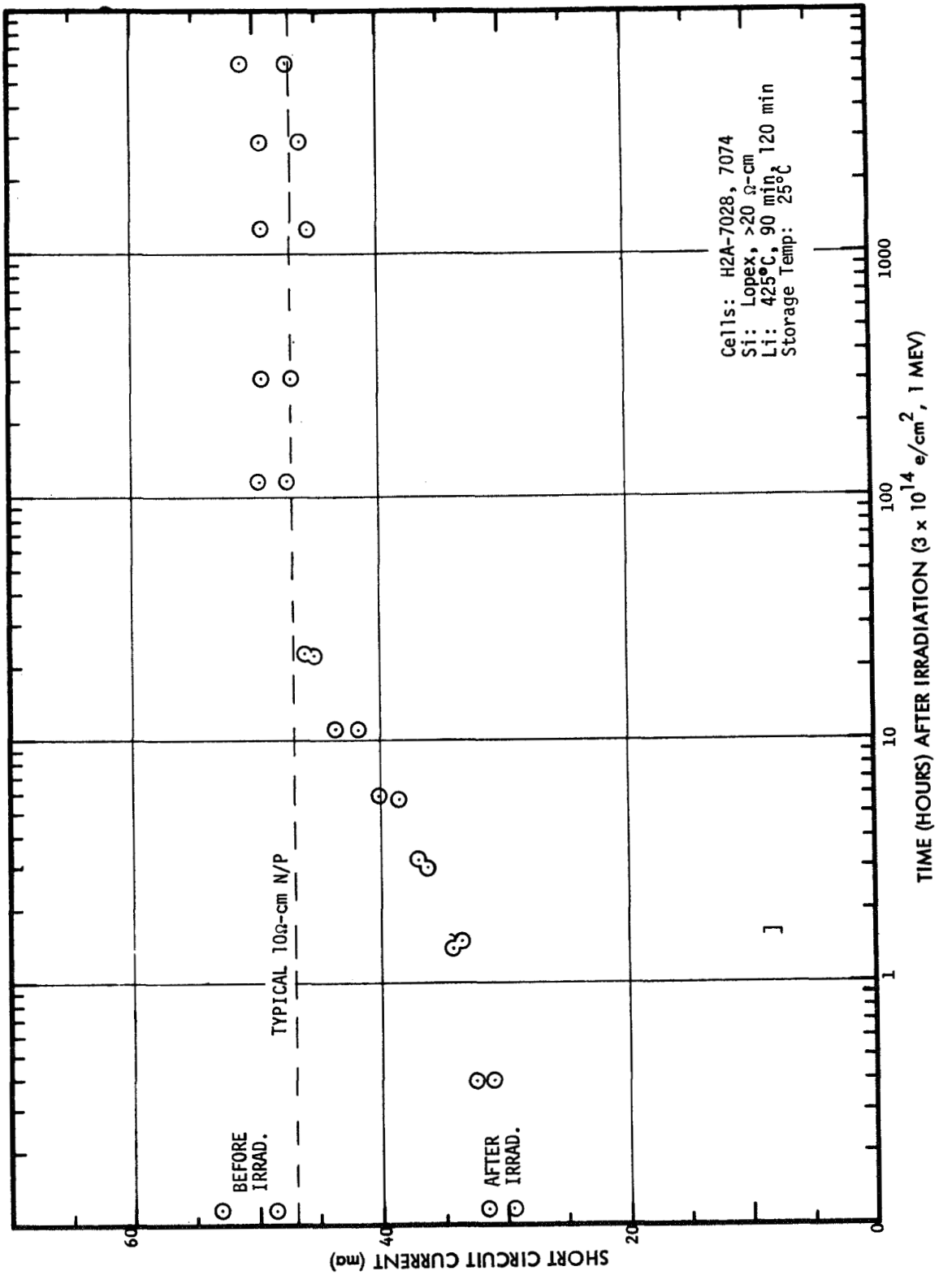


FIGURE 39- RECOVERY OF GROUP H2A SOLAR CELLS, $3 \times 10^{14} e/cm^2$

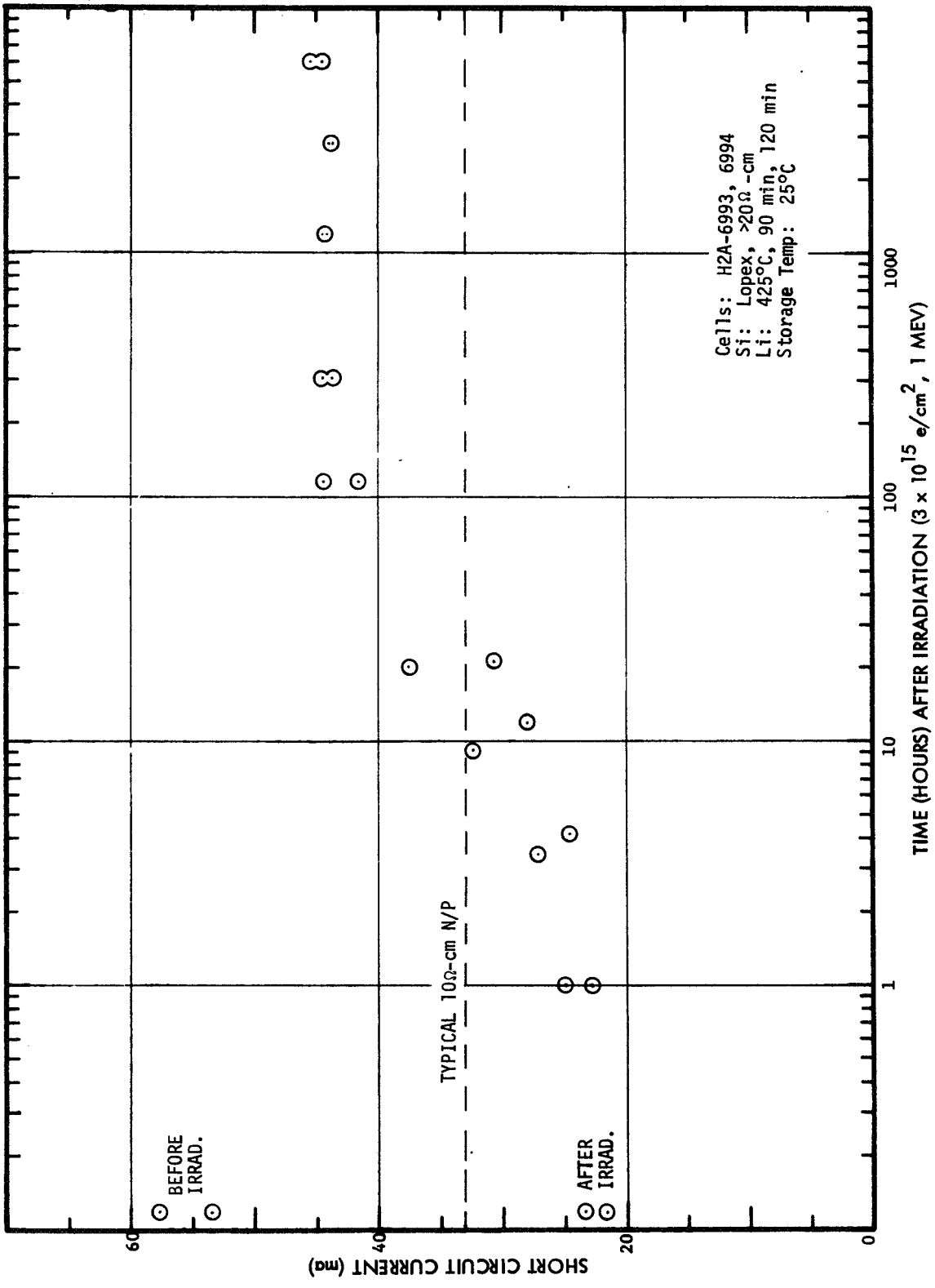


FIGURE 40. RECOVERY OF GROUP H2A SOLAR CELLS, $3 \times 10^{15} e/cm^2$

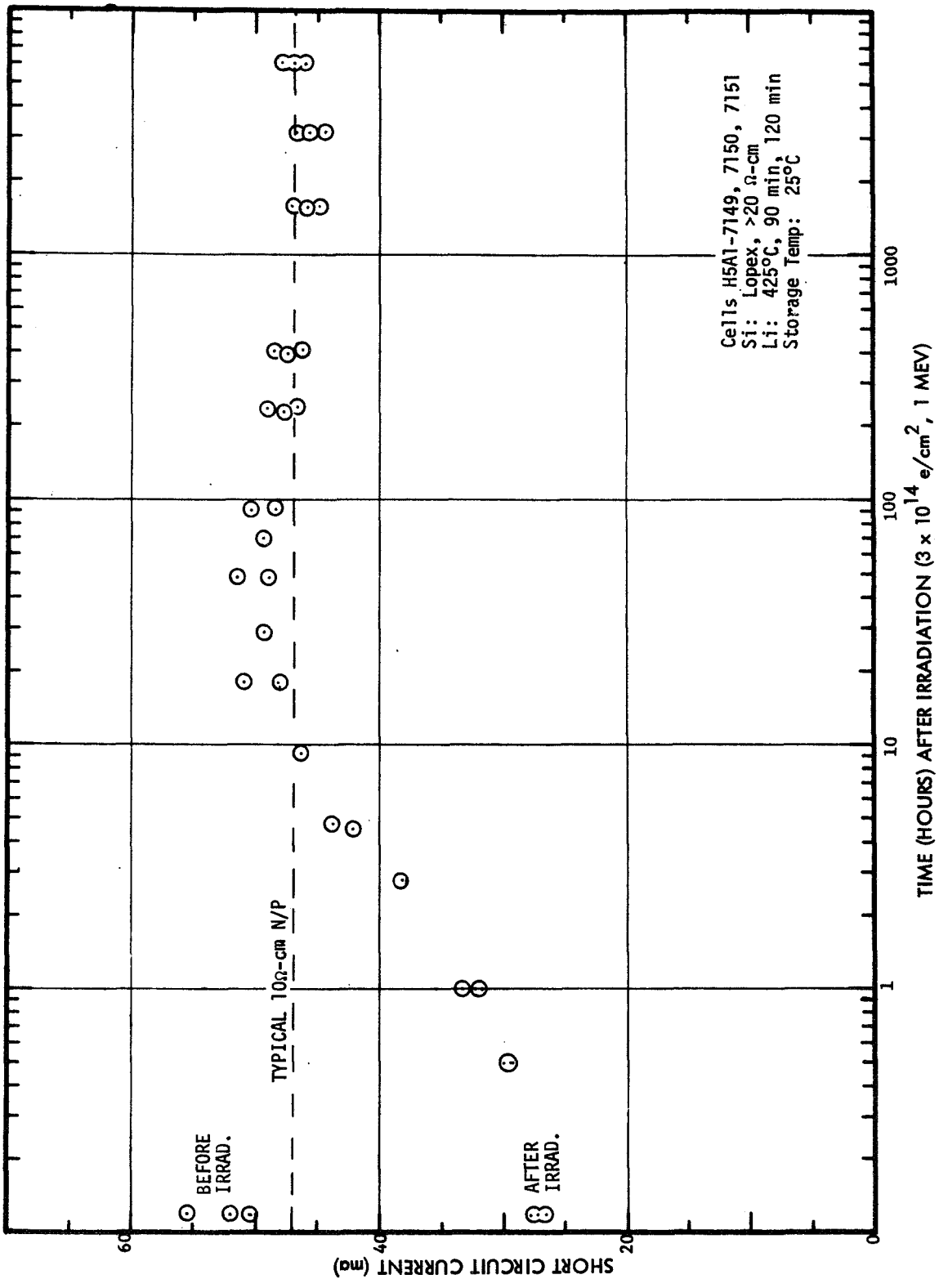


FIGURE 41- RECOVERY OF GROUP H5A1 SOLAR CELLS, $3 \times 10^{14} e/cm^2$

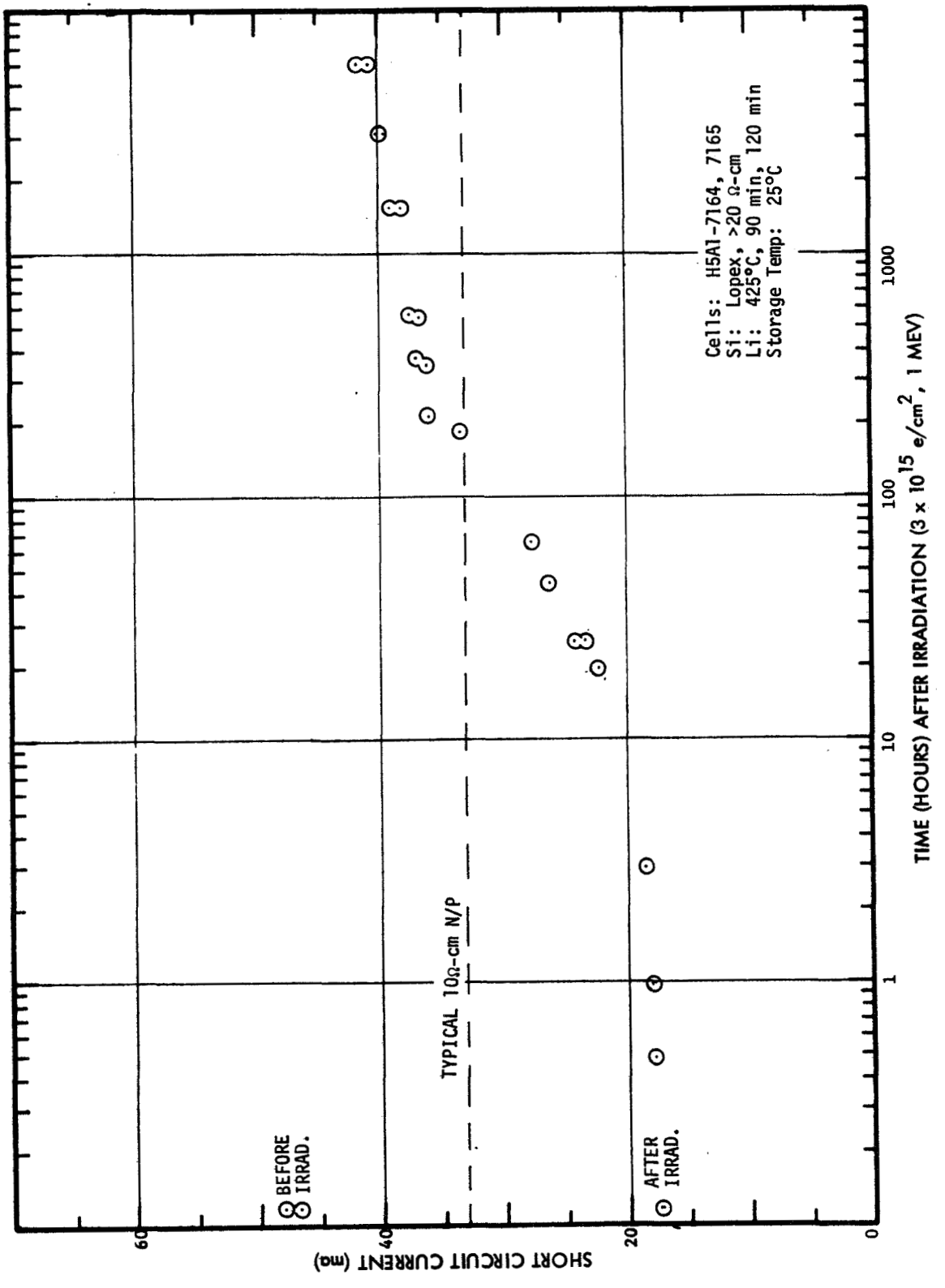


FIGURE 42. RECOVERY OF GROUP H5A1 SOLAR CELLS, $3 \times 10^{15} e/cm^2$

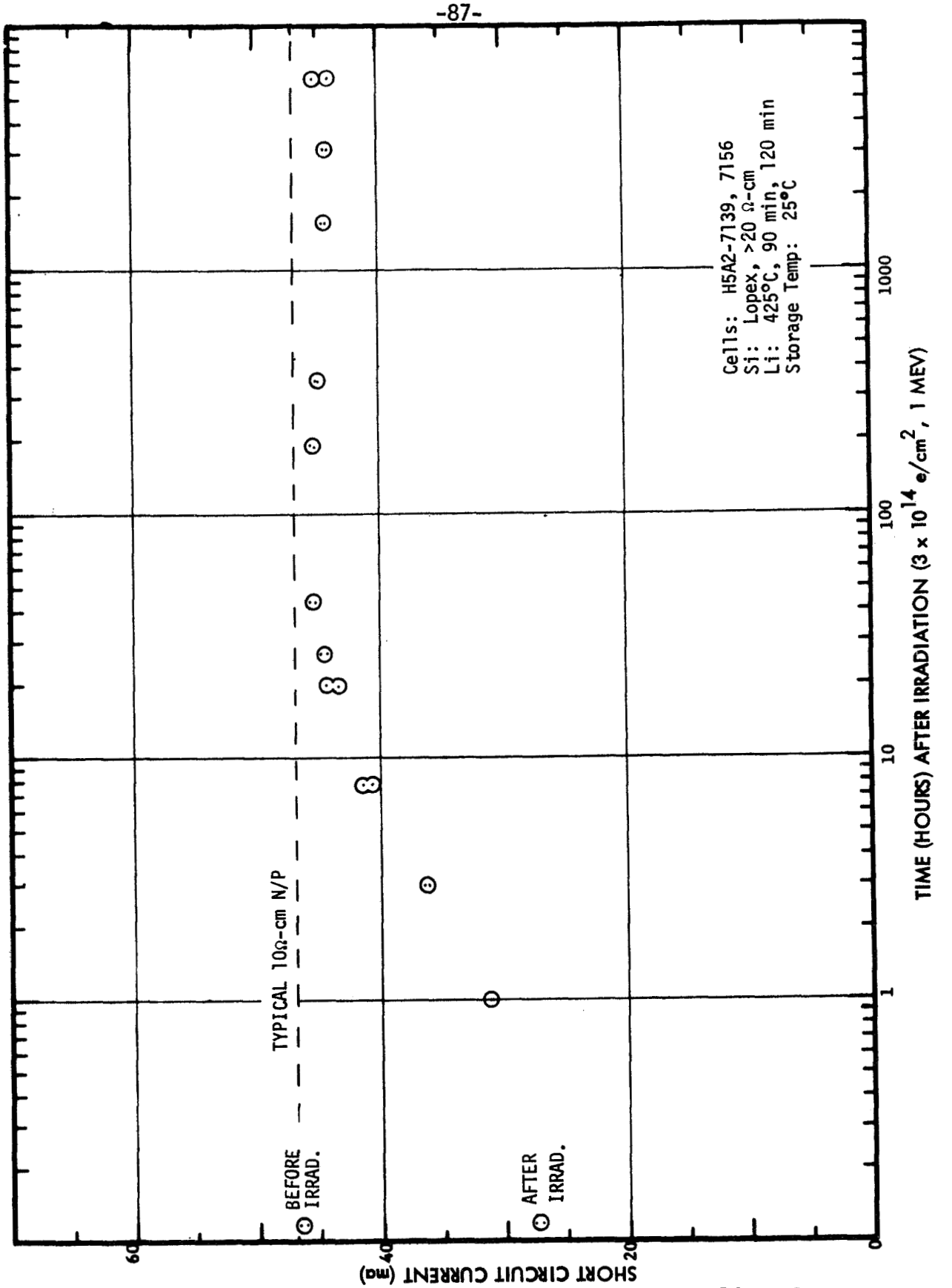


FIGURE 43 - RECOVERY OF GROUP H5A2 SOLAR CELLS, $3 \times 10^{14} e/cm^2$

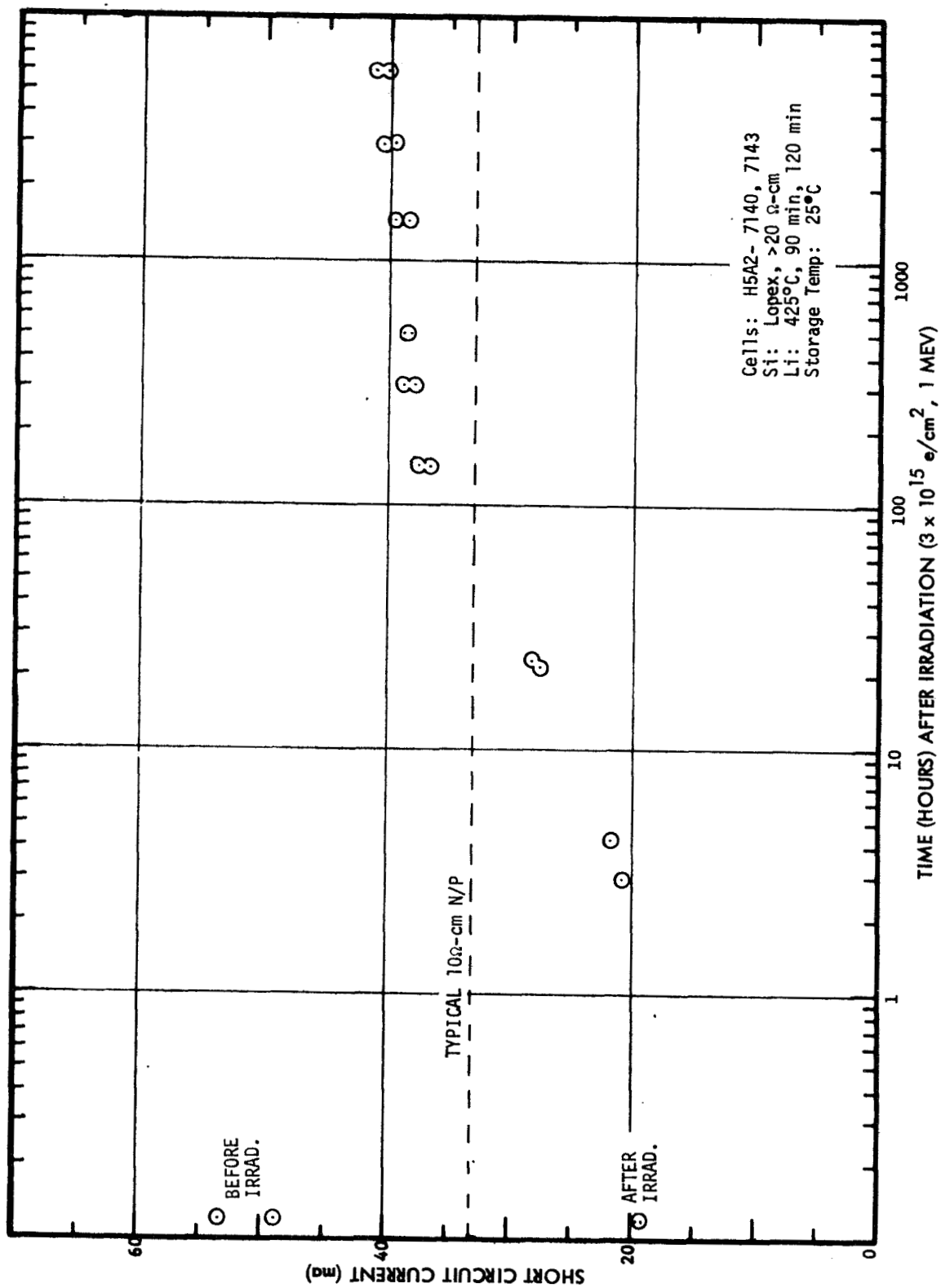


FIGURE 44 - RECOVERY OF GROUP H5A2 SOLAR CELLS, $3 \times 10^{15} e/cm^2$

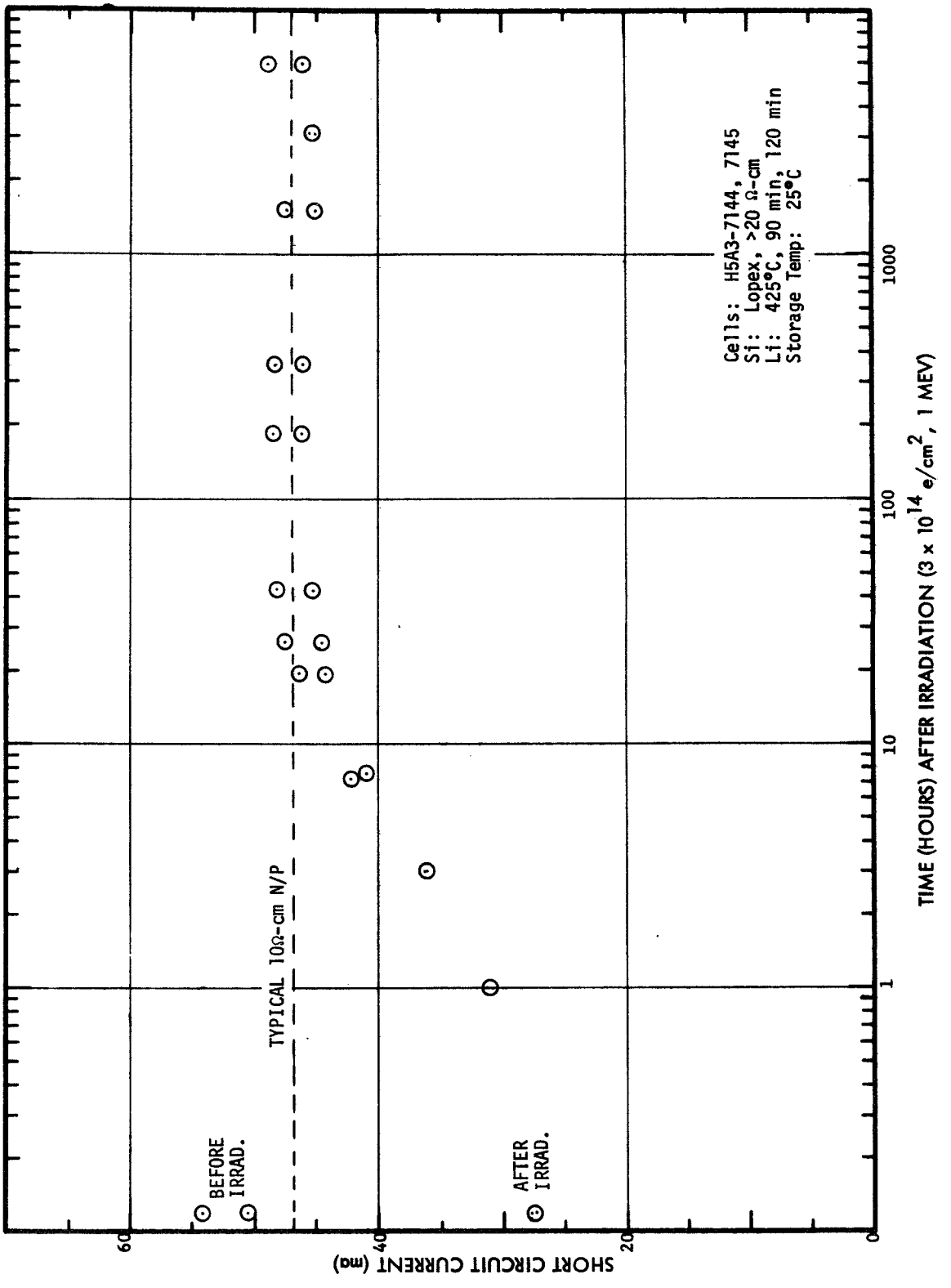


FIGURE 45 - RECOVERY OF GROUP H5A3 SOLAR CELLS, $3x10^{14}e/cm^2$

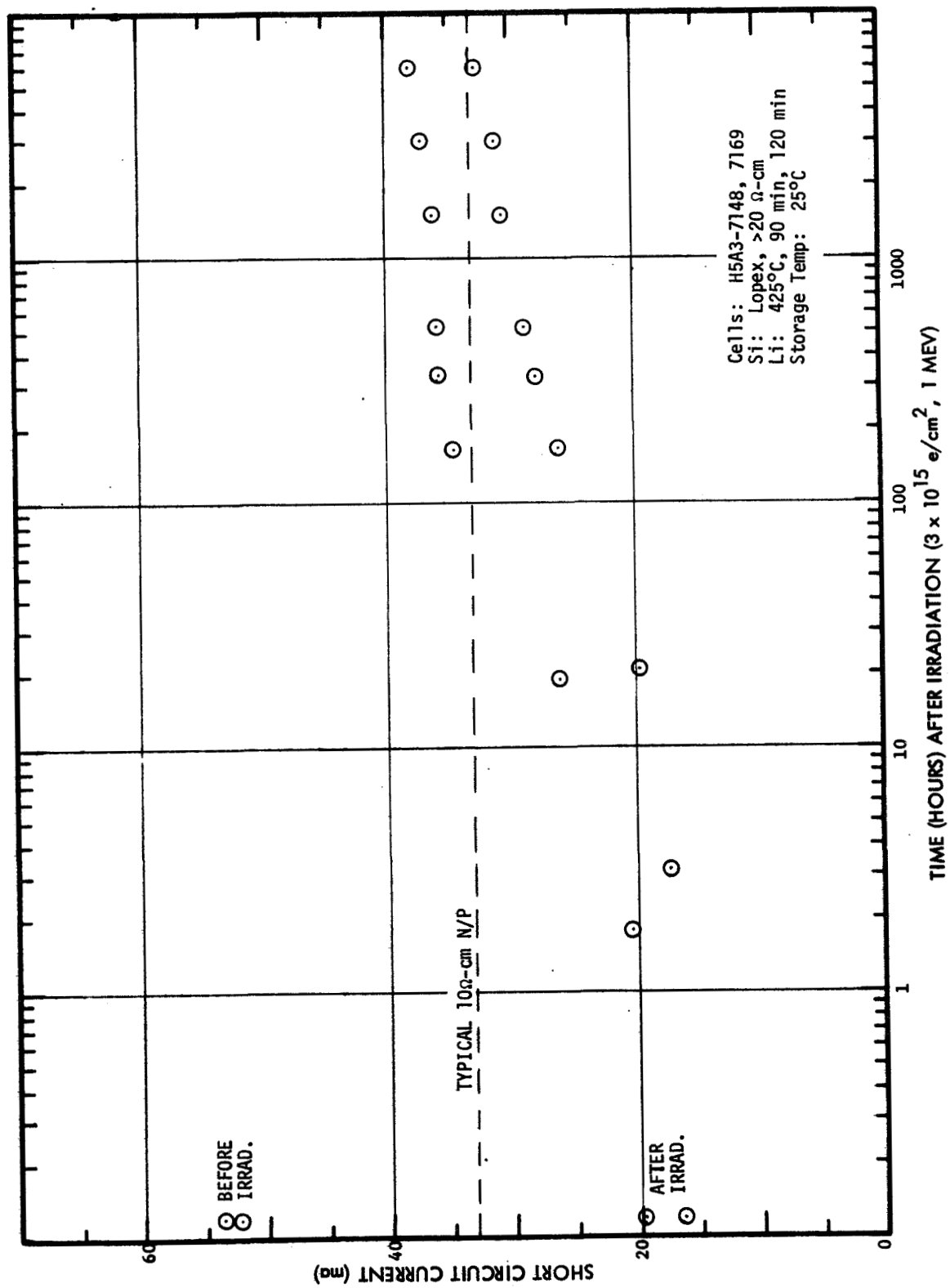


FIGURE 46 - RECOVERY OF GROUP H5A3 SOLAR CELLS, $3x10^{15}e/cm^2$

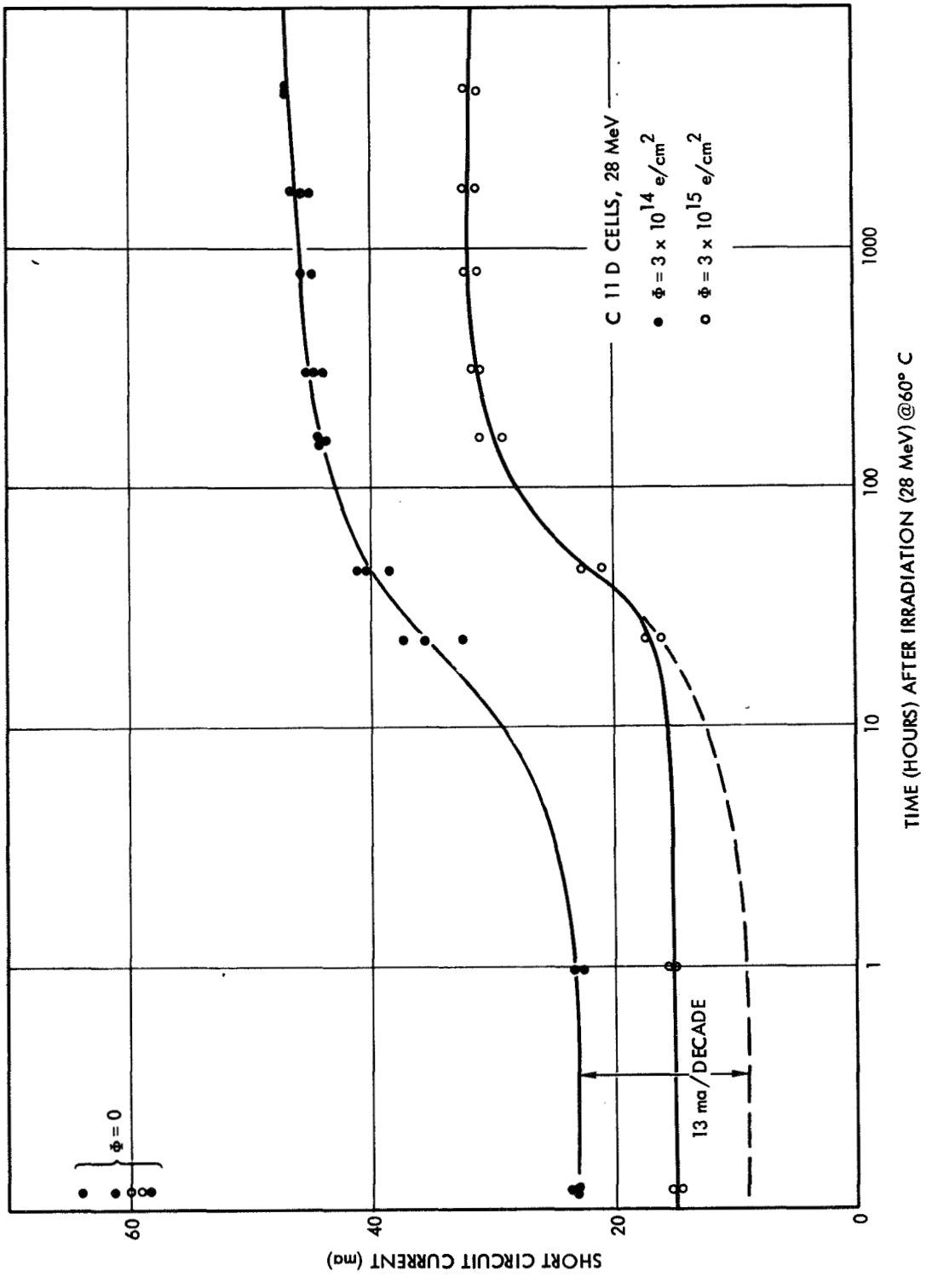


FIGURE 47. SHORT CIRCUIT CURRENT RECOVERY, 28 MeV

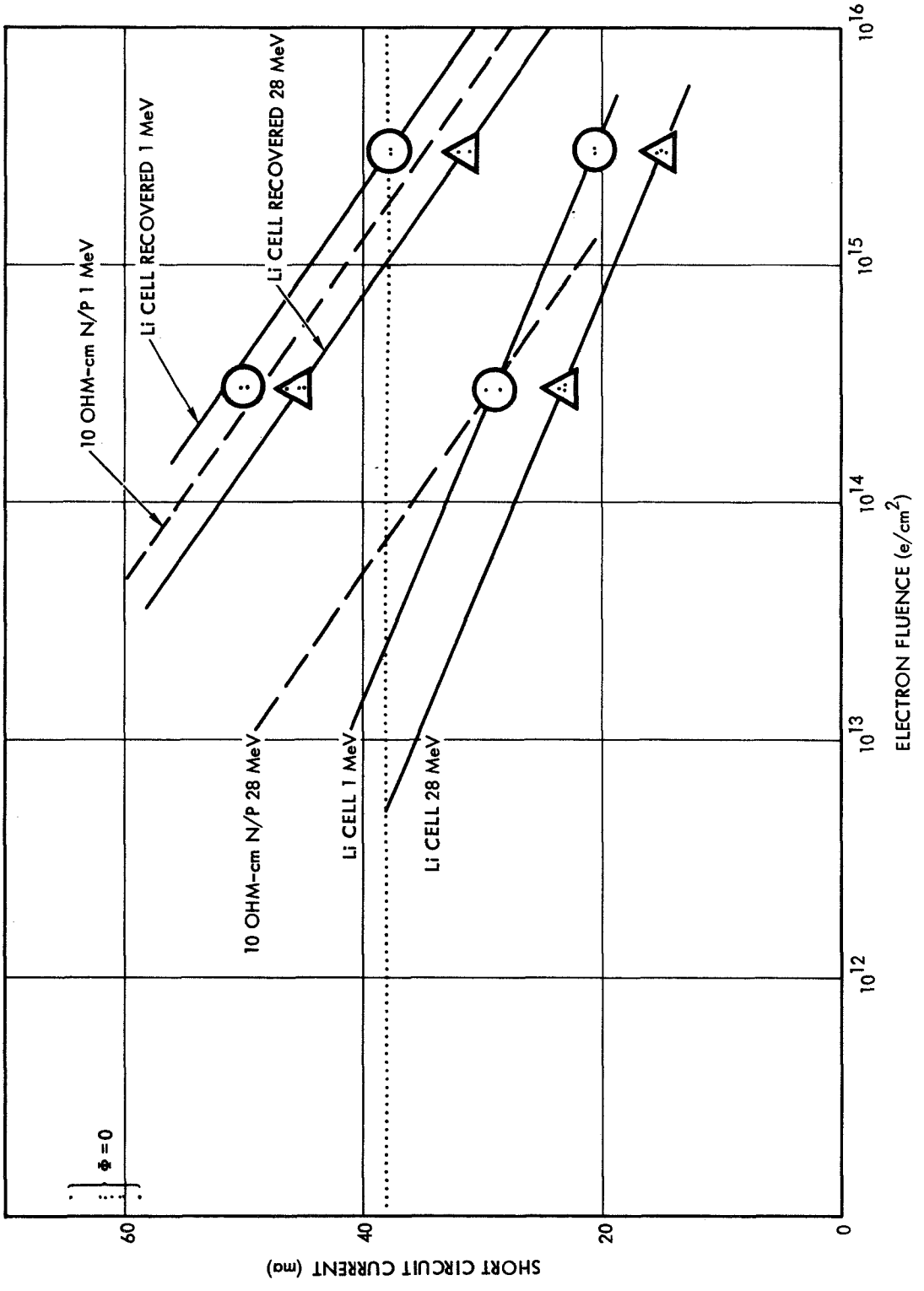


FIGURE 48. SHORT CIRCUIT CURRENT VERSUS ELECTRON FLUENCE

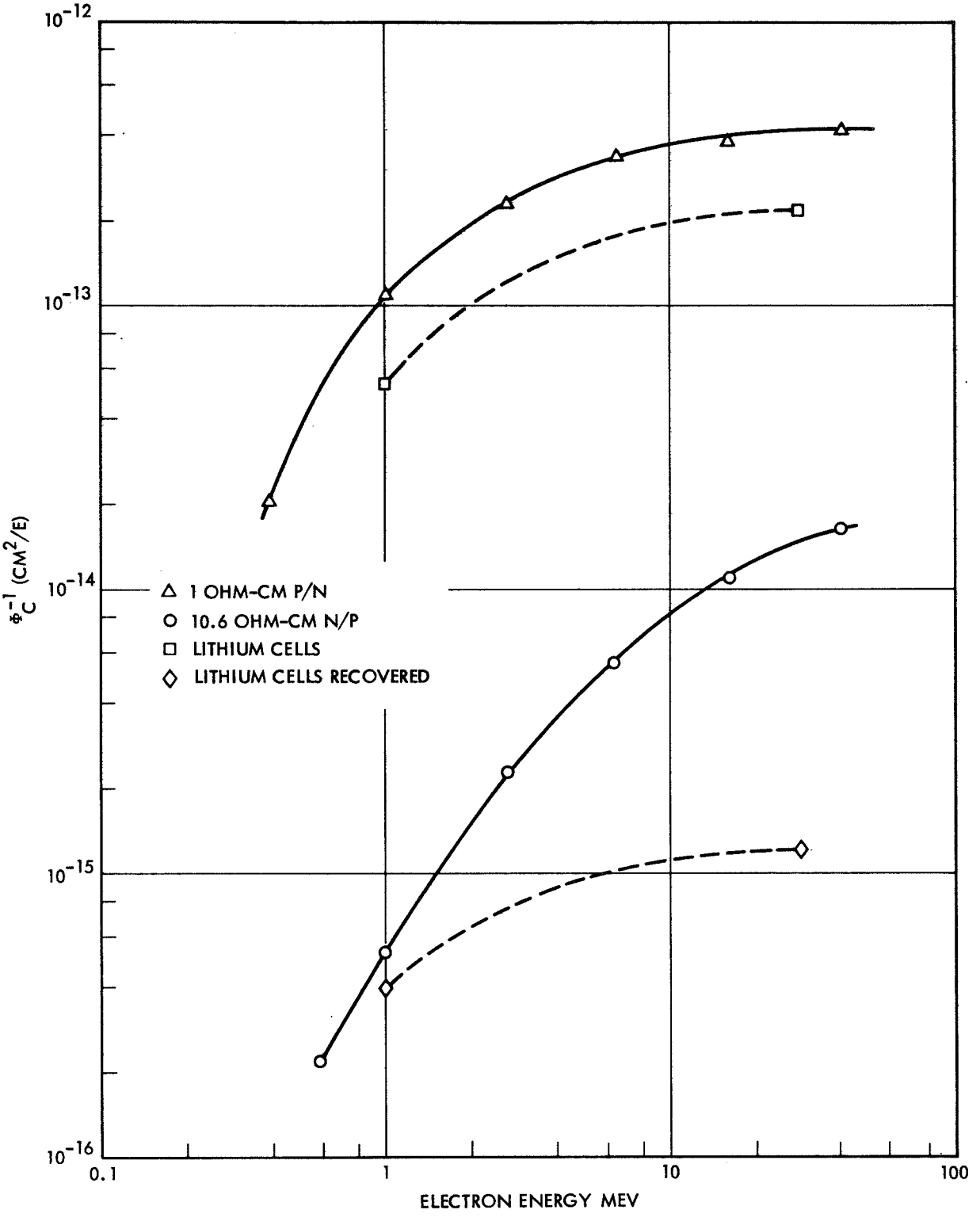


FIGURE 49. CRITICAL FLUENCE VERSUS ELECTRON ENERGY

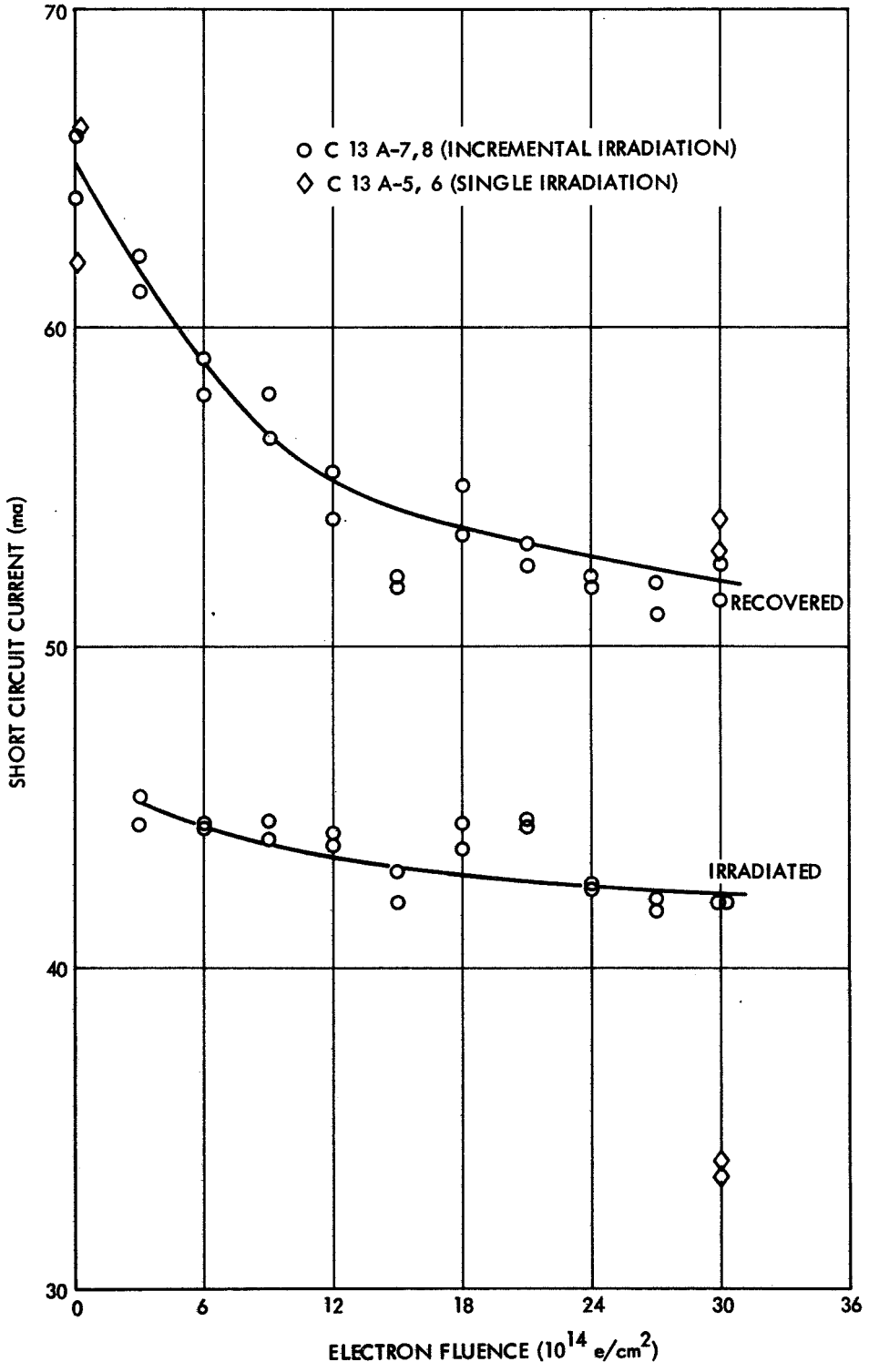


Figure 50. Short Circuit Current Changes During Incremental Irradiation

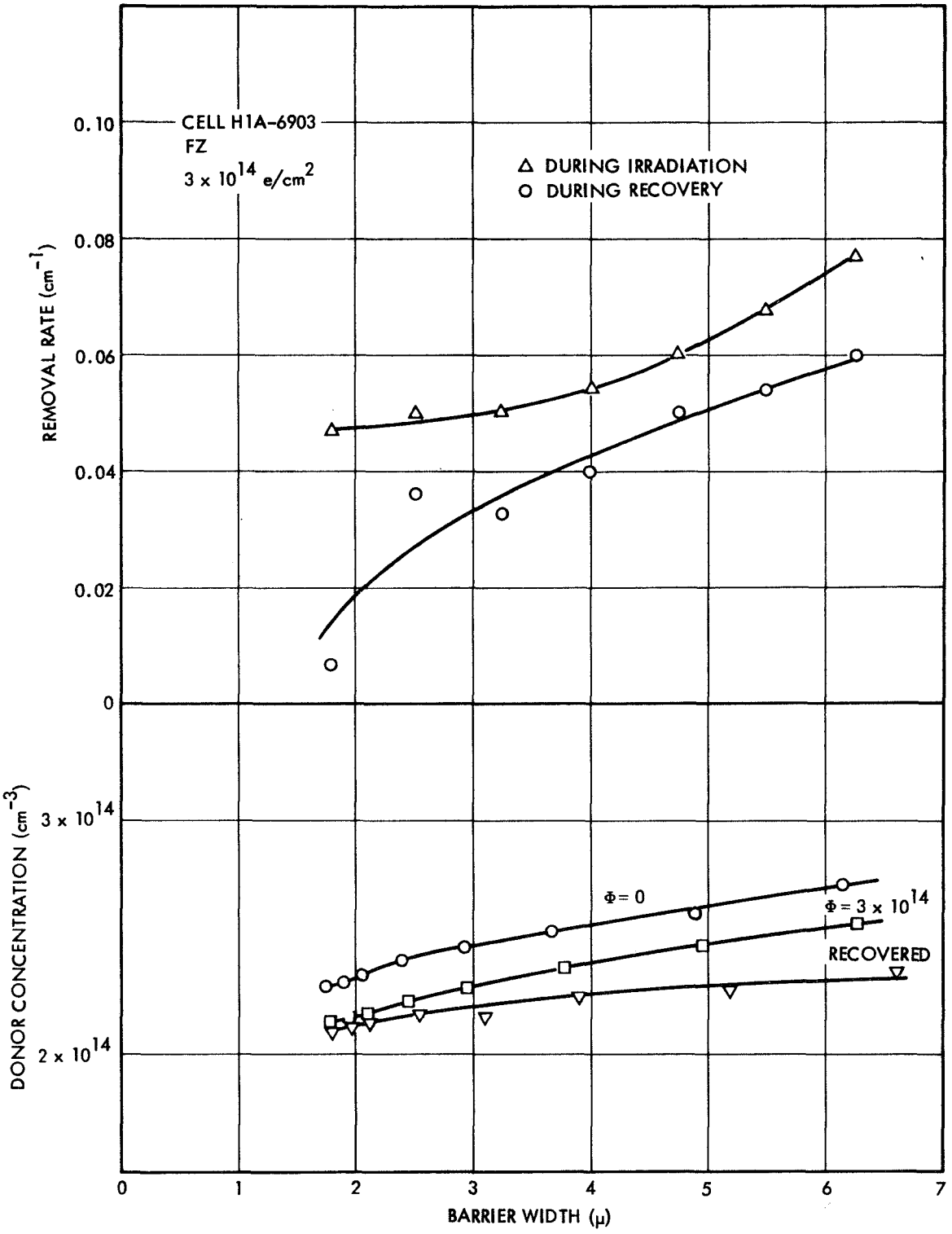


FIGURE 51. CARRIER REMOVAL IN CELL H1A-6903

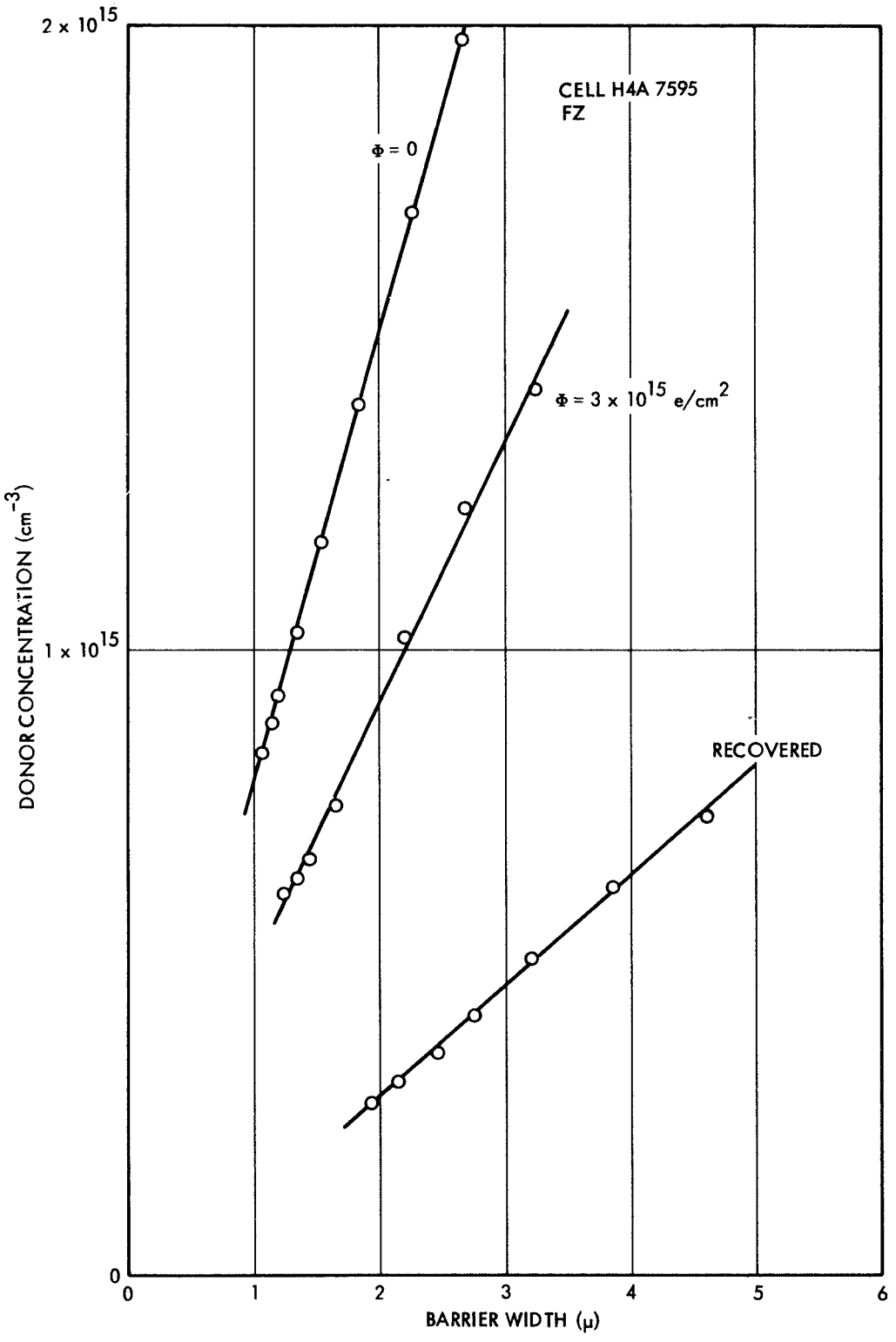


FIGURE 52. CARRIER REMOVAL IN CELL H4A-7595

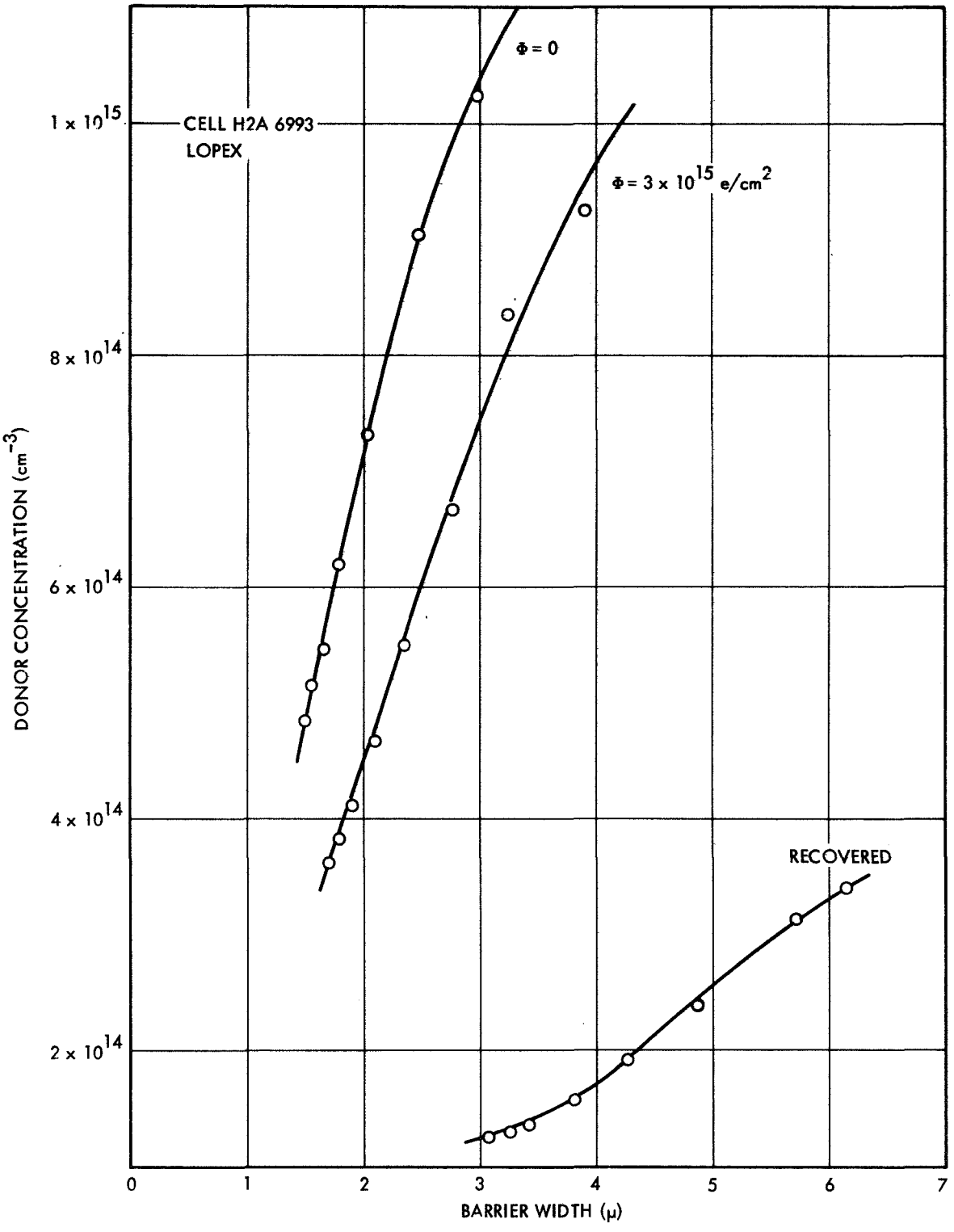


FIGURE 53. CARRIER REMOVAL IN CELL H2A-6993

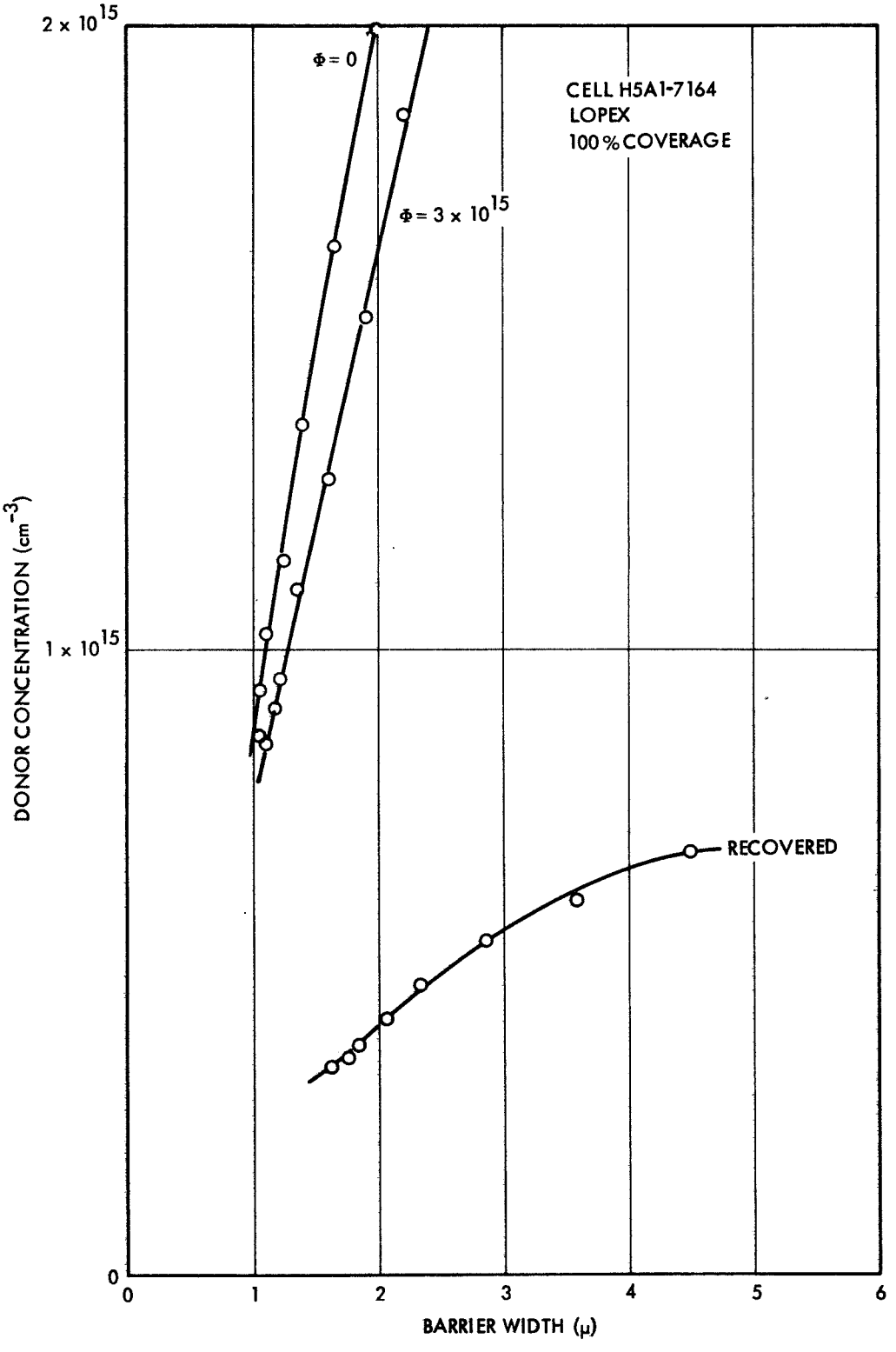


FIGURE 54. CARRIER REMOVAL IN CELL H5A1-7164

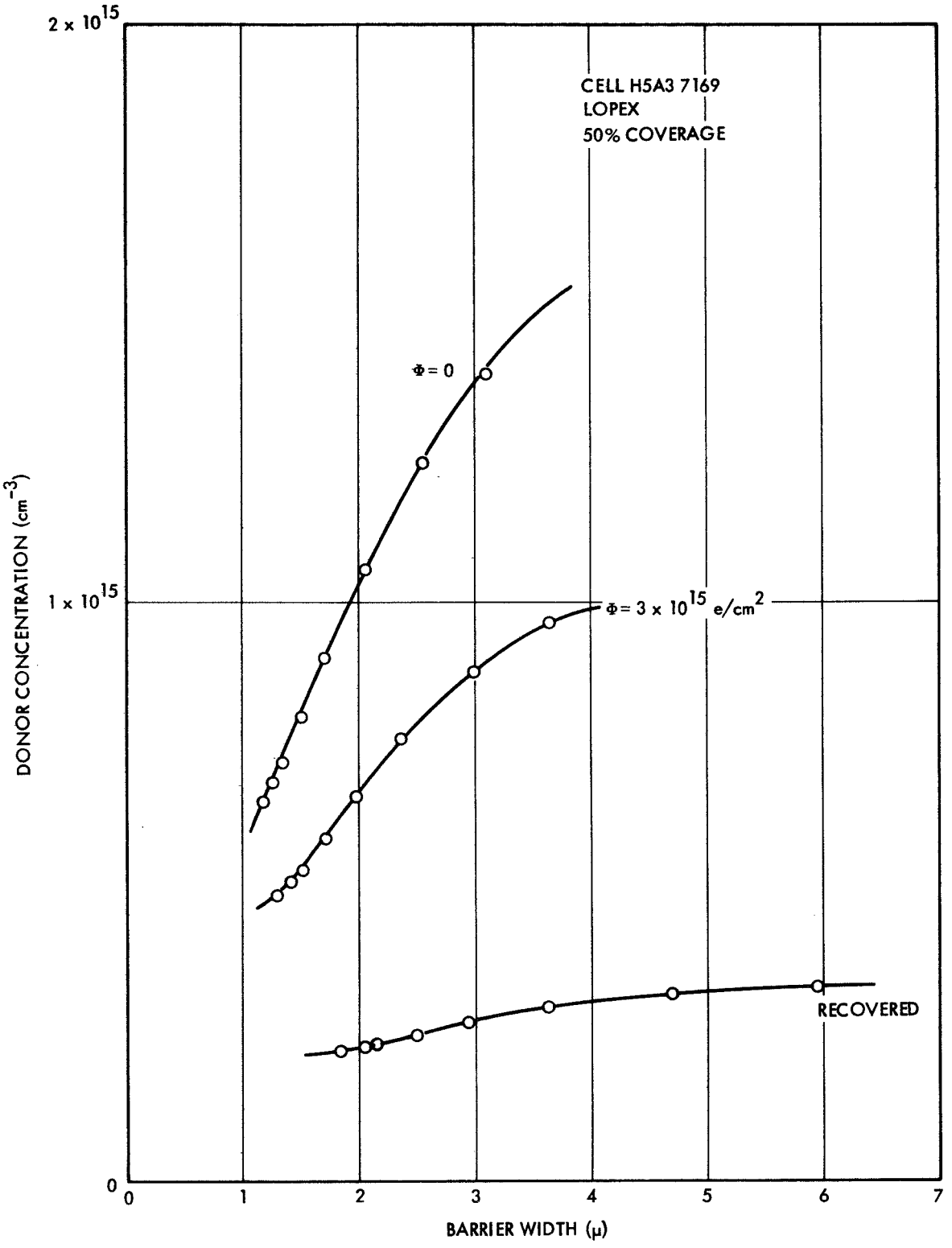


FIGURE 55. CARRIER REMOVAL IN CELL H5A-7169

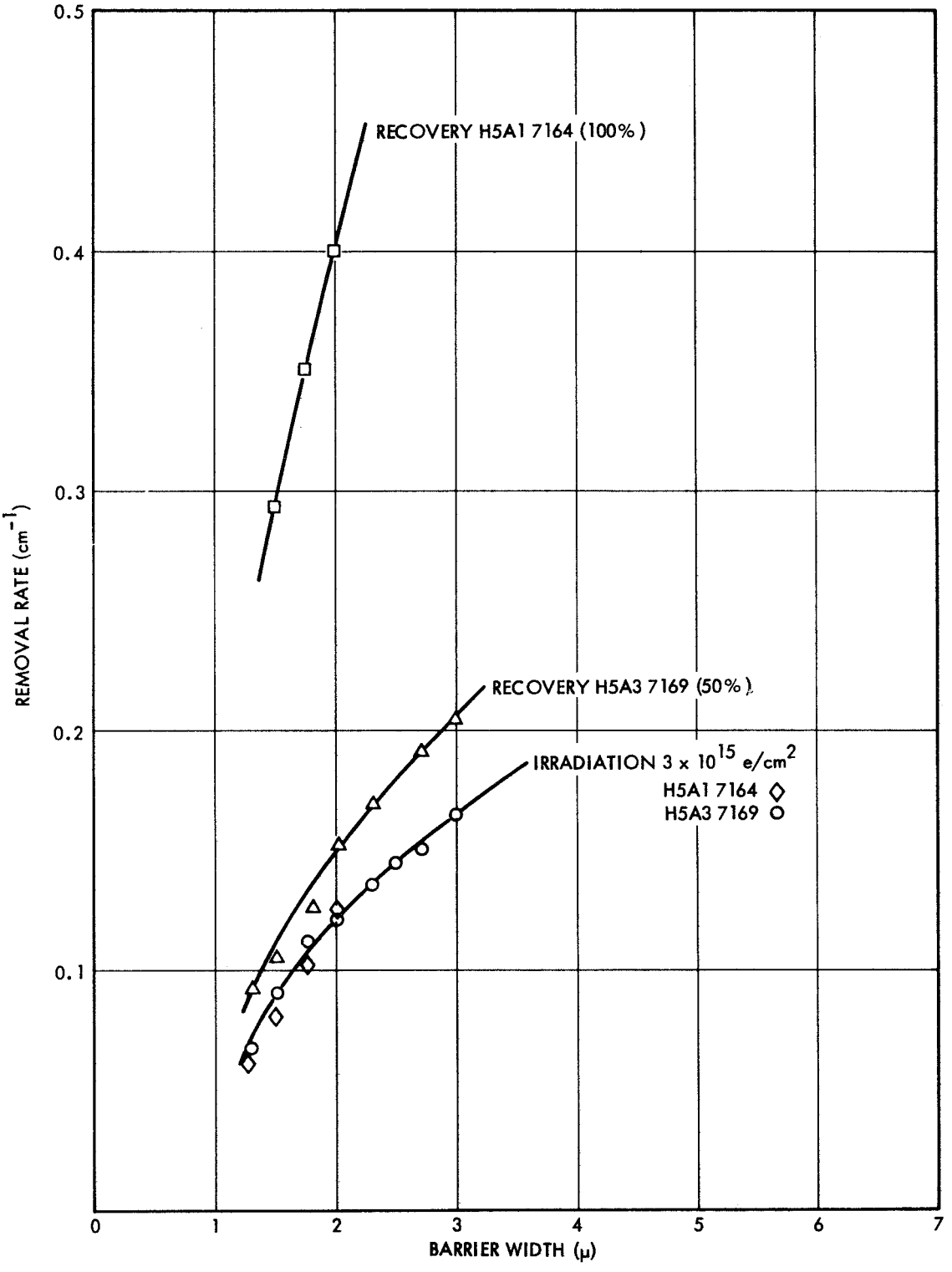


FIGURE 56. REMOVAL RATE, HELIOTEK, LOPEX

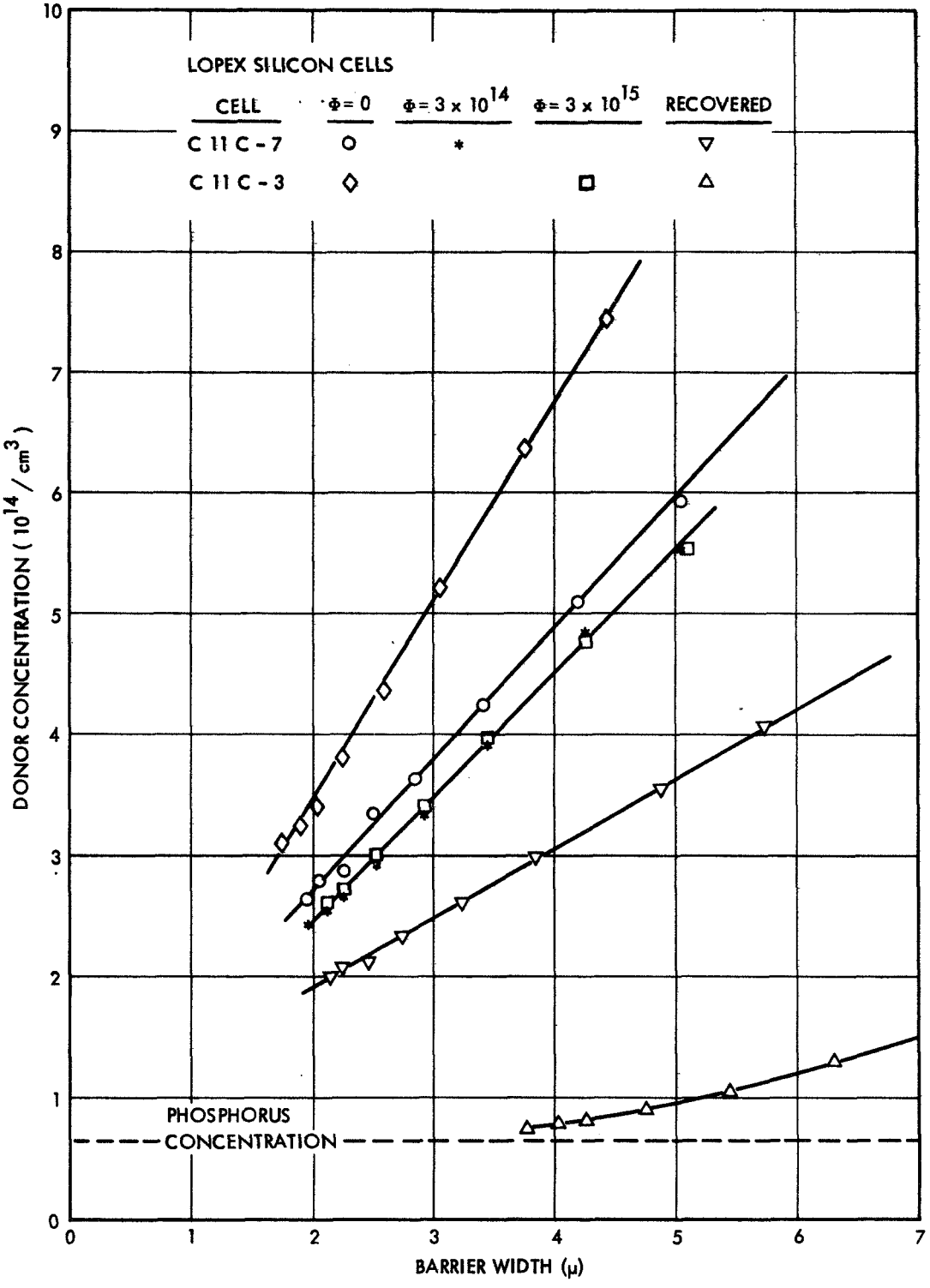


FIGURE 57. CARRIER REMOVAL IN CELLS OF C11C GROUP

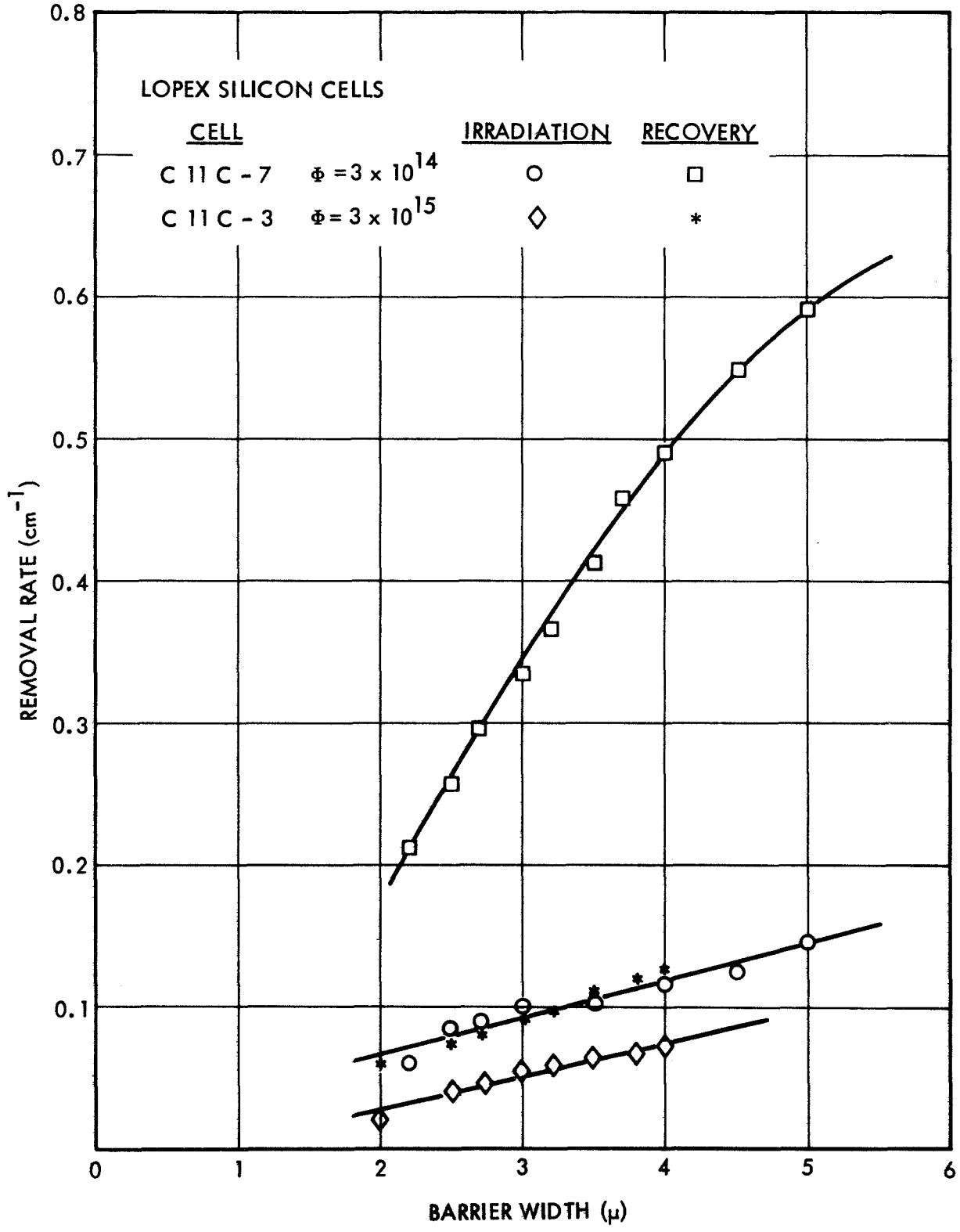


FIGURE 58. REMOVAL RATES OF CELLS OF C11C GROUP

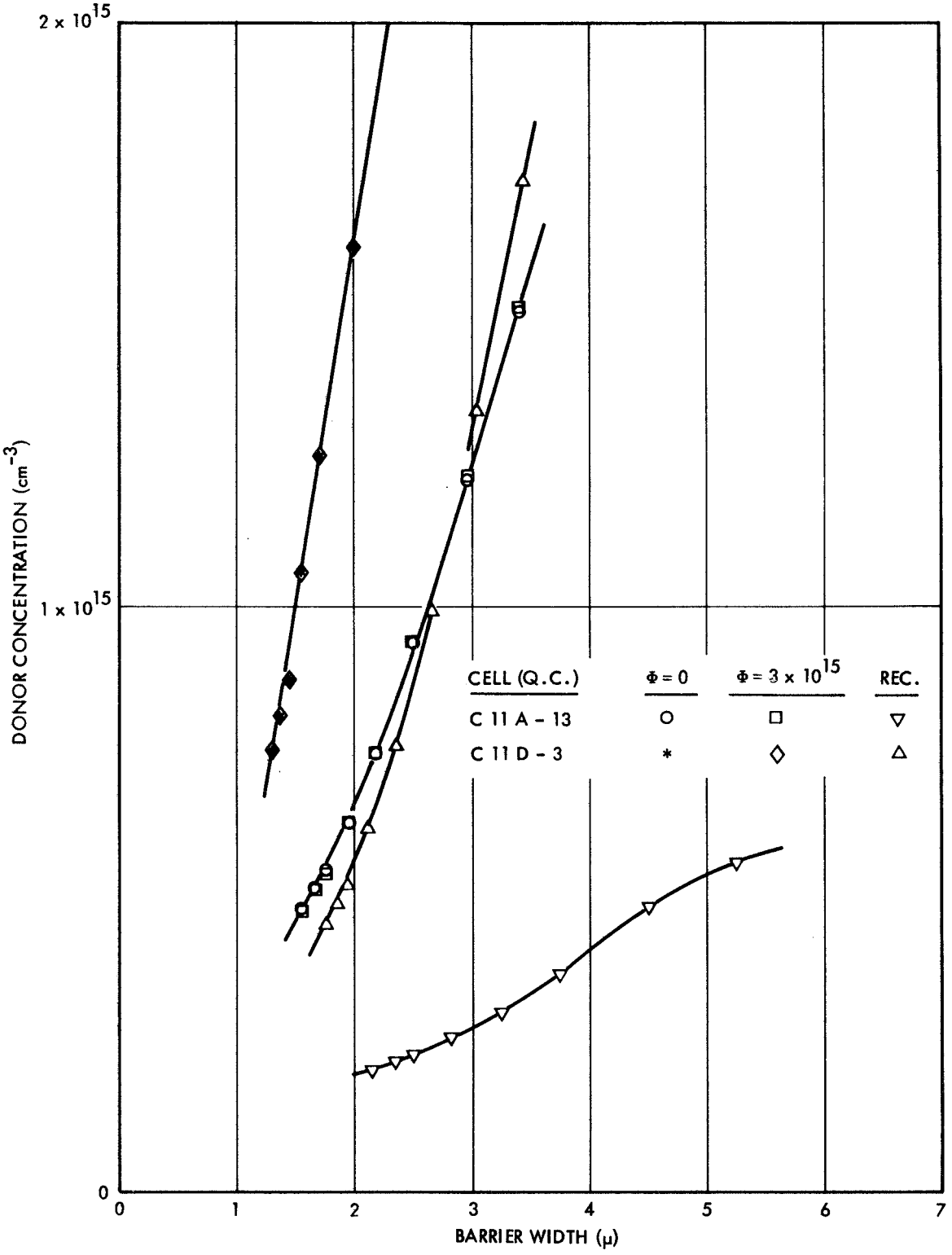


FIGURE 59. CARRIER REMOVAL IN CELL OF C11A & C11D GROUPS

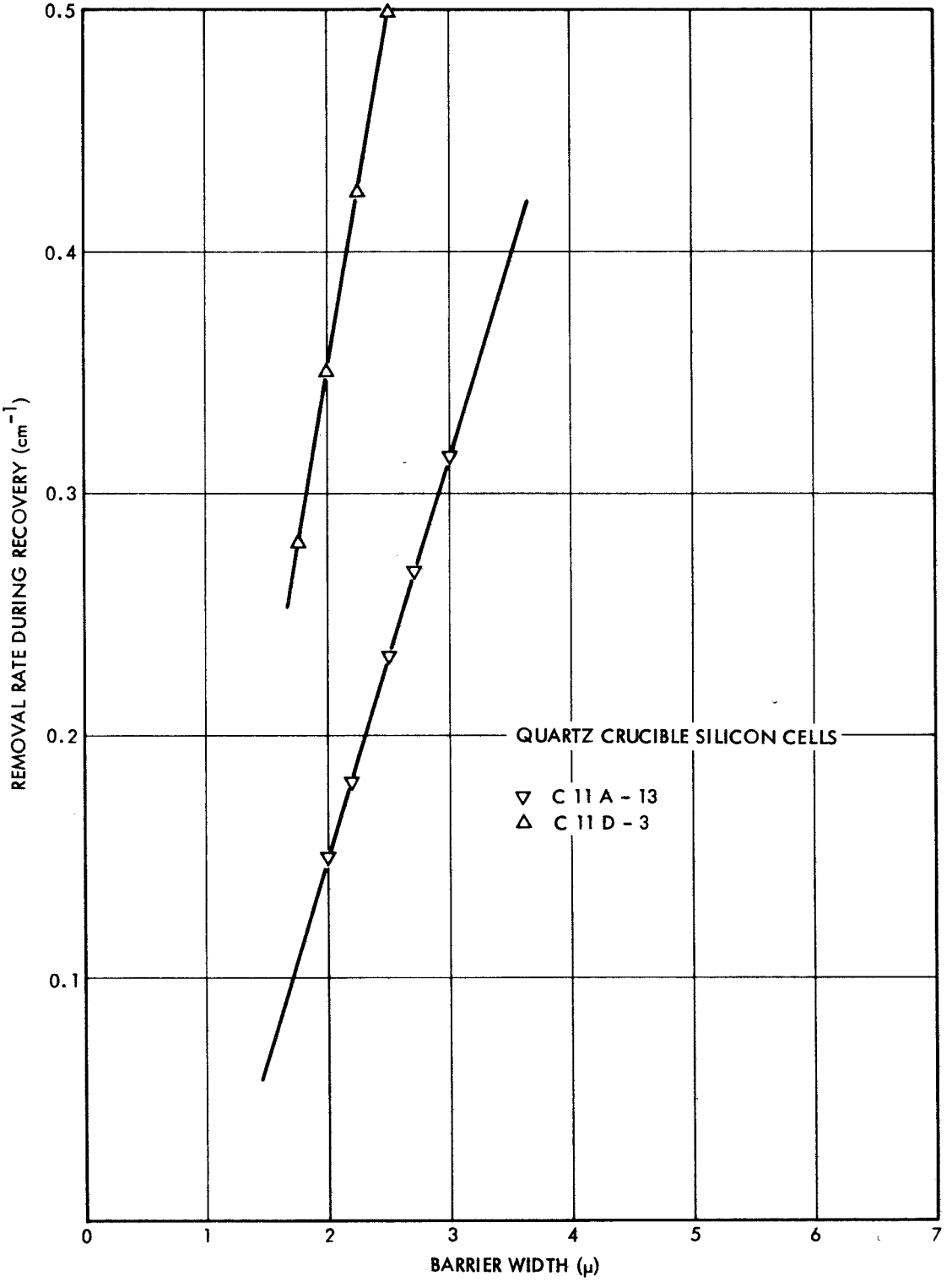


FIGURE 60. REMOVAL RATES OF CELLS OF C11A & C11D GROUPS

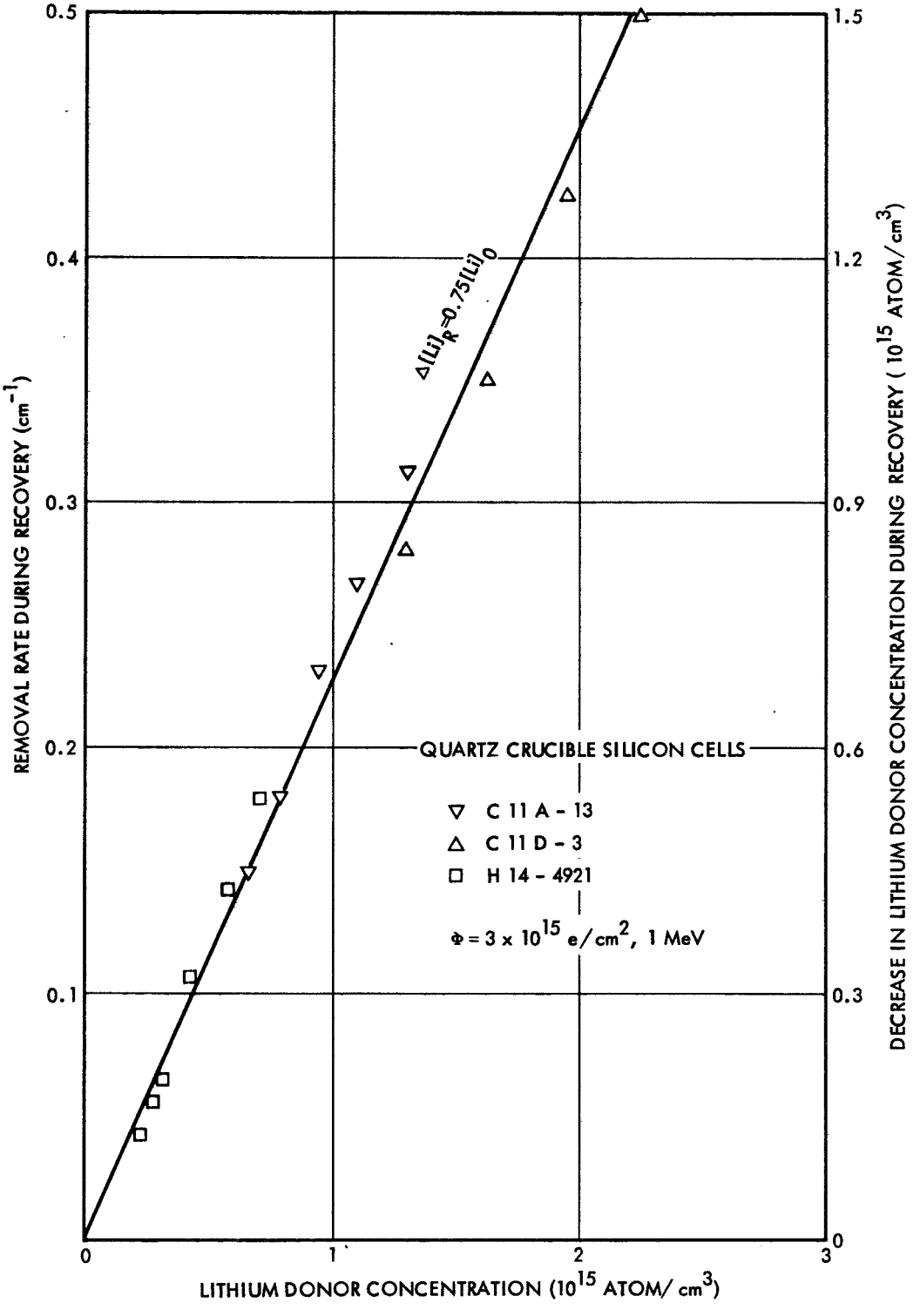


FIGURE 61. REMOVAL RATE VERSUS LITHIUM DONOR CONCENTRATION

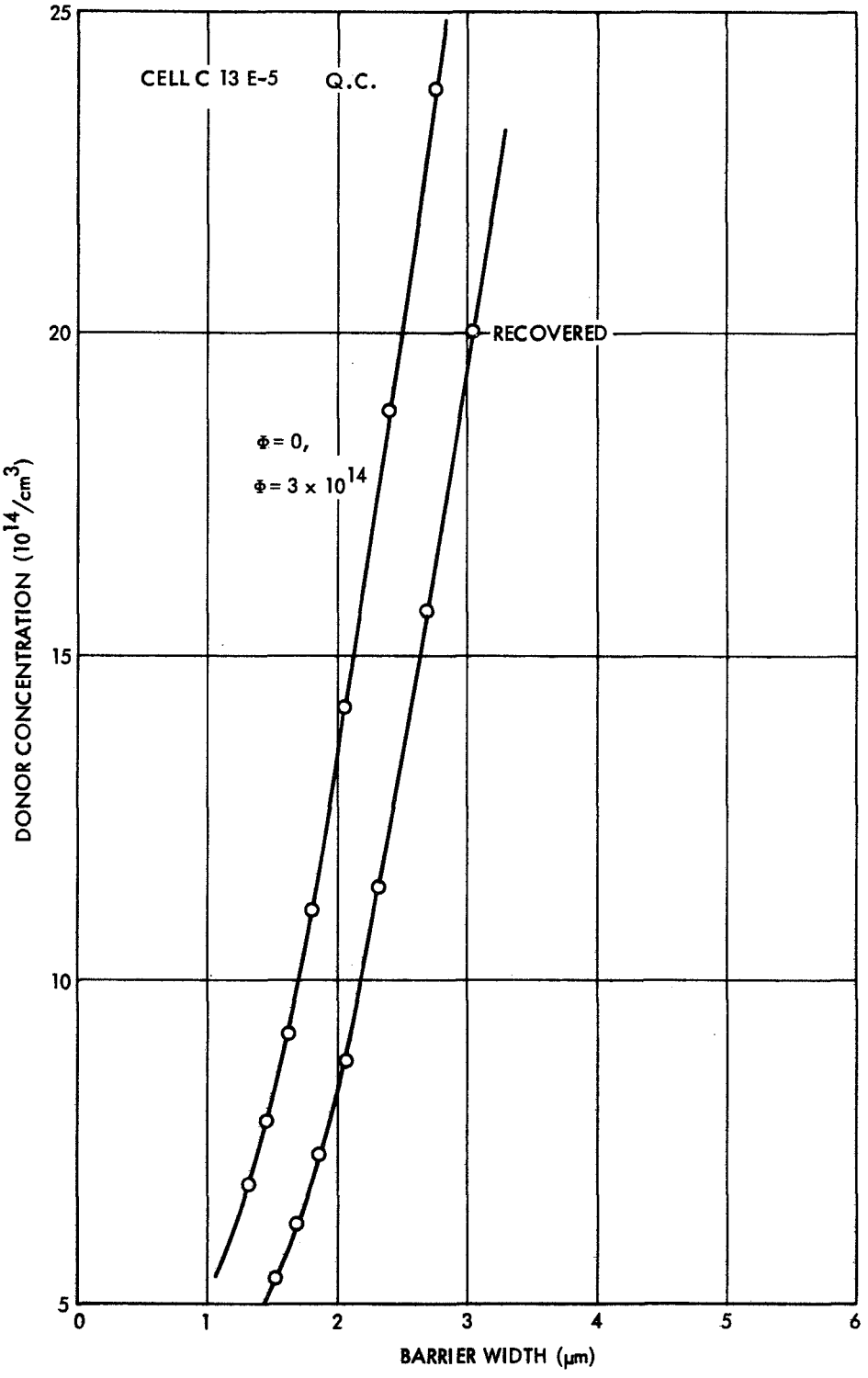


Figure 62. Donor Concentration versus Barrier Width
C13A-6

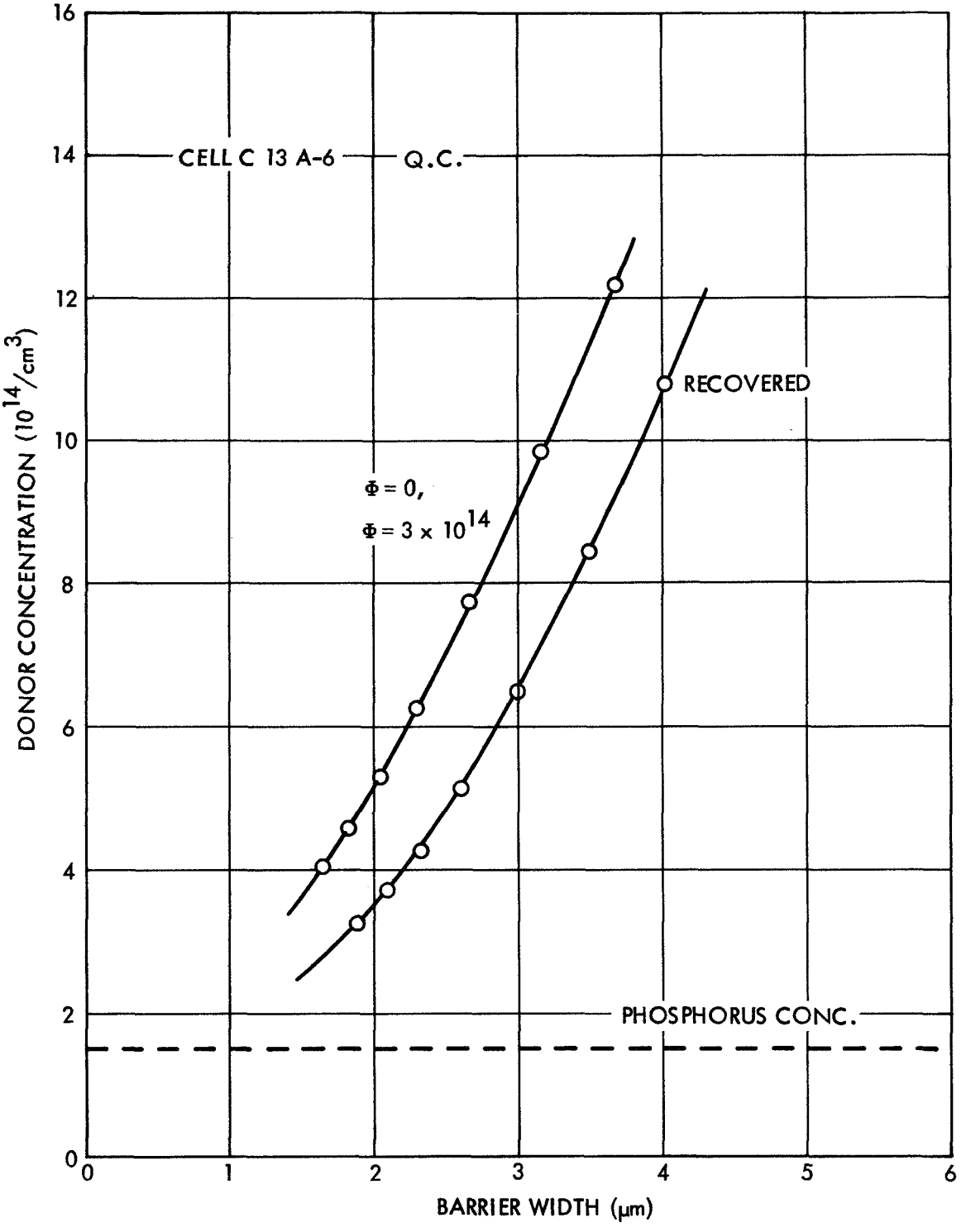


Figure 63. Donor Concentration versus Barrier Width, C13E-5

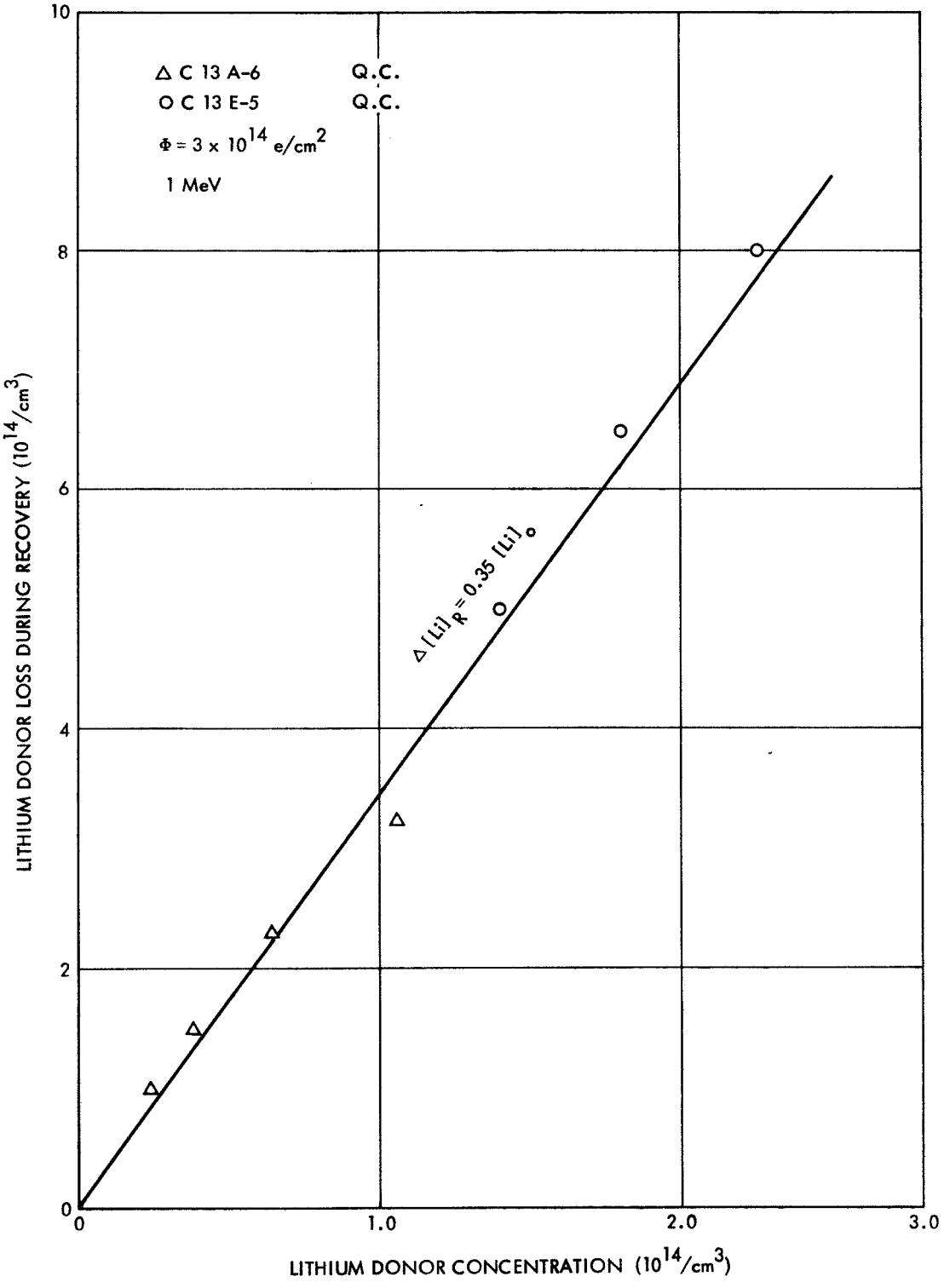


Figure 64. Lithium Donor Loss During Recovery, $3 \times 10^{14}$ e/cm$^2$

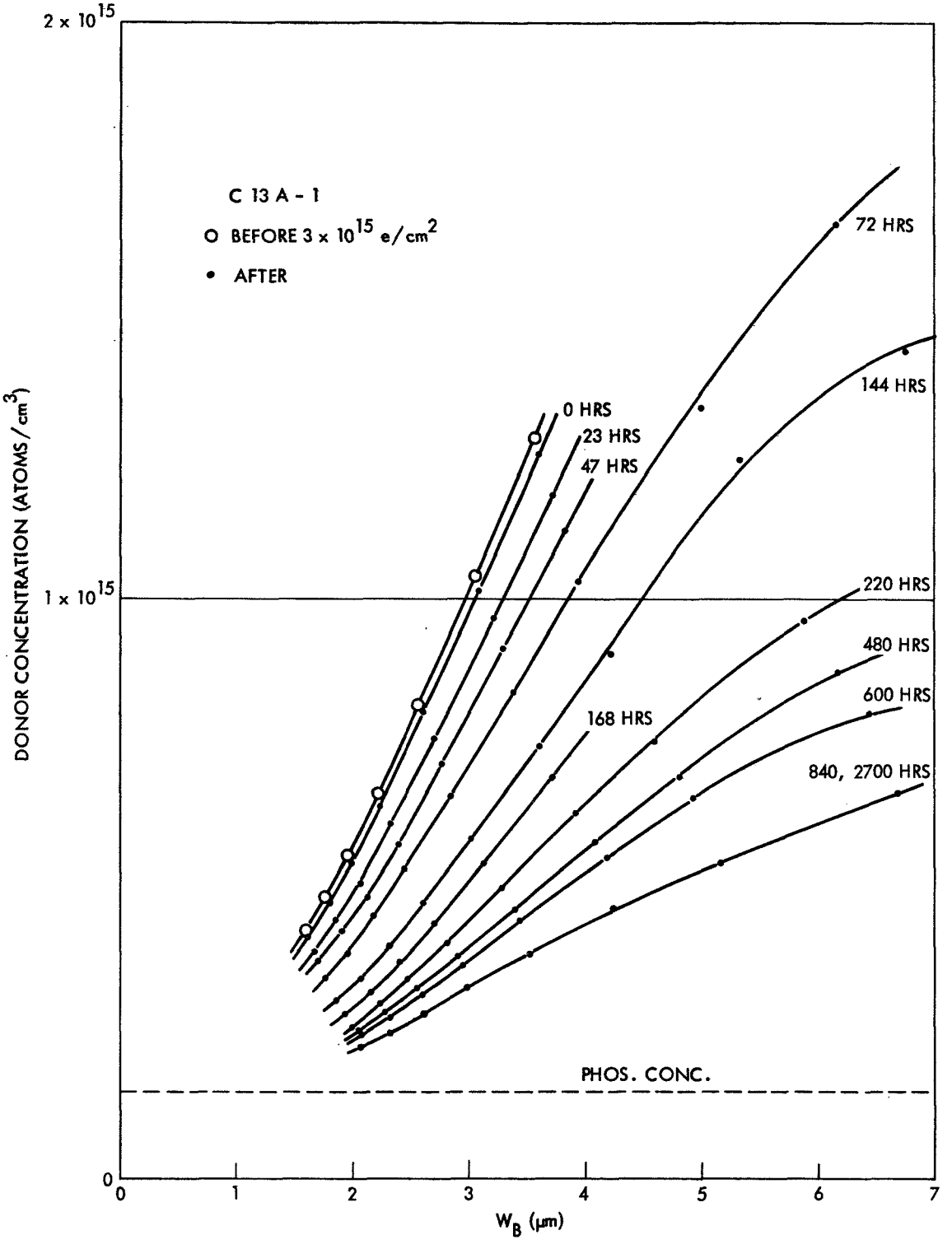


Figure 65. Donor Concentration During Recovery, C13A-1

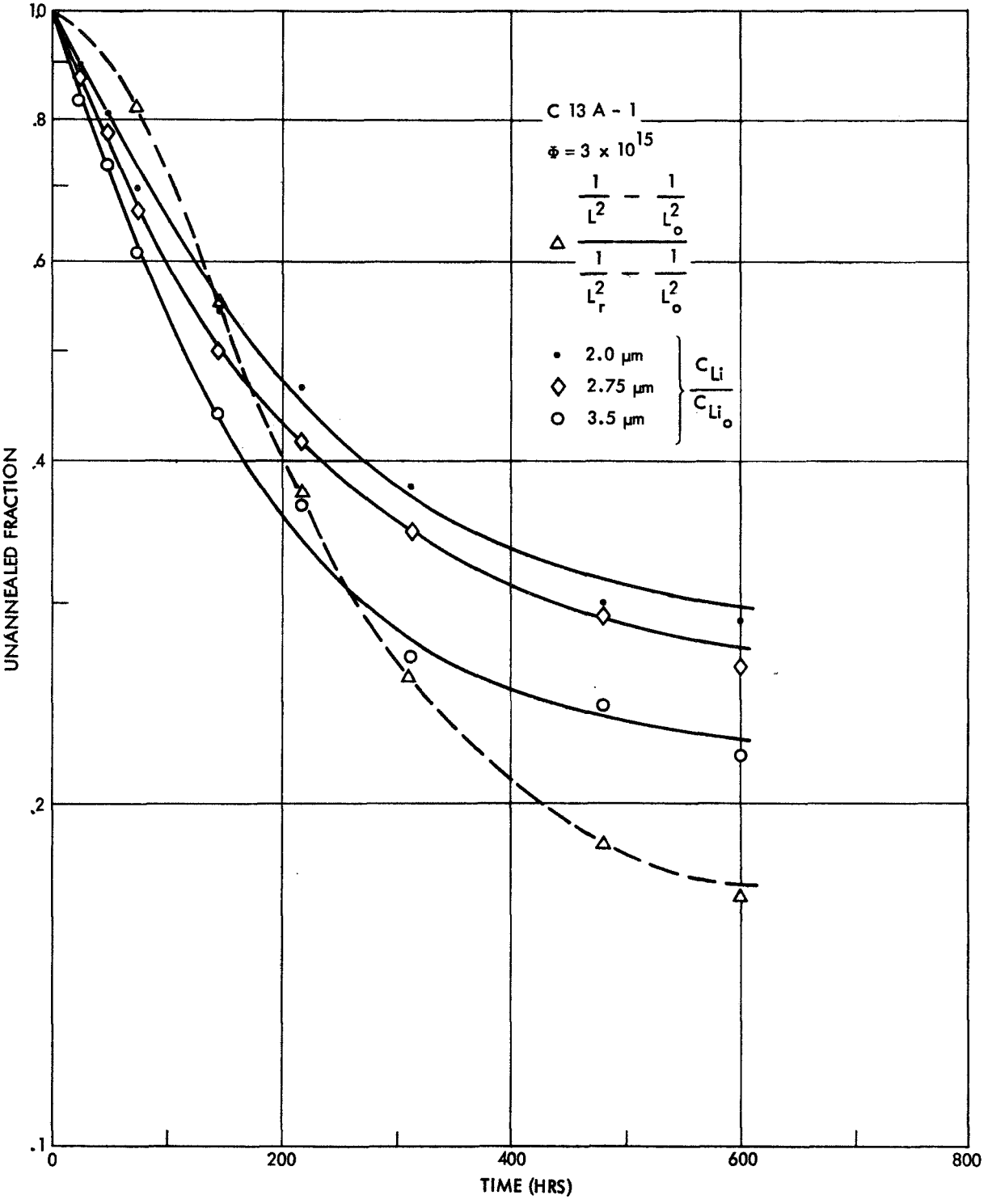


Figure 66. Change in Lithium Donor Concentration and Diffusion Length During Recovery, C13A-1

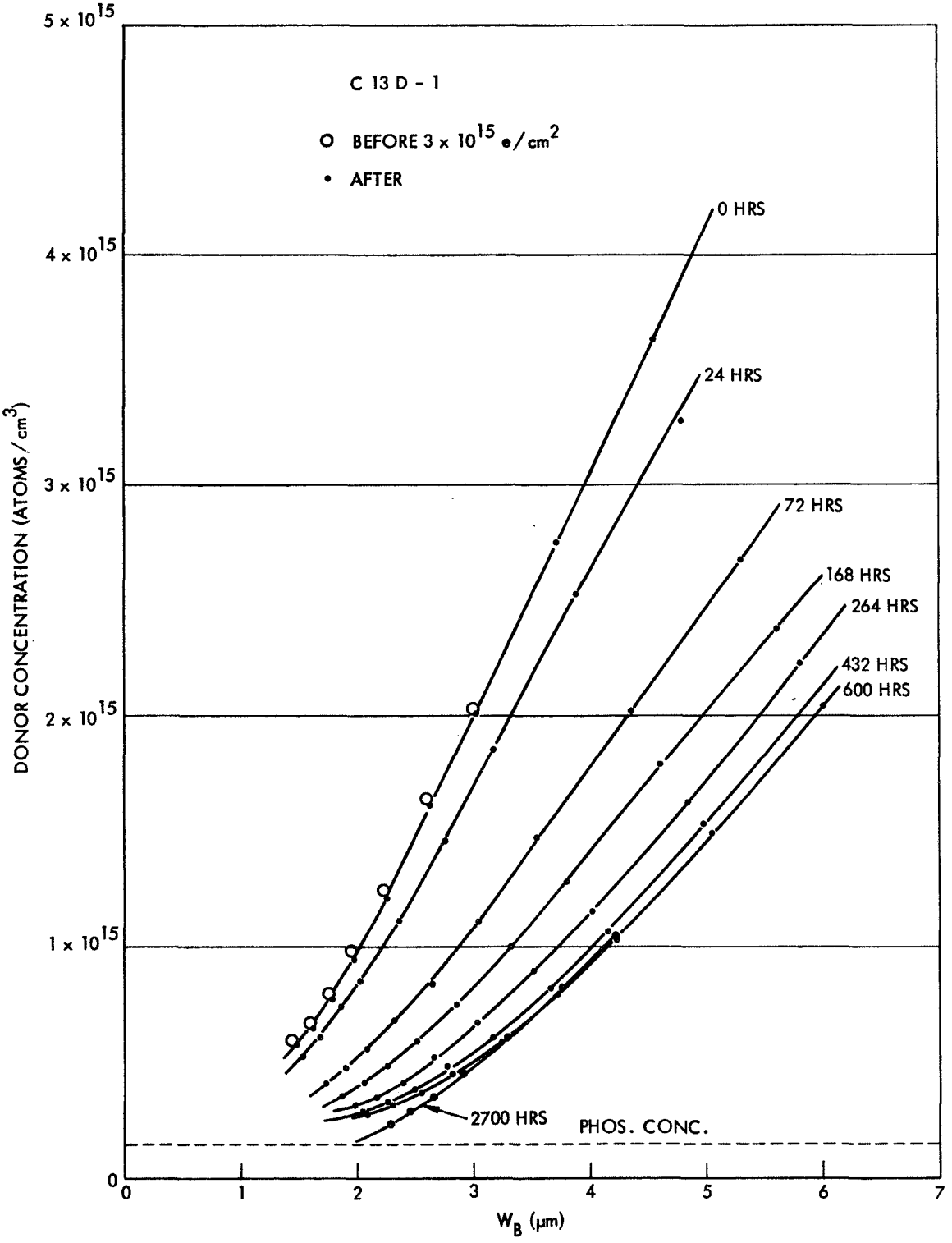


Figure 67. Donor Concentration During Recovery, C13D-1

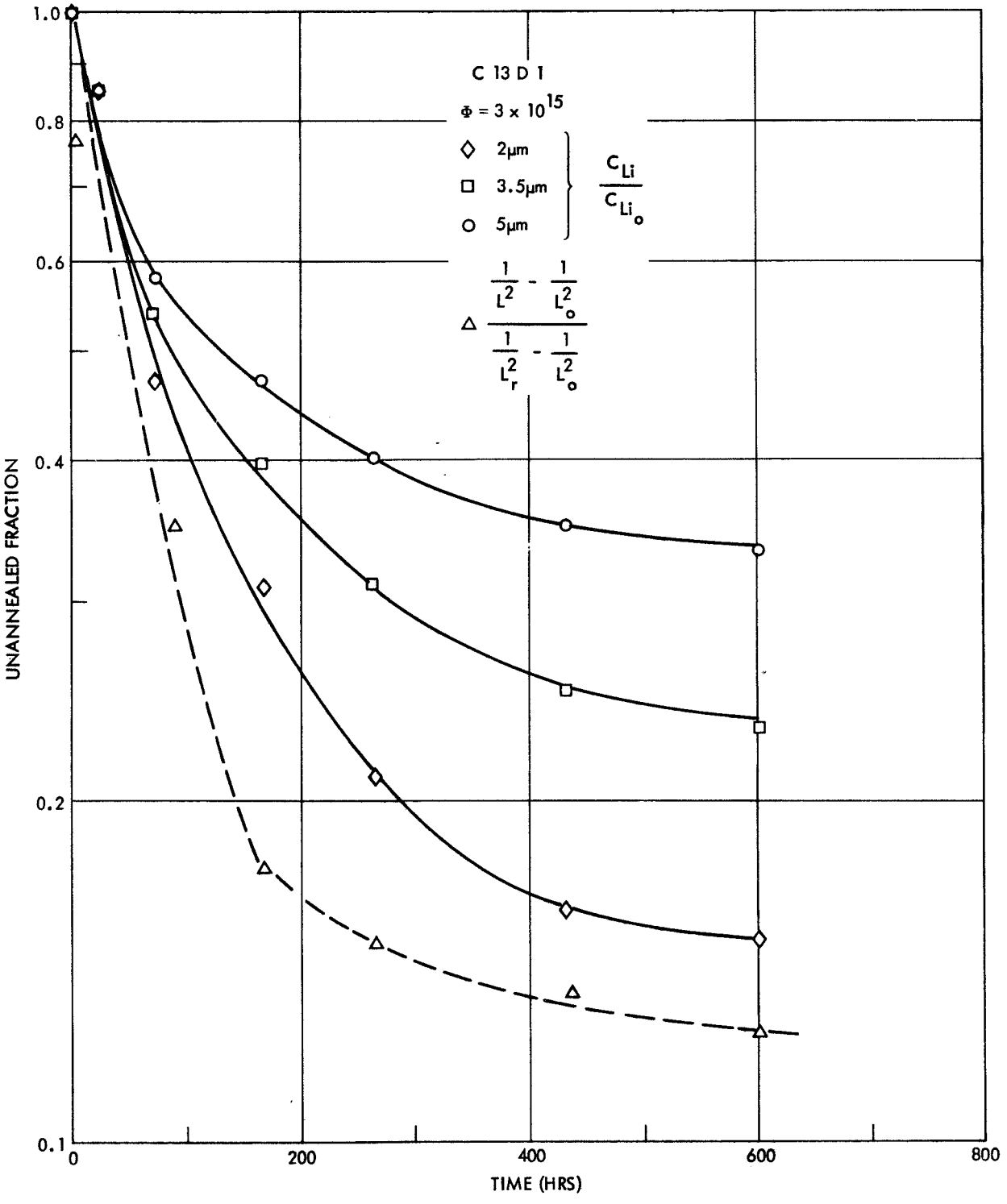


Figure 68. Change in Lithium Donor Concentration and Diffusion Length During Recovery, C13D-1

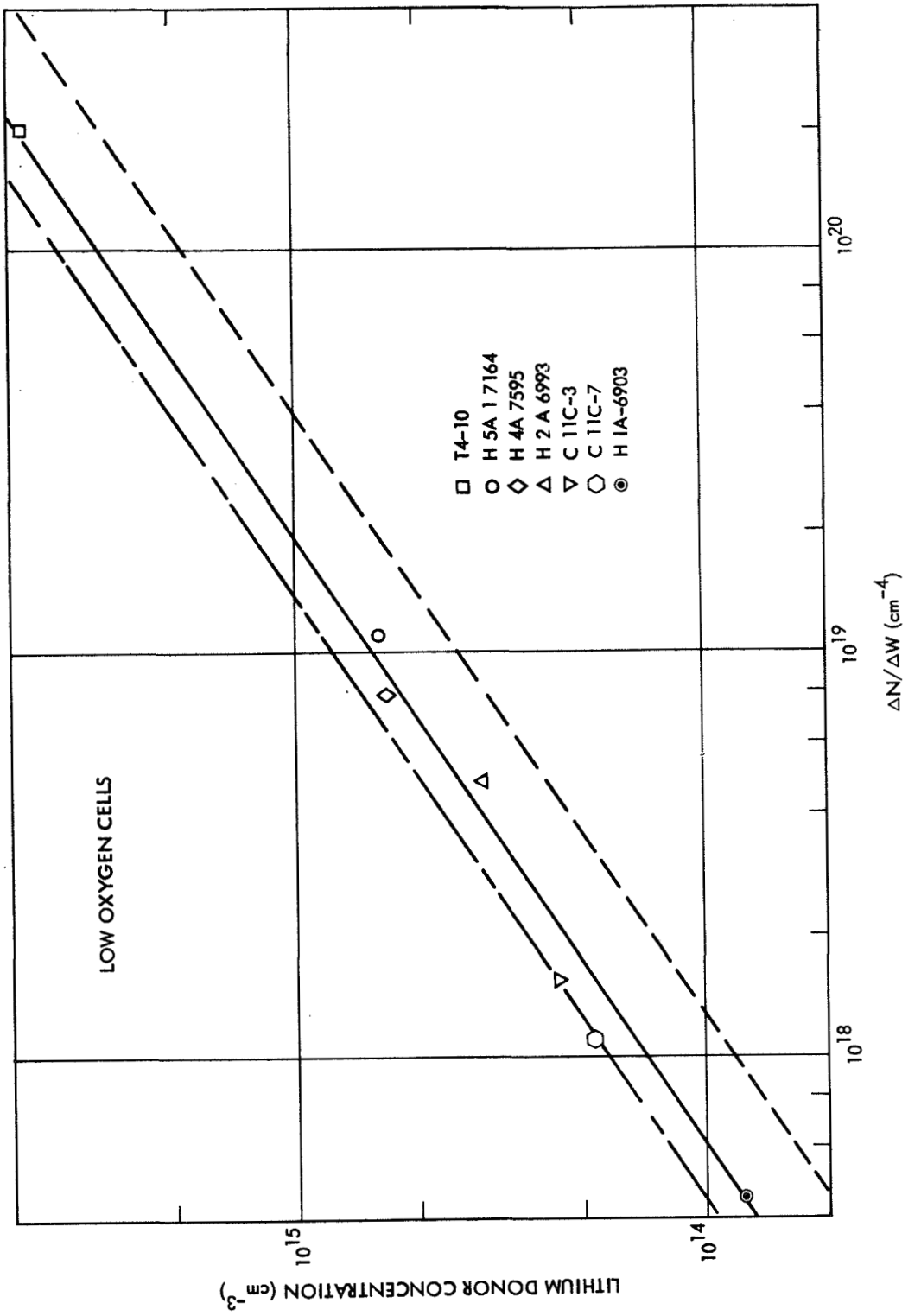


Figure 69. Lithium Donor Concentration versus Gradient, Low Oxygen Cells

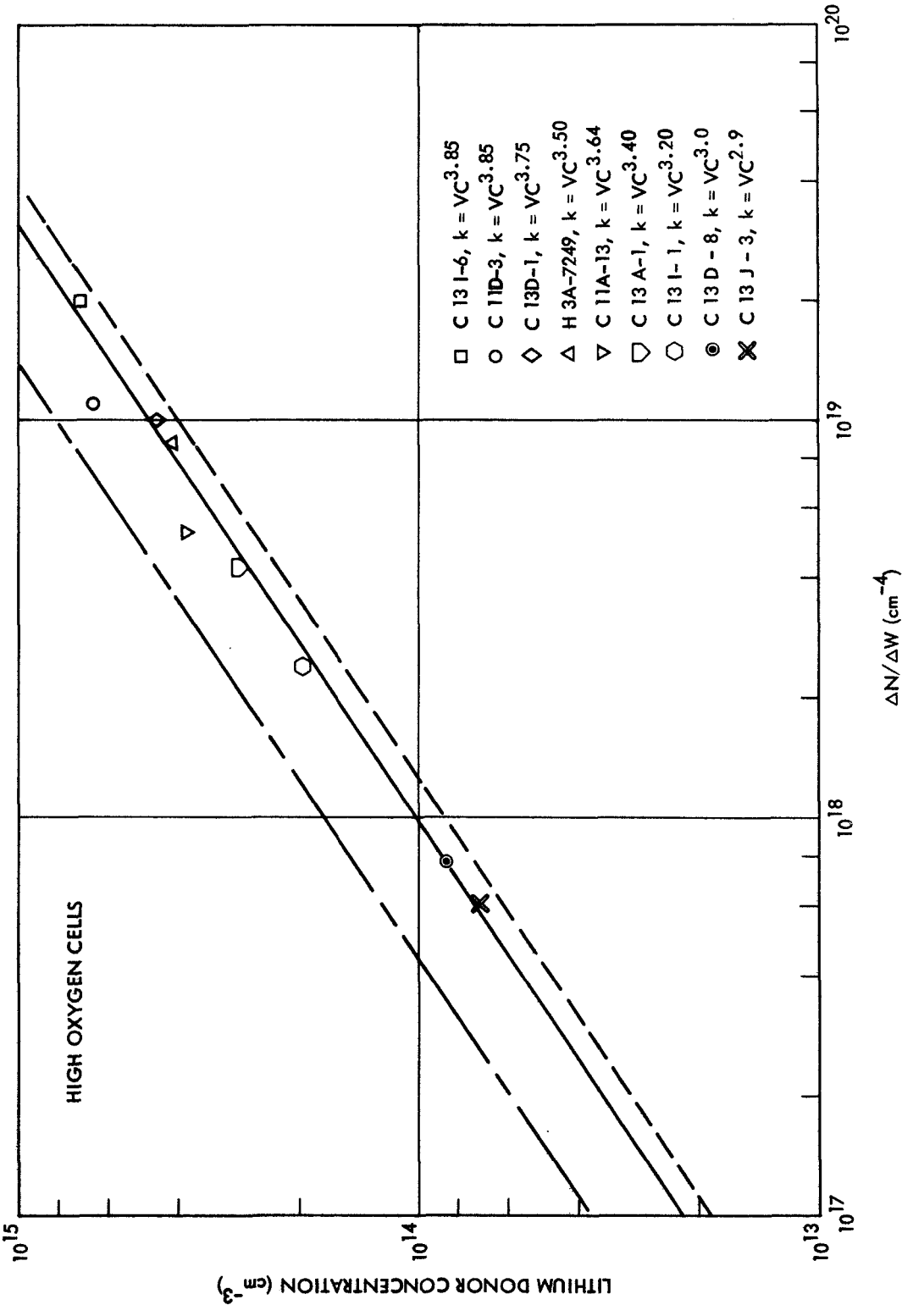


Figure 70. Lithium Donor Concentration versus Gradient, High Oxygen Cells

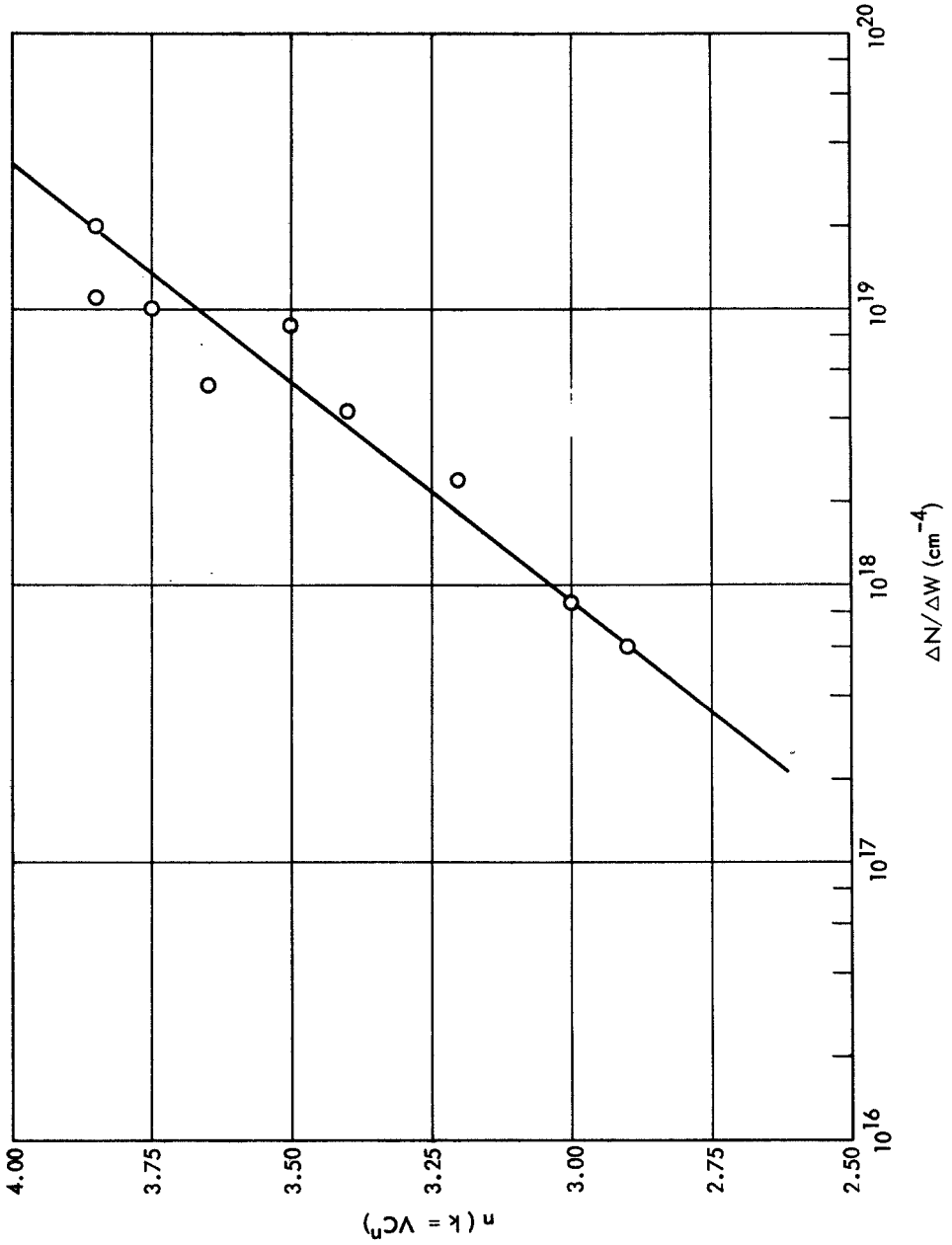


Figure 71. Exponent "n" versus Gradient, High Oxygen Cells

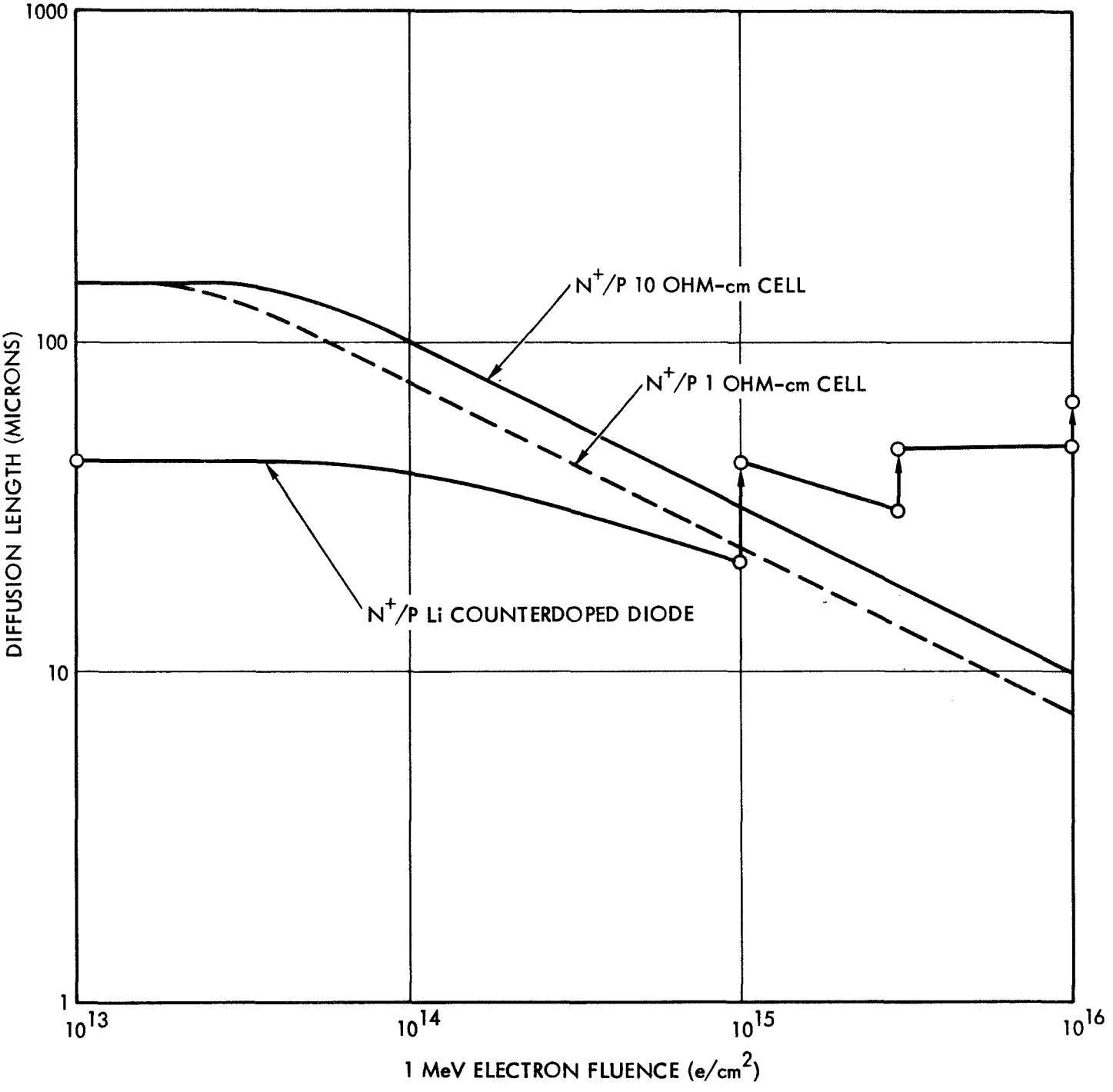


FIGURE 72. LITHIUM COUNTERDOPED DIODE, WACKER FZ

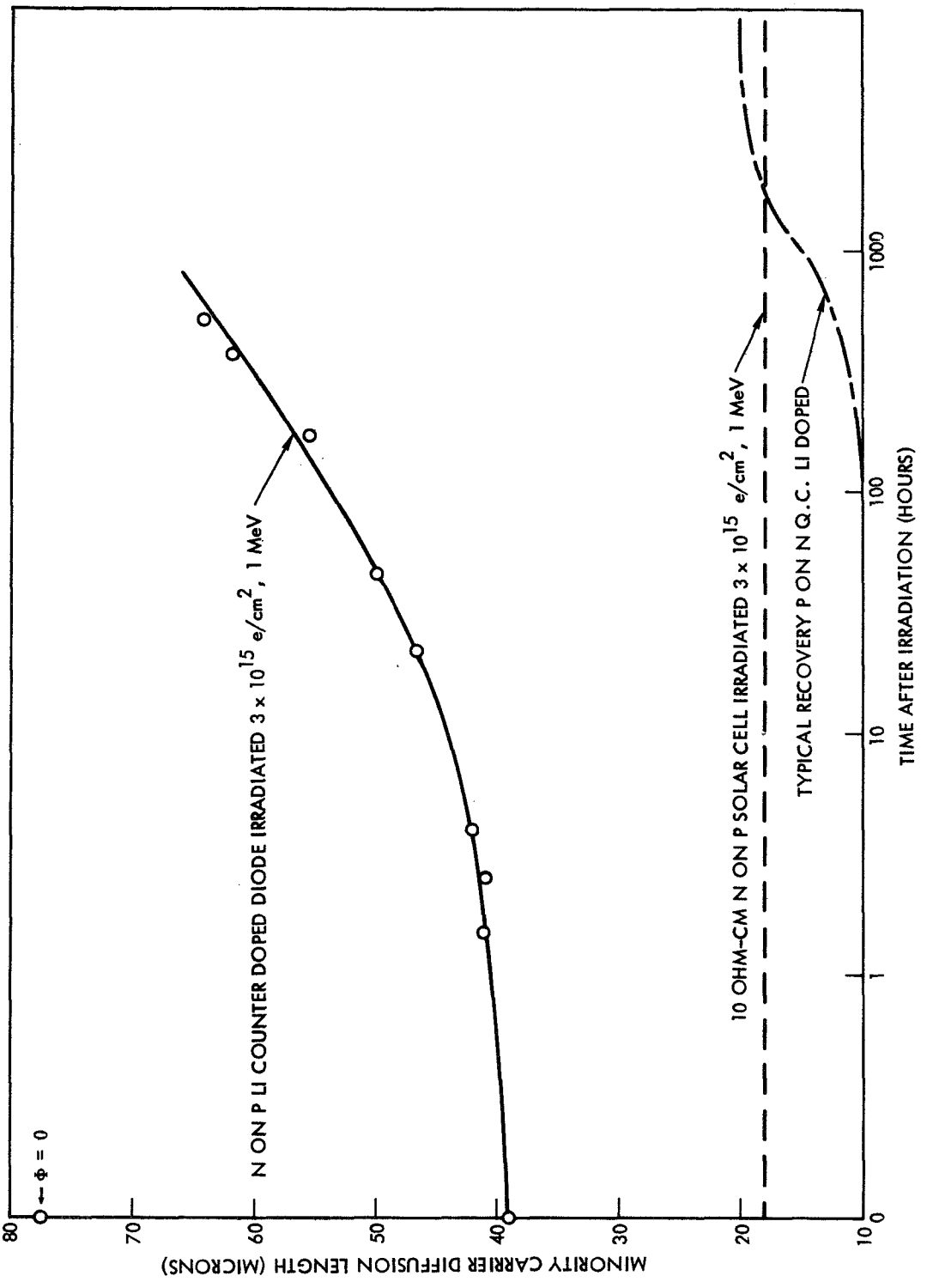


FIGURE 73. LITHIUM COUNTERDOPED DIODE, T.I. LOPEX

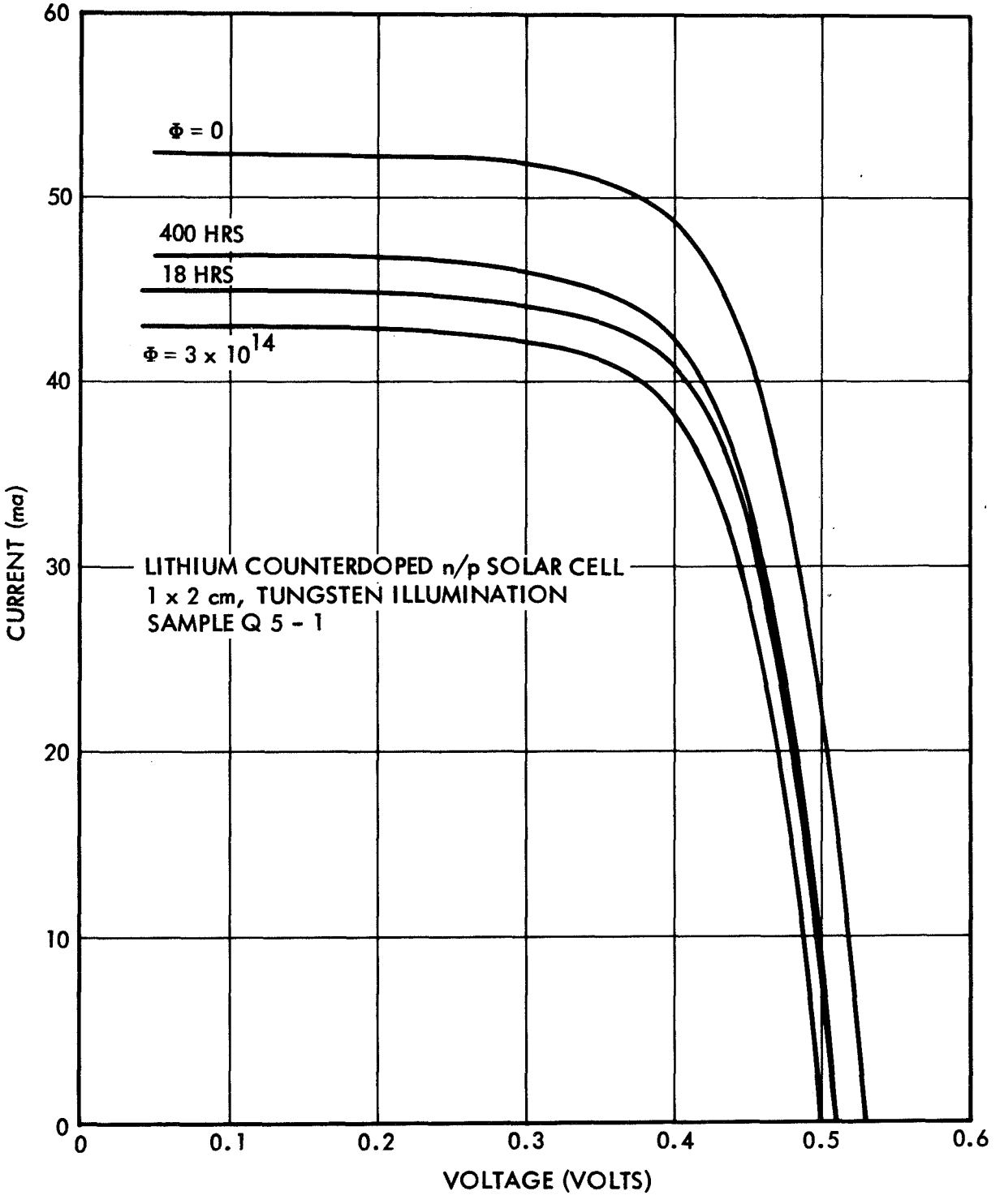


FIGURE 74. LITHIUM COUNTERDOPED n/p SOLAR CELL